Carbon cycling: The role of Methane and Copper in an early ocean analogue, Lake Matano

By

Arne Sturm

Submitted to the graduate degree program in Geology and the Graduate Faculty of the University of Kansas in partial fulfillment of the requirements for the degree of Doctor of Philosophy

_____
David A. Fowle, Chair

_____
Jennifer A. Roberts

_____
Luis A. González

_____
J. Douglas Walker

_____
Edward F. Peltier

Date Defended: December 11. 2015

The Dissertation Committee for Arne Sturm
certifies that this is the approved version of the following dissertation:

Carbon cycling: The role of Methane and Copper in an early ocean analogue, Lake Matano

_____
Chairperson David A. Fowle

Date approved: February 2. 2016

Abstract

Arne Sturm, Ph.D.
Department of Geology, December 2015
University of Kansas

This dissertation examines the carbon cycle of a modern ferruginous environment (Lake Matano, Indonesia), with a primary focus on the critical role of methane in carbon redistribution in this system. In addition, the mobility and availability of copper (Cu) (an essential component of microbial enzymatic systems related to methane oxidation) was evaluated in this iron-dominated, aquatic ecosystem. Fieldwork was conducted over several years to acquire the necessary samples and measurements that were used for constraining and modeling the lakes water budget, carbon cycle and copper mobility. It was determined that microbial methane oxidation was unusually high in the water column of this lake, providing possibly the highest anaerobic oxidation rates for this important greenhouse gas reported in freshwater or marine settings. Furthermore because of the nutrient limitations of the lake and its minimal photosynthetic activity it was shown that methane plays a key role in this carbon cycle and as a substrate for organic matter production, which in turn can be used as an energy source, and for cell growth. Ultimately some of this organic matter produced from methane will be buried and subsequently lithified. The availability of copper is intimately tied to this carbon cycle by its link to methanotrophy, as copper is a central part of the pMMO enzyme, which regulates enzyme expression and increases methanotrophic efficiency, and is therefore of paramount importance for the rates of methanotrophy occurring. Unexpectedly Cu is not entirely removed through sorption and co-precipitation by Fe and Mn oxides as often presumed in ferruginous and manganous environments where a lot of Fe(oxy)hydroxides and Mn oxides are present. It was

found instead to be largely associated with organic matter and undergoing significant redistribution under microbial respiration between a variety of solid phases, including sulfide minerals. These discoveries deliver important insights into both the bioenergetics and microbial enzymatic evolution in the ferruginous basins of Precambrian Eons, through the continued study of one of their best modern analogue systems.

Acknowledgments

I would like to dedicate this work to my Mother Gigi (Gertrud) Sturm-Krumsiek (Apr. 18 1951-Dec. 8. 2013), who was always there for me with support, encouragement, love and inspiration.

I would like to acknowledge the many people without whose contribution this work would have not been possible. I thank my committee for being available on many occasions on short notice and their patience during this process. I would like to especially thank Dr. Jennifer Roberts, for scientific discussion and teachings of Laboratory procedures, and the privilege of working in her laboratory. Beyond this I would like to thank Dr. Roberts for the moral and financial support she provided, even though I was not directly under her supervision or co supervision. Dr. Luis Gonzales I would like to thank for the use of his laboratory, and arranging financial support for my final semesters, as well as many humoring encouraging conversations during my time at KU. I would like to thank Carriayne, Jones, Sean Crowe and Simon Poulton for Scientific Discussions and help with fieldwork and analysis. Don Canfield and Bo Thamdrup I would like to especially thank for the usage of their Lab and Scientific discussions. Manny thanks to my Advisor Dr. David Fowle for financial support, scientific discussions and encouragement and a lot of patience. Finally I would like to thank Dr. Sean A. Crowe, without whom I would not be submitting this work, he has been an immense mentor, inspiring and encouraging in many ways. He has also been a great friend throughout these times.

Finally I would like to thank my family for all the sacrifices that they have made, the many missed Christmases and other holidays and occasions. A special thanks to Maureen Logan and Nero, who have been by my side for the last few years and put up with many long working nights and trips away from home. Thank you Maureen, I could have not done this without you and Nero.

Table of Contents

List of Figures

List of Tables

Chapter 1: Introduction

Lake Matano is a tropical permanently stratified lake on Sulawesi Island, Indonesia and among the 10 deepest lakes on earth with a depth of approximately 590 m. The lake is of tectonic origin and is hosted in a graben structure cryptodepression, with its surface residing at an elevation of 380m above mean sea level. Its basin is relatively small and has an area of approximately 436km^2, the lake itself has a surface area of 164 km^2 and is estimated to be between 2-10 Ma old (Brooks, 1950). The basin was created by rapid uplift and consists dominantly of highly weathered ultramafic bedrock of ophiolitic origin mainly containing pyroxenes (Golightly, 1981), in addition there is a limestone and chert outcrop on south west shore of the lake. As a result of high weathering rates, the basins bedrock is covered by thick lateritic soils (10-30m), rich in iron and manganese, overlaying plateaus and the steep to gently sloping topography of the basin.

Lake Matano is currently one of the most intensely studied early Earth ocean analogues (Crowe et al., 2008a; Crowe et al., 2011; Crowe et al., 2014; Crowe et al., 2008b; Crowe et al., 2007; Jones et al., 2011; Katsev et al., 2010; Kuntz et al., 2015; Wicaksono et al., 2015; Zegeye et al., 2012) and indeed is likely one of the most appropriate to study the biogeochemistry of both modern and paleo ferruginous aquatic environments. Early investigations into this system examined the unique physical and geochemical characteristics of the lake and to evaluate if they could lead to catastrophic release of carbon dioxide or methane (it was deemed safe soon after and the result was published in (Crowe et al., 2011)). However the long term stability of these geochemical conditions has likely co-evolved with a unique microbial community (e.g. (Crowe et al., 2014)). The ferruginous conditions in the lake, together with its dearth of sulfate and ultra

low nutrient concentration are conditions indicative of those that are postulated to have dominated early Earth ocean chemistry (Canfield et al., 2008; Planavsky et al., 2011; Poulton and Canfield, 2011). The interplay between these geochemical parameters has clearly played a significant role in development and shaping of microbial metabolisms (Canfield et al., 2006) through geologic time, as well as in the adaptability of microbes in these elemental deserts. Based on the rock record of nutrient availability, stable isotope (C, N, S, O) measurements and the evaluation of what redox states predominated, there have been a number of conceptual models developed for what the carbon cycle in an early earth ferruginous environment looked like, in terms of primary production, carbon mineralization, deposition and lithification (Bartley and Kah, 2004; Des Marais, 1997; Des Marais, 2002; Fennel et al., 2005; Konhauser, 2007; Schidlowski, 1993).

In the Anthropocene, primary production on our planet is dominated by photosynthesis (Field et al., 1998), however the importance of chemoautotrophy cannot be ignored for poorly irradiated environments The main function of primary production is to convert inorganic carbon into a carbon form that it usable for anabolic reactions (e.g. biomass creation) and this carbon in turn is the underpinning for the bioenergetics of a broad and deep food web and the remainder is buried in the sediments of oceans or lakes, where the refractory components are typically lithified and buried until exposed to the atmosphere again by geological processes. Here within this dissertation I present evidence for a carbon cycle in which primary production is nearly equally supported by intensely cycled methane, as it is by anoxygenic prototrophy (Crowe et al., 2008a), and oxygenic phototrophy. This redistribution of primary production likely influences bio-signatures and thus our interpretation of paleoenvironments. The behavior of the

micronutrient copper in this ferruginous environment was also examined and the influence it has on biological processes and their evolution through time.

Methane Biogeochemistry

Methane (CH_4) is a critical component of the global carbon cycle, as it is often an intermediate or end product of organic matter degradation in soils and aqueous systems and is readily released by industrial processes and other anthropogenic activity such as biomass burning due to incomplete combustion. Methane's importance as a greenhouse gas is undeniable, and according to (Lashof and Ahuja, 1990) and (Albritton et al., 1995) methane has a global warming effect that is 25 times higher on a weight comparison than carbon dioxide (CO_2) based on a 14.5 year residence time for CH_4 and one century comparison . This in turn leads to a contribution of 14.6% to the total global radiative forcing (Dlugokencky et al., 1998; Lelieveld et al., 1998; Intergovernmental panel on climate change (IPCC) 4th assessment report Table 2.1) even with its low (1843 ppbv (EPA location Hawaii)) atmospheric abundance. Carbon dioxide continues to be the primary greenhouse gas with over 50% of global radiative forcing (IPCC 4th assessment report Table 2.1). However, concentrations of methane have increased in the atmosphere by more than a factor of two, from 750-1840 ppbv, compared to preindustrial levels (Cicerone and Oremland, 1988) and have never been this high in the previous 160,000 years (Raynaud et al., 1988). It remains somewhat enigmatic as to why methane values have risen this rapidly over the last 300 years, however this lack of clarity suggests that there are a wide variety of sinks and sources for methane that are not well constrained or have even been evaluated. Anthropogenic methane production is an estimated 375 Tg y^{-1} (Prather et al., 1995), which is about twice of the estimated naturally occurring emissions. Therefore the assumption that human activity is

responsible for the recent increase is very reasonable. Natural sources of methane release include lakes, wetlands, and similar freshwater systems. Furthermore termites, geological release, burning of biomass (through lightning strikes) and soil depending on its moisture content, temperature and other conditions can be either a sink or source of methane (Prather et al., 1995).

Freshwater ecosystems such as wetlands and lakes are among the largest natural contributors of atmospheric methane release, with freshwater lakes being responsible for 6-16 % of natural global methane emissions (Bastviken et al., 2004), even though they cover less than 1% of earth surface (Downing et al., 2006). It should be noted that artificially created water storage reservoirs fall into this category as well and contribute nearly 20% of the global anthropogenic emissions (St Louis et al., 2000). Oceans despite their size only contribute 1-4 % to the annual methane flux (Cicerone and Oremland, 1988; Seiler, 1984), more recent studies even suggest contributions of less then 1% (Rhee et al., 2009). The remainder of methane is released from cattle intestines, rice agriculture, termites, and the largest contribution from industrial processes (Conrad, 2009). Indeed, native and constructed wetlands are critical components of the global carbon cycle, supporting some of the most biologically productive ecosystems on Earth where they degrade and store large amounts of carbon under aerobic and anaerobic conditions. In all of these environments microbial processes contribute to more then 2/3 of methane released into the atmosphere (Reeburgh, 2007). Typically, methane sinks and sources are closely coupled both in proximity to each other and ecologically. In most natural freshwater systems methanogens will convert organic carbon, often fermentation byproducts (e.g. formate (CH_3OO^-), H_2 etc.), under anaerobic conditions into methane (Eq 1 and 2).

$$CO_2 + 4\ H_2 \rightarrow CH_4 + 2\ H_2O \qquad (1)$$

$$CH_3COOH \rightarrow CH_4 + CO_2 \quad (2)$$

Methanogenesis can account for 30-80% of all anaerobic carbon mineralization, (Bédard and Knowles, 1991; Fallon et al., 1980; Kuivila et al., 1988; Rudd and Hamilton, 1978) hence converting between 20 to 59% of particulate carbon to methane (Wetzel, 2001). However a significant proportion of this produced methane never enters the atmosphere. Methanotrophy, (usually defined as) the microbial oxidation of methane using oxygen, whereby these microorganisms metabolize methane to produce fixed carbon and energy, can consume between 30 and 99% of this methane. Evidence for this biogeochemical process is typically found at the oxic anoxic interface in the water or sediments and is facilitated by methanotrophic bacteria (Bastviken et al., 2008; Bastviken et al., 2002; Fallon et al., 1980; Frenzel et al., 1990; Kankaala et al., 2006; Kuivila et al., 1988; Liikanen et al., 2002; Utsumi et al., 1998b). Chemical redox stratification in the environment provides boundary conditions for the presence of methanogenesis and methanotrophy. In most near-surface environments a redox ladder (Canfield and Thamdrup, 2009), where electron acceptors are utilized in order of thermodynamic favorability controls this stratification e.g. O_2 is exhausted first, followed by nitrite (NO_2^-), nitrate (NO_3^-), manganese (Mn), iron (Fe), sulfate(SO_4^{-2}) and CO_2. For this reason methanotrophy and methanogenesis are not only directly linked by the carbon cycle but also through physical parameters for example, physical stratification has to be present in order to enable the formation of necessary geochemical gradients. The distribution of redox active elements are of particular importance here as most methanogens will not operate if oxygen concentrations are above 10 ppm as several enzyme and cofactors involved in the organisms metabolism are oxygen sensitive (Ragsdale and Kumar, 1996; Schönheit et al., 1981).

Furthermore sulfate and other redox couples (Fe, NO_3^-, NO_2^-) in the anaerobic zone will promote other anaerobic carbon degradation pathways such as, sulfate reduction, iron reduction and de-nitrification, which can outcompete methanogens for substrates such as H_2 and acetate (Achtnich et al., 1995; Lovley and Phillips, 1987; Winfrey et al., 1977). Indeed sulfate levels of more than 30 uM have been suggested to inhibit methanogenesis e.g. (Lovley and Klug, 1986) via a switch over from methanogenesis to sulfate reduction. In many freshwater systems sulfate concentrations are low and will be depleted quickly in the diffusion driven transport environment of sediments thereby facilitating methanogenesis through redox stratification. This spatial distribution is often very narrow with methanogenesis present only a few centimeters or less (Koizumi et al., 2003; Kuivila et al., 1989) below the sulfate reduction zone.

Methane oxidizing microorganisms have been demonstrated to oxidize methane using a variety of electron acceptors. For example methanotrophy will usually occur in a narrow suboxic zone, with oxygen concentrations greater then 120 μM impeding this process (Harrits and Hanson, 1980). The niche environment for these bacteria that has the correct balance of oxygen and methane is typically found in boundary layers that are produced via physical stratification. In sediments this stratification is more readily produced and maintained as it is typically removed from physical mixing events. To date the highest rates for aerobic methane oxidation have been observed near the bottom of the oxycline boundary layer, where methane concentrations are high and oxygen concentrations are diminishing (Bastviken et al., 2002; Harrits and Hanson, 1980; Liikanen et al., 2002; Rudd et al., 1974; Utsumi et al., 1998b). In turnover events in lakes total lake specific methane oxidation can increase substantially (Harrits and Hanson, 1980), when waters with high methane concentrations are mixed with oxygenated waters. In this case there is no diffusion limited transport of either substrate nor electron

acceptor, though if oxygen concentrations are too high there can be inhibition of methane oxidation. Methane may also be oxidized in the anoxic zone of sediments or water columns in lakes and oceans, utilizing several naturally occurring electron acceptors (e.g. sulfate, nitrate, nitrite, and manganese and iron oxides), which are present and most likely accessible in stratified boundary layers. These alternative electron acceptors were first suggested by (Hinrichs et al., 1999; Mason, 1977; Zehnder and Brock, 1980) and then demonstrated (Beal et al., 2009; Boetius et al., 2000; Raghoebarsing et al., 2006), though the evidence for Fe and Mn dependent oxidation of methane was not conclusive and may have failed to rule out other electron acceptors.

The narrow spatial region in which methane oxidation occurs makes this biogeochemical process sensitive to perturbations in physical parameters. For example an increase in temperature could lead to higher methane production, releasing more of the methane to the atmosphere via increased diffusional transport, higher carbon lability (Westrich and Berner, 1988) or by occasional saturation and bubble occurrence (Crill and Martens, 1983), transporting methane rapidly to the atmosphere. Increased temperature may also have some negative effects on methane emissions, by increasing methane consumption rates (Kelly and Chynoweth, 1981), drying up methane producing freshwater systems, and increasing the earth albedo due to more water vapor (clouds) in the atmosphere.

Rates for aerobic methanotrophy are considered well constrained for many systems (Bastviken et al., 2002; Deangelis and Scranton, 1993; Guerin and Abril, 2007; Howard et al., 1971; Jannasch, 1975; Liikanen et al., 2002; Lilley et al., 1988; Rudd and Hamilton, 1975; Utsumi et al., 1998a; Utsumi et al., 1998b; Venkiteswaran and Schiff, 2005), but anaerobic methane oxidation (AOM) rates on the other hand is not well documented. The anaerobic pathway can depend on several electron donors (Table 1), which in some systems coexist and

therefore it is not as trivial to separate quantitatively which process may contributed to AOM. In many stratified systems we can often only estimate the net flux of CH_4 to the atmosphere, yet without a knowledge of the mechanisms and rates of all processes influencing carbon cycling of these ecosystems it is unlikely that we can predict the results of geochemical or climate perturbations particularly in paleo environments.

Copper Biogeochemistry

Copper (Cu) is not very abundant in the near-surface and usually is only present in trace concentrations in most aqueous environments. As a micronutrient Cu is a cofactor in many microbial enzymatic systems that are essential for several important microbial metabolic pathways such as denitrification, photosynthesis, iron oxidation and methanotrophy. Copper availability is often critical for these pathways to function although paradoxically, high concentrations of Cu can have an adverse and even poisonous effect on microbes (Brand et al., 1986). For most microbial organisms these concentrations are usually not much higher then what they need for their enzyme synthesis, presenting a delicate balance in these environments. As aqueous copper concentrations do not really reflect true copper availability and Cu^{2+} is the relevant species for uptake by microorganisms, Cu^{2+} concentrations are usually used to determine effects of Cu on biota (Brand et al., 1986).

Copper cycling has critical implications in both modern and ancient ferruginous environments, Cu availability in an aqueous systems is very much dependent on the redox conditions and distribution of other redox active elements such as iron, sulfate and oxygen. In modern settings with a well oxygenated atmosphere, oxygen will prevail in the surface waters, poor mixing and stratification will essentially lead to oxygen depletion and anoxia. Copper

solubility differs greatly under ferruginous, euxinic and oxic conditions. Under oxic conditions Cu is strongly sequestered with Fe, Mn oxides and organic matter through sorption and complexation reactions. In anoxic zones Cu is typically liberated from the Fe and Mn phases by reductive dissolution, and ultimately in many sulfate bearing systems maybe scavenged by sulfide that was produced as a byproduct of sulfate reduction (Canfield et al., 2005). The bioavailability and reactivity of solid phase reservoirs of Cu may have profound implications for the productivity and choice of metabolism in aquatic systems. While the fate of Cu has been evaluated in modern euxinic environment it has not been examined to the same extent in ferruginous environments which has been predicted by majority of Precambrian research to be rendered unavailable for enzymatic systems and thus used as a boundary condition for the evolution of many enzymatic systems.

In this dissertation I investigated several facets of the carbon cycle in Lake Matano, Sulawesi, Indonesia (Figure 1) with special focus on the role of methane in this oligotrophic environment. The trace nutrient copper was also investigated as it usually plays an important role in methane biogeochemistry and can have a significant impact on methane distribution in aquatic environments. Our collaborative research group (Dr. Fowle, Dr. Canfield, Dr. Crowe and Dr. Jones) has been studying Lake Matano's geochemistry for over 10 years and this lake presents us with a tremendous natural laboratory for studies relating to early Earths ferruginous oceans (Crowe et al., 2008b). The stratified nature and its unique geochemical composition make the lake ideal to investigate specific mechanisms and rates of methane oxidizing metabolisms, which is the focus of Chapter 2. Sulfate and nitrate are almost absent, near detection limits (0.2 and 0.25 nmol l^{-1} respectively) in the lake; therefore they are eliminated naturally as electron

acceptors suitable (Table 1) for anaerobic oxidation of methane (AOM), though the other two electron acceptors, iron and manganese, have high concentrations, with up to 150 μM and 12 μM respectively. As most alternative electron acceptors (beyond Fe and Mn) are present at concentrations that are thermodynamically not feasible I was able to determine aerobic vs. anaerobic rates of methane oxidation, providing novel insights into how anaerobic rates are coupled to Iron and/or Manganese reduction (Crowe et al., 2011) and the assimilation and recycling of carbon from methane back into the carbon cycle of the lake.

In Chapter 3 I undertook a broad investigation of the other elements of the carbon cycle of the lake using stable isotopes, geochemistry and hydrological modeling. The stratified nature of the lake provided the opportunity to establish a proper mass balance of carbon, as the DIC, CH_4 and particulate organic matter (POM) concentrations are in or near steady state throughout the lake. The magnitude of photosynthesis primary production (PP) values immediately suggested that the carbon budget in Lake Matano is unique and its low productivity likely a result of the low nutrient availability in the lake. The aquatic ecosystem is therefore considered to have quite low net primary production (through photosynthesis), but my work investigated the potential for degradation products from detrital organic matter (supplied from terrestrial sources) to fuel chemoautotrophic primary production namely by methanogenesis and methanotrophy. This change in the carbon flow and involvement of metabolisms that are thought to be mainly reserved for sediment digenesis has a profound influence on the isotopic signature of most carbon involved. If we considered Lake Matano as an analogue for the early earth Oceans then isotopic signatures and trace element proxies for redox in these ancient systems must consider that net primary production may have looked much different in an oligotrophic ferruginous environment.

In Chapter 4 I investigated the copper (Cu) cycle of Lake Matano, I evaluated the distribution, fate and cycling of Cu in lake Matano through careful evaluation of trace aqueous concentrations and examination of particulate bound copper. Solid phases were further evaluated by applying a selective metal extraction scheme to discriminate between Mn, Fe and organic phases. The extraction results taken together with geochemical modeling and synchrotron based μXRF mapping were used to infer how copper behaves as it moves through the water column. Total Copper concentrations in this lake are extremely low in the aqueous and solid phases as postulated in paleoenvironments. However, even though Cu is surrounded in an environment with copious Fe and Mn oxides present, it is not exclusively controlled by these phases, but instead displays a strong association with organic matter (much likely produced and recycled in the lake) suggesting bioavailability even in this challenging system. In the anoxic zone where Cu might be predicted to be liberated after Fe and Mn reduction it is instead but re-associated with sulfide and organic phases. This result is striking, as sulfide concentrations are extremely low and provides some tantalizing insights into Cu-S associations their impact on enzyme evolution in ferruginous environments.

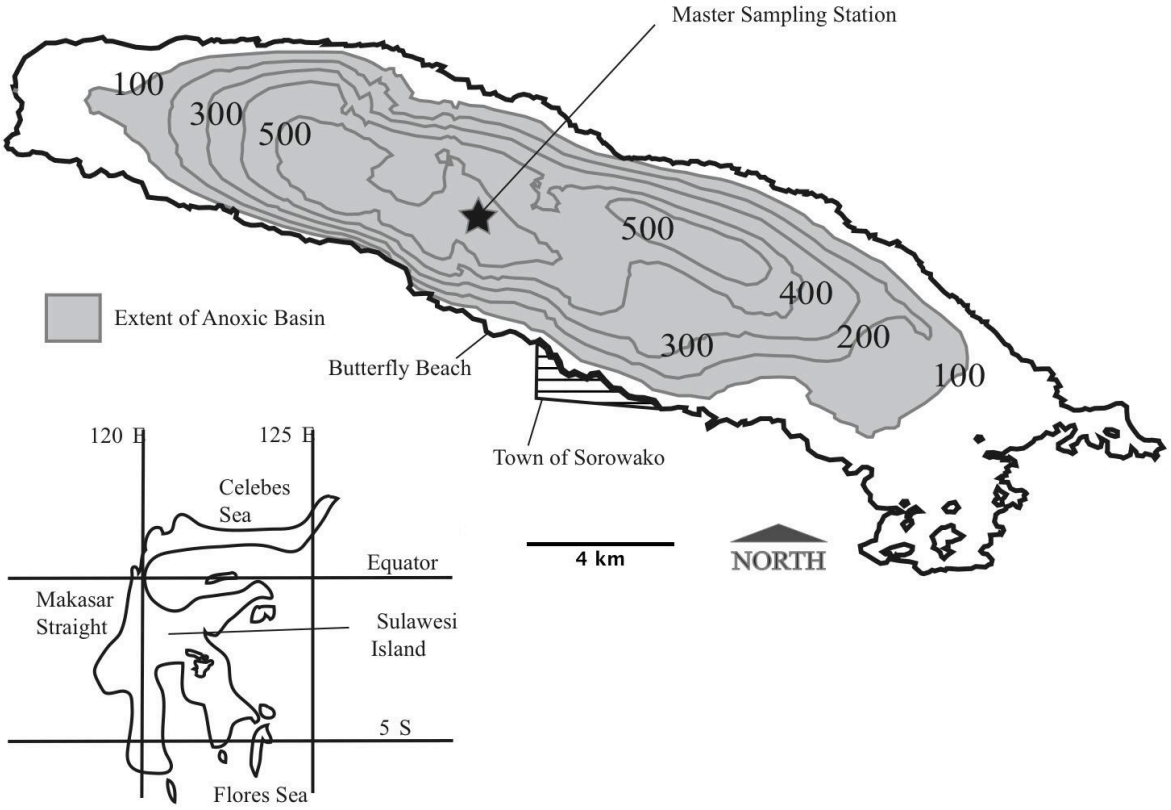

Figure 1 Map of Lake Matano and its anoxic basin.

Reaction	$\Delta G^{0'}$ in kJ mol^{-1} CH_4	Reference
$5CH_4 + 8NO_3^- + 8H^+ \rightarrow 5CO_2 + 4N_2 + 14H_2O$	-765	Raghoebarsing et al., 2006
$3CH_4 + 8NO_2^- + 8H^+ \rightarrow 3CO_2 + 4N_2 + 10H_2O$	-928	Raghoebarsing et al., 2006
$CH_4 + 8Fe(OH)_3 + 15H^+ \rightarrow HCO_3^- + 8Fe^{2+} + 21H_2O$	-572.2	Crowe et al., 2011
$CH_4 + 4MnO_2 + 7H^+ \rightarrow HCO_3^- + 4Mn^{2+} + 5H_2O$	-789.9	Crowe et al., 2011
$CH_4 + SO_4^- \rightarrow HCO_3^- + HS^- + H_2O$	-20 to -30	Boetius et al., 2000; Valentine et al., 2000

Table 1 Mass action equations and their corresponding Gibbs Free energy.

References:

Achtnich, C., Bak, F., Conrad, R., 1995. Competition For Electron-Donors Among Nitrate Reducers, Ferric Iron Reducers, Sulfate Reducers, And Methanogens In Anoxic Paddy Soil. Biology and Fertility of Soils, 19(1): 65-72.

Albritton, D.L., Derwent, R.G., Isaksen, I.S.A., Lal, M., Wuebbles, D.J., 1995. Trace gas radiative forcing indices. Climate Change 1994 Radiative Forcing of Climate Change, Intergovernmental Panel on Climate Change.

Bartley, J.K., Kah, L.C., 2004. Marine carbon reservoir, C-org-C-carb coupling, and the evolution of the Proterozoic carbon cycle. Geology, 32(2): 129-132.

Bastviken, D., Cole, J., Pace, M., Tranvik, L., 2004. Methane emissions from lakes: Dependence of lake characteristics, two regional assessments, and a global estimate. Global Biogeochem. Cycles, 18(4): GB4009.

Bastviken, D., Cole, J.J., Pace, M.L., Van de Bogert, M.C., 2008. Fates of methane from different lake habitats: Connecting whole-lake budgets and CH4 emissions. J. Geophys. Res., 113(G2): G02024.

Bastviken, D., Ejlertsson, J., Tranvik, L., 2002. Measurement of methane oxidation in lakes: A comparison of methods. Environmental Science & Technology, 36(15): 3354-3361.

Beal, E.J., House, C.H., Orphan, V.J., 2009. Manganese- and Iron-Dependent Marine Methane Oxidation. Science, 325(5937): 184-187.

Bédard, C., Knowles, R., 1991. Hypolimnetic O2 Consumption, Denitrification, and Methanogenesis in a Thermally Stratified Lake. Canadian Journal of Fisheries and Aquatic Sciences, 48(6): 1048-1054.

Boetius, A. et al., 2000. A marine microbial consortium apparently mediating anaerobic oxidation of methane. Nature, 407(6804): 623-626.

Brand, L.E., Sunda, W.G., Guillard, R.R.L., 1986. Reduction of marine-phytoplankton reproduction rates by copper and cadmium. Journal of Experimental Marine Biology and Ecology, 96(3): 225-250.

Brooks, J.L., 1950. Speciation in ancient lakes. Quarterly Review of Biology, 25: 131-176.

Canfield, D.E. et al., 2008. Ferruginous conditions dominated later neoproterozoic deep-water chemistry. Science, 321(5891): 949-952.

Canfield, D.E., Rosing, M.T., Bjerrum, C., 2006. Early anaerobic metabolisms. Philosophical Transactions of the Royal Society B-Biological Sciences, 361(1474): 1819-1834.

Canfield, D.E., Thamdrup, B., 2009. Towards a consistent classification scheme for geochemical environments, or, why we wish the term 'suboxic' would go away. Geobiology, 7(4): 385-392.

Canfield, D.E., Thamdrup, B., Kristensen, E., 2005. Aquatic Geomicrobiology. Advances in Marine Biology, 48. Elsevier Academic Press, 640 pp.

Cicerone, R.J., Oremland, R.S., 1988. Biogeochemical aspects of atmospheric methane. Global Biogeochem. Cycles, 2(4): 299-327.

Conrad, R., 2009. The global methane cycle: recent advances in understanding the microbial processes involved. Environmental Microbiology Reports, 1(5): 285-292.

Crill, P.M., Martens, C.S., 1983. Spatial And Temporal Fluctuations Of Methane Production In Anoxic Coastal Marine-Sediments. Limnology and Oceanography, 28(6): 1117-1130.

Crowe, S.A. et al., 2008a. Photoferrotrophs thrive in an Archean Ocean analogue. Proceedings of the National Academy of Sciences of the United States of America, 105(41): 15938-15943.

Crowe, S.A. et al., 2011. The methane cycle in ferruginous Lake Matano. Geobiology, 9(1): 61-78.

Crowe, S.A. et al., 2014. Deep-water anoxygenic photosythesis in a ferruginous chemocline. Geobiology, 12(4): 322-339.

Crowe, S.A. et al., 2008b. The biogeochemistry of tropical lakes: A case study from Lake Matano, Indonesia. Limnology and Oceanography, 53(1): 319-331.

Crowe, S.A. et al., 2007. Reductive dissolution of trace metals from sediments. Geomicrobiology Journal, 24(3-4): 157-165.

Deangelis, M.A., Scranton, M.I., 1993. Fate of methane in the Hudson River and estuary. Global Biogeochemical Cycles, 7(3): 509-523.

Des Marais, D.J., 1997. Isotopic evolution of the biogeochemical carbon cycle during the Proterozoic Eon. Organic Geochemistry, 27(5-6): 185-193.

Des Marais, D.J., 2002. Biogeochemical carbon cycles during the Archean and early Proterozoic. Geochimica Et Cosmochimica Acta, 66(15A): A178-A178.

Dlugokencky, E.J., Masarie, K.A., Lang, P.M., Tans, P.P., 1998. Continuing decline in the growth rate of the atmospheric methane burden. Nature, 393(6684): 447-450.

Downing, J.A. et al., 2006. The Global Abundance and Size Distribution of Lakes, Ponds, and Impoundments. Limnology and Oceanography, 51(5): 2388-2397.

Fallon, R.D., Harrits, S., Hanson, R.S., Brock, T.D., 1980. The Role of Methane in Internal Carbon Cycling in Lake Mendota during Summer Stratification. Limnology and Oceanography, 25(2): 357-360.

Fennel, K., Follows, M., Falkowski, P.G., 2005. The co-evolution of the nitrogen, carbon and oxygen cycles in the Proterozoic ocean. American Journal of Science, 305(6-8): 526-545.

Field, C.B., Behrenfeld, M.J., Randerson, J.T., Falkowski, P., 1998. Primary production of the biosphere: Integrating terrestrial and oceanic components. Science, 281(5374): 237-240.

Frenzel, P., Thebrath, B., Conrad, R., 1990. Oxidation Of Methane In The Oxic Surface-Layer Of A Deep Lake Sediment (Lake Constance). FEMS Microbiology Ecology, 73(2): 149-158.

Golightly, J.P., 1981. Nickeliferous Laterite Deposits. Economic Geology, 75th Aniversary Volume: 710-735.

Guerin, F., Abril, G., 2007. Significance of pelagic aerobic methane oxidation in the methane and carbon budget of a tropical reservoir. Journal of Geophysical Research-Biogeosciences, 112(G3): Article: G03006.

Harrits, S.M., Hanson, R.S., 1980. Stratification Of Aerobic Methane-Oxidizing Organisms In Lake Mendota, Madison, Wisconsin. Limnology and Oceanography, 25(3): 412-421.

Hinrichs, K.U., Hayes, J.M., Sylva, S.P., Brewer, P.G., DeLong, E.F., 1999. Methane-consuming archaebacteria in marine sediments. Nature, 398(6730): 802-805.

Howard, D.L., Frea, J.I., Pfister, R.M., 1971. The potential for Methane-carbon cycling in lake Erie, Proc.14th International Association of Great Lakes Research, University of Toronto, Toronto, Ontario, pp. 236-240.

Jannasch, H.W., 1975. Methane Oxidation In Lake Kivu (Central Africa). Limnology and Oceanography, 20(5): 860-864.

Jones, C. et al., 2011. Biogeochemistry of manganese in ferruginous Lake Matano, Indonesia. Biogeosciences, 8(10): 2977-2991.

Kankaala, P., Huotari, J., Peltomaa, E., Saloranta, T., Ojala, A., 2006. Methanotrophic activity in relation to methane efflux and total heterotrophic bacterial production in a stratified, humic, boreal lake. Limnology and Oceanography, 51(2): 1195-1204.

Katsev, S. et al., 2010. Mixing and its effects on biogeochemistry in the persistently stratified, deep, tropical Lake Matano, Indonesia. Limnology and Oceanography, 55(2): 763-776.

Kelly, C.A., Chynoweth, D.P., 1981. The Contributions Of Temperature And Of The Input Of Organic-Matter In Controlling Rates Of Sediment Methanogenesis. Limnology and Oceanography, 26(5): 891-897.

Koizumi, Y., Takii, S., Nishino, M., Nakajima, T., 2003. Vertical distributions of sulfate-reducing bacteria and methane-producing archaea quantified by oligonucleotide probe hybridization in the profundal sediment of a mesotrophic lake. FEMS Microbiology Ecology, 44(1): 101-108.

Konhauser, K.O., 2007. Introduction to Geomicrobiology. Blackwell Publishing, 440 pp.

Kuivila, K., Murray, J., Devol, A., Novelli, P., 1989. Methane production, sulfate reduction and competition for substrates in the sediments of Lake Washington☆. Geochimica Et Cosmochimica Acta, 53(2): 409-416.

Kuivila, K.M., Murray, J.W., Devol, A.H., Lidstrom, M.E., Reimers, C.E., 1988. Methane cycling in the sediments of lake washington. Limnology and Oceanography, 33(4): 571-581.

Kuntz, L.B., Laakso, T.A., Schrag, D.P., Crowe, S.A., 2015. Modeling the carbon cycle in Lake Matano. Geobiology, 13(5): 454-461.

Lashof, D.A., Ahuja, D.R., 1990. Relative Contributions of Greenhouse Gas Emissions to Global Warming. Nature, 344(6266): 529-531.

Lelieveld, J., Crutzen, P.J., Dentener, F.J., 1998. Changing concentration, lifetime and climate forcing of atmospheric methane. Tellus Series B-Chemical and Physical Meteorology, 50(2): 128-150.

Liikanen, A., Huttunen, J.T., Valli, K., Martikainen, P.J., 2002. Methane cycling in the sediment and water column of mid-boreal hyper-eutrophic Lake Kevaton, Finland. Archiv Fur Hydrobiologie, 154(4): 585-603.

Lilley, M.D., Baross, J.A., Dahm, C.N., 1988. Methane production and oxidation in lakes impacted by the May 18, 1980 Eruption of Mount St. Helens. Global Biogeochem. Cycles, 2(4): 357-370.

Lovley, D.R., Klug, M.J., 1986. Model For The Distribution Of Sulfate Reduction And Methanogenesis In Fresh-Water Sediments. Geochimica Et Cosmochimica Acta, 50(1): 11-18.

Lovley, D.R., Phillips, E.J.P., 1987. Competitive Mechanisms for Inhibition of Sulfate Reduction and Methane Production in the Zone of Ferric Iron Reduction in Sediments. Applied and Environmental Microbiology, 53(11): 2636-2641.

Mason, I., 1977. Methane as a carbon source in biological denitrification. Journal Water Pollution Control Federation, 49(5): 855-857.

Planavsky, N.J. et al., 2011. Widespread iron-rich conditions in the mid-Proterozoic ocean. Nature, 477(7365): 448-U95.

Poulton, S.W., Canfield, D.E., 2011. Ferruginous Conditions: A Dominant Feature of the Ocean through Earth's History. Elements, 7(2): 107-112.

Prather, M. et al., 1995. Other trace gases and atmospheric chemistry. In: Houghton, J.T. et al. (Eds.), Climate Change 1994. Cambridge University Press, Cambridge (UK), pp. 73–126.

Raghoebarsing, A.A. et al., 2006. A microbial consortium couples anaerobic methane oxidation to denitrification. Nature, 440(7086): 918-921.

Ragsdale, S.W., Kumar, M., 1996. Nickel-containing carbon monoxide dehydrogenase/acetyl-CoA synthase. Chemical Reviews, 96(7): 2515-2539.

Raynaud, D., Chappellaz, J., Barnola, J.M., Korotkevich, Y.S., Lorius, C., 1988. Climatic and CH4 cycle implications of glacial-interglacial CH4 change in the Vostok ice core. Nature, 333(6174): 655-657.

Reeburgh, W.S., 2007. Oceanic methane biogeochemistry. Chemical Reviews, 107(2): 486-513.

Rhee, T.S., Kettle, A.J., Andreae, M.O., 2009. Methane and nitrous oxide emissions from the ocean: A reassessment using basin-wide observations in the Atlantic. Journal of Geophysical Research-Atmospheres, 114.

Rudd, J.W.M., Hamilton, R.D., 1975. Factors Controlling Rates Of Methane Oxidation And Distribution Of Methane Oxidizers In A Small Stratified Lake. Archiv Fur Hydrobiologie, 75(4): 522-538.

Rudd, J.W.M., Hamilton, R.D., 1978. Methane Cycling In A Eutrophic Shield Lake And Its Effects On Whole Lake Metabolism. Limnology and Oceanography, 23(2): 337-348.

Rudd, J.W.M., Hamilton, R.D., Campbell, N.E., 1974. Measurement Of Microbial Oxidation Of Methane In Lake Water. Limnology and Oceanography, 19(3): 519-524.

Schidlowski, M., 1993. Proterozoic carbon cycle. Nature, 362(6416): 117-118.

Schönheit, P., Keweloh, H., Thauer, R.K., 1981. Factor F420 degradation in Methanobacterium thermoautotrophicum during exposure to oxygen. Fems Microbiology Letters, 12(4): 347-349.

Seiler, W., 1984. Contribution of biological processes to the global budget of CH4 in the atmosphere. In: Klug, M.J., Reddy, C.A. (Eds.), Current Perspectives in Microbial Ecology. American Society for Microbiology, Washington D.C., pp. 468-477.

St Louis, V.L., Kelly, C.A., Duchemin, E., Rudd, J.W.M., Rosenberg, D.M., 2000. Reservoir surfaces as sources of greenhouse gases to the atmosphere: A global estimate. Bioscience, 50(9): 766-775.

Utsumi, M. et al., 1998a. Oxidation of dissolved methane in a eutrophic, shallow lake: Lake Kasumigaura, Japan. Limnology and Oceanography, 43(3): 471-480.

Utsumi, M. et al., 1998b. Dynamics of dissolved methane and methane oxidation in dimictic Lake Nojiri during winter. Limnology and Oceanography, 43(1): 10-17.

Venkiteswaran, J.J., Schiff, S.L., 2005. Methane oxidation: isotopic enrichment factors in freshwater boreal reservoirs. Applied Geochemistry, 20(4): 683-690.

Westrich, J.T., Berner, R.A., 1988. The Effect Of Temperature On Rates Of Sulfate Reduction In Marine-Sediments. Geomicrobiology Journal, 6(2): 99-117.

Wetzel, R.G., 2001. Limnology - Lake and River Ecosystems. Academic Press, San Diego, California.

Wicaksono, S.A., Russell, J.M., Bijaksana, S., 2015. Compound-specific carbon isotope records of vegetation and hydrologic change in central Sulawesi, Indonesia, since 53,000 yr BP. Palaeogeography Palaeoclimatology Palaeoecology, 430: 47-56.

Winfrey, M.R., Nelson, D.R., Klevickis, S.C., Zeikus, J.G., 1977. Association of Hydrogen Metabolism with Methanogenesis in Lake Mendota Sediments. Applied and Environmental Microbiology, 33(2): 312-318.

Zegeye, A. et al., 2012. Green rust formation controls nutrient availability in a ferruginous water column. Geology.

Zehnder, A.J.B., Brock, T.D., 1980. Anaerobic methane oxidation - Occurrence and ecology. Applied and Environmental Microbiology, 39(1): 194-204.

Chapter 2: Rates and pathways of CH_4 oxidation in ferruginous Lake Matano, Indonesia

Abstract:

This study evaluates rates and pathways of methane (CH_4) oxidation and uptake using ^{14}C-based tracer experiments throughout the oxic and anoxic waters of ferruginous Lake Matano, Indonesia. Microbial methane oxidation rates in Lake Matano are low ($3.8x10^{-2}$ μmol l^-) compared to other lakes, but are sufficiently high to preclude strong CH_4 fluxes to the atmosphere. In addition to aerobic CH_4 oxidation, which takes place in Lake Matano's oxic mixolimnion, we also detected CH_4 oxidation in Lake Matano's anoxic ferruginous waters. Here, CH_4 oxidation proceeds in the apparent absence of oxygen (O_2) and instead appears to be coupled to nitrate (NO_3^-), nitrite (NO_2^-), iron (Fe) or manganese (Mn) reduction. Throughout the lake, the fraction of CH_4 carbon that is assimilated versus oxidized to carbon dioxide (CO_2) is high (up to 92%), indicating extensive CH_4 conversion to biomass and underscoring the importance of CH_4 as a carbon and energy source in Lake Matano and potentially other ferruginous or low productivity aquatic environments.

1. Introduction

Methane (CH_4) is a critical component of the global carbon cycle and is a potent greenhouse gas (Cicerone and Oremland, 1988; Conrad, 2009; Kroeger et al., 2011). Dramatic changes in global climate throughout Earth's history have been linked to alterations in the global

CH_4 cycle (Kroeger et al., 2011; Sloan et al., 1992; Zeebe et al., 2009). Biogenic methane is produced in the environment as the end product of organic matter degradation via methanogenesis, either through acetate fermentation or CO_2 reduction, in freshwater and marine sediments and soils. A significant fraction of this CH_4 is then consumed through microbially catalyzed oxidation directly within soils and sediments, or within water columns. Microbial oxidation of CH_4 can take place aerobically, with O_2 as the electron acceptor, or anaerobically (anaerobic oxidation of methane (AOM)), typically with sulfate (SO_4^{2-}) as the electron acceptor (Boetius et al., 2000; Devol et al., 1984; Martens and Berner, 1974; Reeburgh, 1980). There are several other thermodynamically favorable electron acceptors (Fe^{+3}, Mn^{+3}, NO_2^-, NO_3^-) that provide even more energy (Table 1) then sulfate, still AOM by sulfate seems to be a highly active and widely distributed pathway which in many cases may be directly tied to the unavailability of other electron acceptors. Indeed sulfate-dependent anaerobic CH_4 oxidation consumes most of the CH_4 produced in marine sediments (Devol et al., 1984;Knittel and Boetius, 2009;Martens and Berner, 1974;Reeburgh, 2007;Treude et al., 2005) and is therefore the largest natural sink for CH_4 on the planet (Reeburgh, 2007). The scarcity of SO_4^{2-} in freshwater settings, however, is thought to largely preclude AOM, and thus aerobic CH_4 oxidation is believed to dominate CH_4 consumption in these environments.

Large uncertainties accompany CH_4 budgets for freshwater environments due to physical and chemical diversity of lake, wetland and soil systems, (Liikanen and Martikainen, 2003;Liikanen et al., 2003;Luesken et al., 2011a). In the large intervals of diffusion-limited marine sediments where CH_4 oxidation occurs, AOM likely represents a more effective environment for CH_4 consumption than aerobic methanotrophy. Primarily, this can be attributed to physical parameters such as the thickness of the diffusion layer in which the oxidation of CH_4

occurs. AOM coupled to SO_4^{2-} usually takes place in a more extensive diffusion layer than aerobic methanotrophy. Sulfate concentrations are generally also much higher in marine systems, for this reason freshwater systems may be not as effective at total CH_4 removal compared to their marine counterparts. Thus, freshwater systems emit proportionally much more CH_4 to the atmosphere (Capone and Kiene, 1988;Conrad, 2009).

Recently, evidence has emerged for AOM utilizing alternative electron acceptors. Nitrate dependent AOM takes place in enrichment cultures from NO_3^- and NO_2^- rich canal waters (Raghoebarsing et al., 2006) and wastewater systems (Kampman et al., 2012;Luesken et al., 2011a;Luesken et al., 2011b;Shen and Hu, 2012). Isolates of *Methylomirabilis oxyfera* conduct nitrate-dependent CH_4 oxidation through a novel denitrifying pathway (Ettwig et al., 2010). Other NO_3^--dependent CH_4 oxidizing archaea couple NO_3^- reduction to ammonium (NH_4^+) with CH_4 oxidation (Haroon et al., 2013). Despite abundant documentation of NO_3^- dependent AOM in lab settings and wastewaters, its broader significance in dilute natural environments is largely unknown at this time. However, natural systems rich in NO_3^- with rapid N-cycling, such as freshwater lakes, estuaries and wetlands, should have the potential to oxidize immense amounts of CH_4 through NO_3^- dependent AOM (Joye et al., 1999). Evidence for Fe and Mn dependent CH_4 oxidation is also accruing, and has been proposed to explain geochemical evidence for AOM in freshwater environments in the apparent absence of SO_4^{-2} (Crowe et al., 2008a;Crowe et al., 2011;Lopes et al., 2011;Nordi et al., 2013;Sivan et al., 2011). However, these environmental observations remain unsubstantiated, and AOM in these systems has not been confirmed by process rate measurements or shown through microbial isolation and pure culture laboratory experiments.

Lake Matano, Sulawesi Island, Indonesia, hosts the largest, deepest, and oldest known ferruginous basin on Earth (Crowe et al., 2008a; Crowe et al., 2008b). This system offers a unique opportunity to examine CH_4 biogeochemistry under conditions with very low natural SO_4^{2-} concentrations and an abundant supply of Fe and Mn oxyhydroxides. In general, tropical lakes are understudied by comparison to their temperate counterparts and, therefore, further examination of the CH_4 biogeochemistry in such systems is needed to constrain global CH_4 budgets. Furthermore, with chemistry and physics analogous to those proposed for the Precambrian oceans, Lake Matano also affords opportunities to test models for the marine CH_4 cycle throughout much of Earth's history. To better constrain CH_4 biogeochemistry in Lake Matano, tropical lakes, and ferruginous environments in general, we have determined CH_4 oxidation rates with a suite of oxic and anoxic incubations using ^{14}C labeled CH_4. These rate measurements are interpreted with respect to the availability of oxidants to place constraints on the pathways of CH_4 oxidation throughout the lake.

2. Materials and Methods

2.1 Sampling and general analyses

Samples were retrieved from a deep-water master station (2°28'00''S and 121°17'00''E) (Crowe et al., 2008b) in May 2010. For deep and shallow water sampling (i.e. <100 m or >140 m) 5 L Go-Flow (Niskin; General Oceanics, Miami, FL, USA) bottles were used with a manual winch setup and a Furuno FCV585 sonar device for bottle placement by echolocation, achieving an accuracy and precision of ±1 m. For samples in intermediate depths (i.e.>100 m, <140 m deep), a pump profiling method was used (Jones et al., 2011) in which water was pumped from depth using a double-cone intake (Jørgensen et al., 1979) sampling a thin (<2 cm) horizontal

layer of water. The intake was fastened to a conductivity, temperature, depth (CTD) probe (Sea and Sun Technology), which allowed for very accurate (~10 cm) vertical sample positioning during pumping. A minimum of three tubing volumes of water was flushed through the tubing and pump system before sampling commenced. Oxygen concentrations, conductivity and temperature were determined using the CTD equipped with the following sensor array: Temperature (SST PT100, accuracy ± 0.005 °C, precision ± 0.001 °C), conductivity (SST 7-pole platinum cell, accuracy ± 0.005 mS cm^{-1}, precision ± 0.0001 mS cm^{-1}), O_2 (Oxyguard Ocean (2009), Oxyguard Profile (2010), detection limit ~1% saturation, precision ± 1% saturation), light (LICOR PAR Sensor 193 SA, Accuracy ± 5%, detection limit 0.01 µmol m^{-2} s^{-1}), and turbidity (Seapoint). In addition to the measurements made using the Oxyguard sensors on the CTD, O_2 concentrations were also determined using the classic Winkler titration (detection limit 6 µmol l^{-1}) (APHA, 1985; Rose and Long, 1988). The position of the oxycline was verified independently in pumped water with surface based measurements using potentiometry with Clark-style microelectrodes (Unisense) (detection limit 0.2 µmol l^{-1}), and by voltammetry using Au/Hg amalgam microelectrodes (1 µmol l^{-1}) (Brendel and Luther, 1995)(data not shown). Samples for measurement of Fe^{2+} concentrations were withdrawn directly from the pump stream or the spout of the Niskin bottle and fixed on site with ferrozine reagent, stored refrigerated (4°C), and analyzed by a standard spectrophotometric method (Stookey, 1970; Viollier et al., 2000) within 8 hours. Nitrite and NO_3^- combined, NO_x was determined by chemiluminescnce (Braman and Hendrix, 1989) , and SO_4^{2-} by ion chromatography (Dionex ICS 1500, with an IONpac AS22 anion column and suppressor). Samples for CH_4 concentrations were withdrawn directly from the Niskin bottle spout or pump tubing via a syringe and needle and introduced directly into pre-evacuated serum bottles with thick butyl rubber stoppers, which were poisoned

immediately with 100 µL of concentrated $HgCl_2$ (Crowe et al., 2011) to prevent methanogenesis or CH_4 oxidation. Methane concentrations were measured by gas chromatography (Agilent Technologies Network GC System 6890N), and depending on concentration, using either Thermal Conductivity Detection (TCD) or Flame Ionization Detection (FID).

2.2 Incubations

2.2.1 General incubation setup

Water for incubations was sampled from the lake as described above and transferred directly into 100 ml glass syringes (110 m, 115 m, 120 m and 130 m) or 60 ml plastic syringes (20 m, 39.5 m, 81.7 m, and 105.2 m). Here it is important to note that the glass syringes were used for the sample depths that were evidently anoxic or in the oxic-anoxic transition zone such as the 110 m depth sample. The plastic syringes were used only for oxic depth intervals. All syringes were flushed with three volumes of water from the depth of interest and were filled without gas headspace. The openings of the syringes were closed with long (1.5 inch) 25 gauge needles, which were plugged with high-density butyl rubber stoppers. The O_2 concentration was measured inside the syringes immediately following sampling with a standard Clark-style O_2 electrode, inserting it into the luer-lock opening of the syringe. Oxygen was below detection (250 nmol l^{-1}) in the syringes from depths 110 m through to 130 m.

Radiolabeled CH_4 dissolved in water (2.3-4.5 nCi/incubation, 5-10 µl of 10 µmol l^{-1} CH_4 at an activity of 45.04 Ci mol^{-1}) was injected into the syringes by inserting a long needle into the luer-lock tip of the syringe in order to prevent the introduction of atmosphere. The syringes were closed immediately after the label addition, and a small amount of water was expelled to insure that there were no air bubbles trapped in the needle closure. The syringes were then incubated

under water in the dark at an ambient temperature of ~28°C for 6 to 18 days, with sampling intervals extending from between 30 minutes to several hours initially to several days at the end. Incubation sampling was conducted by removing the rubber stopper on the end of the syringe needle, flushing a small amount of water out of the needle and then inserting the needle into an evacuated 12.5 ml Exetainer containing 1 ml of 4M NaOH. Once the Exetainer pressure was at equilibrium with the syringe (~1 atm), the needle was removed, plugged with the butyl rubber stopper, and the syringe immediately returned to the water bath. At the end of the incubation period, the O_2 concentration was again measured inside the syringe with a Clark-style O_2 electrode. Oxygen was below detection (250 nmol l^{-1}) in the syringes sampled from 110 m through to 130 m. Exetainers were stored upside down and refrigerated at 4°C except during air transport from Indonesia to Denmark.

2.2.2 Oxygen introduction to glass syringes

To estimate the possible introduction of O_2 into the glass syringes by diffusion along the ground glass syringe piston over the incubation period, we computed the O_2 fluxes along the syringe walls. Fluxes were calculated according to Fick's first law:

$$J = D \frac{\partial [O_2]}{\partial x} \quad (1)$$

Where J is the O_2 flux, D is the calculated O_2 diffusivity (2.55386 x10^{-5} cm^2 s^{-1}) (Reid et al., 1977; Wilke and Chang, 1955), $\partial[O_2]$ is the difference in O_2 concentration between the outside and inside of the syringe, and ∂x the distance along the piston from the outside of the syringe to the water inside. The piston glass is ground along the whole length of insertion, increasing the

diffusion path length ∂x every time the piston was pushed further into the syringe when extracting sample (Table S1). The value for $\partial[O_2]$ was set as a constant, assuming water in the syringes was anaerobic and water outside of the syringes was at saturation with respect to the atmosphere (250 µmol l^{-1}). The variable ∂x depended on the volume remaining in the syringe and ranged from 55 to 153 mm, at 100 and 0 ml syringe volume, respectively. The total O_2 flux into the syringes was calculated by the product of J and the area estimated between the piston wall and the inside of the syringe. This area was conservatively estimated, since tolerances for our syringes were not obtainable, by multiplying the available tolerances (0.0065 mm, Northern Technology and Testing®:http://www.nttworldwide.com/docs/specs100ml.pdf) for glass syringes by 30 to yield an area of 21.5 mm^2. Summaries of possible O_2 introduction rates are given in Table S1, S2 and Figure. S1, S2. Introduction of O_2 into the glass syringes could have occurred at a maximum flux of 11.6 nmol m^{-2} s^{-1}, with the potential to oxidize CH_4 at a maximum rate of 215 nmol l^{-1} d^{-1}.

2.2.3 Oxygen introduction to plastic syringes

To estimate the possible O_2 introduction into the plastic syringes over the incubation period, we computed the O_2 fluxes through the plastic syringe walls. These fluxes were also calculated using Fick's first law with O_2 diffusivity through the polyethylene syringes of D = 4.60×10^{-8} cm^{-2} s^{-1} (Trefry and Patterson, 2001). Different initial O_2 concentrations produce different O_2 gradients for each sample depth, which translate to different diffusion rates. The value for $\partial[O_2]$ was set as a constant with the outside of the syringe at saturation with respect to the atmosphere (250 µmol l^{-1}), and the inside of the syringe set at the measured water column $[O_2]$ for the relevant depth intervals. The O_2 concentrations were expected to remain the same

over the duration of the CH_4 oxidation rate measurements owing to low total respiration rates in Lake Matano (SA Crowe, unpublished data). Diffusion path length ∂x was set to 0.1 cm, the wall thickness of the syringe. The total flux into the syringe was calculated by multiplying *F* by the area of the syringe, which varied linearly from 99.66 cm^2 to 29 cm^2, with a full 60 ml and 10 ml of water in the syringe, respectively. Summaries of O_2 introduction into the plastic syringes are provided in the Supplements and ranged from 0.97 μmol d^{-1} (105m, T_o) to 0.11 μmol d^{-1} (20m, T_F).

2.2.4 Measurement of radioactivity

Samples for the oxidation rate measurements were processed according to previously established methods (Iversen and Blackburn, 1981). Methane was flushed out of the Exetainer for 30 minutes at a flow-rate of 17 ml min^{-1}, via two needles, one needle supplying a CH_4 and air carrier gas mix (2 % CH_4) into the Exetainer and the other leading to a copper catalyst housed in a tube furnace, where the CH_4 was oxidized at 850°C. The CO_2 produced was trapped directly in 20 ml scintillation vials filled with 2-phenylethylamine (4 ml) and methanol (4 ml), which has the capacity to capture 2 orders of magnitude more CO_2 than was produced by the CH_4 combustion. Immediately following CO_2 capture, 10 ml of scintillation cocktail (Ultima Gold XR, Packard) was added to the vials, which were vortexed for 1 minute. The samples were then left to stand for 24 hours before they were counted on the scintillation counter (Perkin-Elmer-Tri-Carb 2910 TR). Methane oxidation efficiency tests were performed and resulted in a CH_4 to CO_2 conversion greater than 99.8 % at carrier-gas CH_4 concentrations of 2 %.

To extract the CO_2 from the remaining liquid in the Exetainer, 1-2 drops of bromothymol blue was added to the sample to monitor sample pH, the sample was placed into an Erlenmeyer

flask along with a 20 ml scintillation vial containing a folded fiberglass filter wet with 4ml of 2-phenylethylamine. The Erlenmeyer flask was sealed with a thick butyl rubber stopper through which a long needle was inserted to inject 2ml of hydrochloric acid (6M) into the Exetainer to exsolve the CO_2. The pH was checked visually after 24 hours and the samples were left for a total of 48 hours, to allow the complete exsolution of CO_2 and its effective entrapment on the phenylethylamine soaked filter. The scintillation vials were removed from the Erlenmeyer flasks; 4 ml of methanol was added to dissolve the precipitate, after which 10 ml of scintillation cocktail was added and the entire contents vortexed for 2 minutes. These samples were then left to stand for 24 hours before scintillation counting. To measure the assimilation of ^{14}C carbon from CH_4 during the incubations, 3 ml of the residual fluid from each Exetainer vial was transferred into a scintillation vial and 10 ml of Scintillation cocktail added. The sample was vortexed for 1 minute, after which it stood for 24 hours before counting. Methane oxidation and assimilation were determined from concentrations and activities using Eq. (2) and Eq. (3). Methane oxidation and assimilation rates were then computed as first order rates from the linear portion of the time series with two or more intervals.

$$[CH_{4oxidized}] = [CH_4]\ {}^{14}CO_2/{}^{14}CH_4 \quad (2)$$

$$[CH_{4\ assimilated}] = [CH_4]\ {}^{14}C_{residual}/{}^{14}CH_4 \quad (3)$$

All data used in rate calculations are tabulated in the (Table S3).

3. Results

3.1 Limnology

The physical structure of Lake Matano in 2010 was much the same as previously observed as can be seen from the density and temperature profiles of previous years (Figure 1 and 2) indicating very stable bottom waters but some variance in the upper waters (0-100 m) hence called mixolimnion. During our sampling expedition the lake was stratified with a persistent pycnocline between 110 and 250 m depth, which separates an oxic mixolimnion from a permanently anoxic monimolimnion. This pycnocline is known to move several meters (5-10m) as a result of a seiche (Katsev et al., 2010) in the lake, and its depth exact depth is therefor hard to determine. The mixolimnion exhibits a previously observed seasonal pycnocline (Crowe et al., 2011), which at the time of sampling was at a depth of 30 m. A slow exchange of water across the persistent pycnocline at 110 m depth causes poorly ventilated bottom waters, which was indicated by the exhaustion of O_2 and the accumulation of Fe^{2+}. Fe^{2+} increases to detectable concentrations (0.2 μmol l^{-1}) just below the depth at which O_2 becomes undetectable (1 μmol l^{-1}) at 112-114 m depth (Figure 3). Due to the rapid oxidation kinetics of Fe^{2+} by O_2, it was unlikely that appreciable concentrations of O_2 coexisted with detectable Fe^{2+}, and we thus define the oxic-anoxic boundary as the layer between the deepest depth of detectable O_2 and the shallowest depth at which Fe^{2+} is detected.

Most of the redox active species (Fe^{2+}, Mn^{2+}, SO_4^{2-}, HS^-) followed the classical redox cascade (Canfield and Thamdrup, 2009; Jones et al., 2011): O_2 and Mn^{2+} overlaped slightly (Figure 3a), which can be explained by the sluggish oxidation kinetics of Mn^{2+} with O_2 (Jones et al., 2011; Luther, 2005; Morgan, 2005). Nitrite and NO_3^- (NO_x) accumulated in the lower mixolimnion (Figure 3b), with a maximum concentration of 6 μmol l^{-1} at 111 m. Fe and Mn particulates (Figure 3c) also exhibited peaks in concentration near the pycnocline (Jones et al.,

2011). Fe^{2+} and NH_4^+ (Figure 3a) were both below detection in the surface waters with a sharp increase at the oxic-anoxic boundary, and had constant deep-water concentrations below approximately 250 m depth.

3.2 Oxic Water column

Methane concentrations in the oxic water column were 0.5 μmol l^{-1} and were oversaturated with respect to the atmosphere. Methane consumption during the 20, 39.5 and 81.7 m incubations was negligible (0.53, 0.65, and 0.13 %) for the time interval in which the rates were measured (Table 2). Rates of dissimilatory CH_4 oxidation (CH_4 oxidation), where CH_4 is converted into CO_2, between 20 m and 39.5 m range from (0.2 to 0.43 nmol l^{-1} d^{-1}) in the fully oxygenated mixolimnion (Figure. 4) and remained almost the same at 81.7 m with 0.37 nmol l^{-1} d^{-1}. Rates of CH_4 assimilation into organic matter (CH_4 assimilation) ranged from 0.13 to 2.43 nmol l^{-1} d^{-1} in the mixolimnion, and summing the rates of CH_4 assimilation with the rates of dissimilatory CH_4 oxidation yielded total CH_4 consumption rates (total consumption) of 0.56 to 2.51 nmol l^{-1} d^{-1}. Oxygen concentrations in the upper water column were near saturation with respect to the atmosphere and were above 200 μmol l^{-1}, though O_2 became depleted with increasing depth and concentrations were 138 μmol l^{-1} at 39.5 m and 58.4 μmol l^{-1} at 81.5 m (Table 2).

3.3 Oxic-Anoxic transition layer

Rates of CH4 oxidation within this layer were between 78 nmol l-1 d-1 at 105 m depth and 527 nmol l-1 d-1 at 110 m depth, rates of CH_4 assimilation ranged from 142 nmol l^{-1} d^{-1} to 3640 nmol l^{-1} d^{-1} (105-110 m). Summing the rates of CH_4 assimilation and dissimilatory CH_4 oxidation yielded total CH_4 consumption in the oxic-anoxic transition layer that ranged from 220

nmol l^{-1} d^{-1} to 4160 nmol l^{-1} d^{-1} (Figure 4). Average O_2 concentrations within this layer were less than 3 μmol l^{-1}, whereas CH_4 concentrations ranged from 6.98 μmol l^{-1} at 105 m to 2.70 μmol l^{-1} at 110 m.

3.4 Upper anoxic zone

With 2.6 μmol l^{-1} of Fe^{2+} at 115 m, the upper monimolimnion is strictly anoxic. Rates of CH_4 oxidation in this layer ranged from 5.6 μmol l^{-1} d^{-1}, at 115 m depth, to 50.1 μmol l^{-1} d^{-1}, at 130 m depth. Rates of CH_4 assimilation were 6.3 μmol l^{-1} d^{-1} at 115 m and 67.2 μmol l^{-1} d^{-1} at 130 m. Total CH_4 consumption at these depths was 11.9 μmol l^{-1} d^{-1} at 115 m, and 117.4 μmol l^{-1} d^{-1} at 130 m. Methane concentrations over the 115 to 130 m depth interval ranged from 12 to 484 μmol l^{-1}, NO_x concentrations were 0.06 to 0.5 μmol l^{-1}, Fe and Mn oxyhydroxide concentrations were 95-170 nmol l^{-1} and 1- 361 nmol l^{-1}, respectively. Sulfate concentrations ranged from 0.6 to 19.6 μmol l^{-1} and SO_4^{2-} reduction rates were on the order of 0.93 - 4.73 nmol l^{-1} d^{-1} over the 115 to 130 m depth interval.

4. Discussion

4.1 Oxidation in the oxic water column

Methane oxidation rates from a variety of well-oxygenated environments (>25 μmol l^{-1}) have been compiled (**Error! Reference source not found.**) to provide a comparison to the rates easured in Lake Matano. The upper mixolimnion maintained CH_4 oxidation rates in the lower range compared to other aquatic environments (**Error! Reference source not found.**). The inetics of aerobic microbial CH_4 oxidation are typically described by a Michaelis-Menten model with half-saturation constants for CH_4 typically between 2 and 26 μmol l^{-1} (Buchholz et al., 1995; Harrits and Hanson, 1980; Lidstrom and Somers, 1984; Remsen et al., 1989) and for O_2

0.14 to 21 μmol l^{-1} (Joergensen, 1985; Lidstrom and Somers, 1984). With CH_4 concentrations below K_m values, CH_4 oxidation rates in the mixolimnion were likely limited by CH_4 availability. Though CH_4 concentrations in Lake Matano's mixolimnion were low, raging from 0.5 to 3 μmol l^{-1}, and below typical K_m values for methanotrophs, they are still well above threshold in vitro concentrations (50 to 150 nmol l^{-1})(Schmidt and Conrad, 1993; Whalen et al., 1990) below which CH_4 oxidizing microbes can no longer access dissolved CH_4. High O_2 concentrations (>120 μmol l^{-1}, or >48 % of saturation) are also known to inhibit CH_4 oxidation (Harrits and Hanson, 1980), and thus at 20 m depth CH_4 oxidation may have also been inhibited by as much as 58 % due to high O_2 concentration; however, below 45 m (<120 μmol l^{-1} O_2) inhibition due to O_2 would be unlikely (Harrits and Hanson, 1980).

4.2 Oxidation in the oxic-anoxic transition layer

Rates for CH_4 oxidation at 105 and 110 m (Figure 4), in the oxic-anoxic transition layer, were higher than in the oxic zone. These rates were within the range reported for comparable freshwater systems (**Error! Reference source not found.**). In all systems in Table 1, O_2 concentrations were reported between 2.5-25 μmol l^{-1} and CH_4 concentrations were in the low μmol l^{-1} range. Lake Matano's rates of CH_4 oxidation in the oxic-anoxic transition layer averaged 219 nmol l^{-1} d^{-1}. This is in the low to mid portion of the range observed in other freshwater bodies, which varies 9 orders of magnitude (Table 1). Since both O_2 and CH_4 concentrations were low within the oxic-anoxic transition zone, the rates were likely dictated by the co-availability of O_2 and CH_4. This is supported by laboratory-based studies of CH_4 oxidation kinetics (Buchholz et al., 1995; Harrison, 1973; Joergensen, 1985; Lidstrom and Somers, 1984).

Given the low O_2 concentrations in this depth interval we sought to constrain the possible

Given the low O_2 concentrations in this depth interval we sought to constrain the possible availability of alternative electron acceptors for CH_4 oxidation through a mass balance approach. Based on mass balance considerations, the O_2 present at 105 m was sufficient to support the measured rates. At 110 m depth, O_2 was below the detection limit (0.25 μmol l^{-1}) of our O_2 sensor. Over the time interval of the rate determination 0.114 μmol l^{-1} O_2 would have been sufficient to oxidize the CH_4 consumed, and therefore if 0.25 μmol l^{-1} O_2 was present, yet under the detection limit of our microsensor measurements, this would provide sufficient O_2 (Table 2). Our calculations also suggest rates of O_2 diffusion into the syringe of between $1.16x10^{-6}$ and $4.21x10^{-7}$ μmol cm^{-2} s^{-1}, could have supplied up to 19 % of the total O_2 needed to match the observed CH_4 oxidation. We argue then, that no alternative electron acceptors were needed to support the observed rates of CH_4 oxidation in the oxic-anoxic transition layer. Nevertheless, total CH_4 consumption at the 110 m depth was 0.448 μmol l^{-1}, with 0.391 μmol l^{-1} contributed to assimilation. If, however, assimilated CH_4 was also oxidized during the assimilation process, the O_2 available would not be sufficient to oxidize this CH_4 and other electron acceptors would need to be considered. Measurements for particulate Fe and Mn were not taken at this depth, but if concentrations are similar to samples below and above this depth, combined concentrations should have been between 30 and 300 nmol l^{-1} and can therefore only account for a fraction of the oxidation needed. Sulfate and NO_x were both present in quantities that would satisfy the demand for electron acceptors, but SO_4^{2-} reduction rates of only a few nmol l^{-1} d^{-1} rules out its involvement in CH_4 oxidation of this magnitude, leaving NO_x as the likely electron acceptor at the depth of 110 m.

4.3 Oxidation in the Anoxic Waters

Methane oxidation was also observed in incubations of water from depths (115 m, 120 m and 130 m) below the oxic-anoxic transition zone (Figure. 4). This observation requires us to carefully consider the possible oxidants available. As above, we first consider possible O_2 contamination by diffusion into the syringes, which ranged from $1.16x10^{-6}$ to $7.28x10^{-7}$ μmol O_2 cm^{-2} s^{-1} (Table S1) and can contribute at most 1.86 %, 11.8 % and 0.216 % at 115, 120 and 130 m respectively, to the observed CH_4 oxidization (Table 2). There are several other possible oxidants (SO_4^{2-}, NO_2^-, NO_3^-, Fe^{3+}, Mn^{4+}) for which reactions are given in Table 3. To validate if these electron acceptors are suitable, we have calculated Δ_rG values for each electron acceptor considering the in situ conditions in Lake Matano. The possible Gibbs free energy space defined by substrate concentrations in Lake Matano is marked in green on the graphs in Figure. 5 along with energies calculated specifically for the three anoxic samples at 115, 120 and 130 m depth. The conditions at which the delta ΔG's are -30 and -15 kJ mol^{-1} (Iso-energies) are marked in blue and red identifying the lowest energies necessary for the generation of ATP and energies observed in similar environments known to support microbial growth, respectively (Caldwell et al., 2008; Hoehler et al., 1994; Valentine and Reeburgh, 2000). These boundaries, hence, are the lowest known amounts of energy at which organisms can grow using these metabolic pathways. All electron acceptors considered provide more than this minimum amount of free energy, except for SO_4^{2-}, which is close to the minimum energies (Figure 5).

Concentrations of electron acceptors and their possible contribution to CH_4 oxidation in %, based on the reactions listed in Table 3, are given in Table 2 for each depth. Nitrite and NO_3^- are combined as NO_x, and Fe^{3+} and Mn^{4+} are referred to as Mn_{part} and Fe_{part}, since they generally exist as particles in these oxidation states. The concentrations of available reactive Fe(III) and

Mn(III/IV) were low, approximately 250-530 nmols l^{-1} cumulative between 115 and 120 m and less than 100 nmols l^{-1} at 130 m, compared to the amount of CH_4 oxidation observed, and could only account for up to 7.7, 22.1 and 0.37 %, respectively, of the CH_4 oxidation measured (Table 2). Possible contribution to the oxidation of CH_4 by NO_x is low at 115 m and considerable at 120 m with 7.6 % and 64 %, but decrease to a negligible 0.8 % at the 130 m depth. Sulfate is the only other significant electron acceptor, and it could account for all the CH_4 oxidation observed at these depths, though at 130 m, SO_4^{2-} was below our detection (>250 nmol l^{-1}). At this concentration SO_4^{2-} could only contribute a maximum of 7.5 % to the CH_4 oxidation observed at 130m depth (Table 2). Low SO_4^{2-} reduction rates that were measured at these depths (< 5 nmol l^{-1} d^{-1}) (Figure. 4c) suggests that CH_4 oxidation coupled to SO_4^{2-} reduction alone cannot support the observed rates of AOM between the depths of 115 to 130 m. We are thus left with some uncertainty as to specific electron acceptors involved in CH_4 oxidation at Lake Matano given our inability to constrain the electron mass balance. It is likely, however, that we have underestimated the concentrations of particulate Fe and Mn (Jones et al., 2011). Particles too small to be retained on 0.2 μm filters, for example, may have escaped measurement. Such small particles have been observed in the lake as nano-particulate aggregates containing Fe and Mn using SEM and TEM (Jones et al., 2011; Zegeye et al., 2012) and would be among the most reactive of all the particles in the system. Though O_2 concentrations were measured in the syringes and all were below our DL (250 nmol l^{-1}), O_2 contamination could have occurred during sample handling but evaded detection due to its consumption by Fe^{2+} prior to measurement. For example, if sampling introduced 1-2 μmol l^{-1} O_2 this could have been rapidly consumed through oxidation of Fe^{2+} supplying 4 to 8 μmol l^{-1} additional reactive Fe oxyhydroxides. The large amount of Fe^{+2} and its rapid oxidation by O_2 makes certain that even though O_2 may have been

introduced into the syringes while extracting samples, Fe^{+3} would have been the electron acceptor that oxidized CH_4. Regardless of the uncertainties in available electron acceptors (NO_x, Fe^{3+}, or Mn^{4+}), the potential rates of anaerobic CH_4 oxidation measured are high, even in comparison to rates measured in other fresh (Iversen et al., 1987; Joye et al., 1999) and marine water columns (Wankel et al., 2010).

4.4 CH_4 assimilation

In Lake Matano a large fraction of CH_4 metabolized (up to 87 %) was assimilated (Figure. 6). The fraction of CH_4 carbon assimilated in Lake Matano is indeed as high as values reported in early isolation and characterization laboratory studies (80 % and 47-70 %) (Brown et al., 1964; Vary and Johnson, 1967). Most studies on temperate lakes report that about one-third of the carbon from CH_4 consumption was assimilated with two-thirds oxidized to CO_2 (Hanson, 1980; Harrits and Hanson, 1980; Lidstrom and Somers, 1984; Rudd et al., 1974). For example, the temperate meromictic Lake 120 of the Experimental Lake Area of Northern Ontario (Rudd et al., 1974), which, like Lake Matano, is persistently stratified, exhibited only 36.8 % assimilation. Perhaps because of its physical and chemical similarities, the most appropriate comparison is Lake Tanganyika, which exhibits on average 26 % assimilation (Rudd, 1980)

We suggest that the high percentage of assimilation in Lake Matano may reflect its highly oligotrophic nature. In more productive systems, excess organic carbon is available for growth, and thus most CH_4 carbon is channeled through dissimilation to CO_2 (Rudd, 1980). Anecdotally, carbon assimilation from CH_4 in marine systems is generally higher than in freshwater systems (Ward et al., 1987) and marine systems are typically more oligotrophic than freshwater.

These relative high rates of CH_4 assimilation suggest that CH_4 may be an important source of carbon for biomass in Lake Matano. Though rates of CH_4 assimilation within the surface waters (10 m, 0.2 nmol $l^{-1}d^{-1}$) are small compared to dark carbon fixation rates (14 nmol $l^{-1}d^{-1}$), the deeper anoxic waters exhibit CH_4 assimilation rates of up to 8.2 μmol $l^{-1}d^{-1}$ (120 m) which exceeds dark carbon fixation rates of 0.24 μmol $l^{-1}d^{-1}$ (at 117.5 m) by 34 times, implicating CH_4 assimilation as the largest carbon fixing process within this depth interval. Considering that the oceans were ferruginous throughout most of early earth history and likely very oligotrophic as well, with similar chemistry to Lake Matano (Crowe et al., 2008a), we may be able to extend some of the observations made to early earth oceans. Therefore in the early earth oceans CH_4 may have been a large part of the carbon cycle and played an important role as a carbon source for microbial growth and primary production. This greater significance of methane in primary production must be considered when investigating stable carbon isotope signatures of carbon buried during these eons. Iron and Mn reduction instead of SO_4 reduction (as it is primarily the case in todays oceans) may have been driving the anaerobic oxidation of CH_4 in the early oceans.

5. Conclusions

Despite the accumulation of CH_4 to relatively high concentrations in Lake Matano's deep monimolimnion, much of this CH_4 is oxidized directly within the lake, precluding strong CH_4 fluxes to the atmosphere. Lake Matano, truly, supports relatively high rates of CH_4 oxidation with some CH_4 apparently oxidized anaerobically (for example, rates of oxidation up to 5.6 μmol CH_4 l^{-1} d^{-1} occur at 115 m depth in the apparent absence of O_2). Alternative electron acceptors that may support measured AOM include NO_x, the oxidized forms of Fe and Mn, and SO_4^{2-}.

Measured rates of SO_4^{2-} reduction are, however, too low to support the measured rate of CH_4 oxidation, therefore we favor NO_x, and oxidized Fe and Mn as the likely electron acceptors. Lake Matano also exhibits unusually high rates of CH_4 assimilation, likely related to its oligotrophic nature. Regardless, such high rates of assimilation and oxidation implicate CH_4 as an important carbon and energy source for microbial growth in Lake Matano. By extension to other oligotrophic ferruginous environments, CH_4 was likely an important contributor to microbial metabolisms in Earth's ferruginous Precambrian oceans.

Acknowledgements:

I thank Alfonso Mucci and Bjørn Sundby, for inspiring discussions, D. Rahim, and S. Rio are acknowledged for sampling and logistical support in Indonesia. B. Thamdrup for lending a tube furnace for CH_4 combustions. The authors are grateful to PT-INCO Tbk for in kind support. The Danish National Research Foundation provided funding for C.J., S.A.C., and D.E.C.. A.S, and D.A.F. were supported by the National Science Foundation grant EAR-0844250.

References:

APHA, 1985. Standard Methods for the Examination of Water and Waste Water, Washington, DC, pp. 413-426.

Boetius, A. et al., 2000. A marine microbial consortium apparently mediating anaerobic oxidation of methane. Nature, 407(6804): 623-626.

Braman, R.S., Hendrix, S.A., 1989. Nanogram Nitrite and Nitrate Determination in Environmental and Biological-Materials by Vanadium(III) Reduction with Chemi-Luminescence Detection. Analytical Chemistry, 61(24): 2715-2718.

Brendel, P.J., Luther, G.W., 1995. Development of a Gold Amalgam Voltammetric Microelectrode for the Determination of Dissolved Fe, Mn, O-2, and S(-Ii) in Porewaters of Marine and Fresh-Water Sediments. Environmental Science & Technology, 29(3): 751-761.

Brown, L.R., Strawinski, R.J., McCleskey, C.S., 1964. Isolation + Characterization Of Methanomonas Methanooxidans Brown + Strawinski. Canadian Journal of Microbiology, 10(5): 791-&.

Buchholz, L.A., Valklump, J., Collins, M.L.P., Brantner, C.A., Remsen, C.C., 1995. Activity of Methanotrophic Bacteria in Green-Bay Sediments. FEMS Microbiology Ecology, 16(1): 1-8.

Caldwell, S.L. et al., 2008. Anaerobic oxidation of methane: Mechanisms, bioenergetics, and the ecology of associated microorganisms. Environmental Science & Technology, 42(18): 6791-6799.

Canfield, D.E., Thamdrup, B., 2009. Towards a consistent classification scheme for geochemical environments, or, why we wish the term 'suboxic' would go away. Geobiology, 7(4): 385-392.

Cicerone, R.J., Oremland, R.S., 1988. Biogeochemical aspects of atmospheric methane. Global Biogeochem. Cycles, 2(4): 299-327.

Conrad, R., 2009. The global methane cycle: recent advances in understanding the microbial processes involved. Environmental Microbiology Reports, 1(5): 285-292.

Crowe, S.A. et al., 2008a. Photoferrotrophs thrive in an Archean Ocean analogue. Proceedings of the National Academy of Sciences of the United States of America, 105(41): 15938-15943.

Crowe, S.A. et al., 2011. The methane cycle in ferruginous Lake Matano. Geobiology, 9(1): 61-78.

Crowe, S.A. et al., 2008b. The biogeochemistry of tropical lakes: A case study from Lake Matano, Indonesia. Limnology and Oceanography, 53(1): 319-331.

Devol, A.H., Anderson, J.J., Kuivila, K., Murray, J.W., 1984. A Model for Coupled Sulfate Reduction and Methane Oxidation in the Sediments of Saanich Inlet. Geochimica Et Cosmochimica Acta, 48(5): 993-1004.

Hanson, R.S., 1980. Ecology and Diversity of Methylotrophic Organisms. In: Perlman, D. (Ed.), Advances in Applied Microbiology. Academic Press, pp. 3-39.

Haroon, M.F. et al., 2013. Anaerobic oxidation of methane coupled to nitrate reduction in a novel archaeal lineage (vol 500, pg 567, 2013). Nature, 500(7468): 567-570.

Harrison, D.E.F., 1973. Studies on the Affinity of Methanol- and Methane-utilizing Bacteria for their Carbon Substrates. Journal of Applied Microbiology, 36(2): 301-308.

Harrits, S.M., Hanson, R.S., 1980. Stratification Of Aerobic Methane-Oxidizing Organisms In Lake Mendota, Madison, Wisconsin. Limnology and Oceanography, 25(3): 412-421.

Hoehler, T.M., Alperin, M.J., Albert, D.B., Martens, C.S., 1994. Field And Laboratory Studies Of Methane Oxidation In An Anoxic Marine Sediment - Evidence For A Methanogen-Sulfate Reducer Consortium. Global Biogeochemical Cycles, 8(4): 451-463.

Iversen, N., Blackburn, T.H., 1981. Seasonal Rates Of Methane Oxidation In Anoxic Marine-Sediments. Applied and Environmental Microbiology, 41(6): 1295-1300.

Iversen, N., Oremland, R.S., Klug, M.J., 1987. Big Soda Lake (Nevada) .3. Pelagic Methanogenesis And Anaerobic Methane Oxidation. Limnology and Oceanography, 32(4): 804-814.

Joergensen, L., 1985. The Methane Mono-Oxygenase Reaction System Studied Invivo By Membrane-Inlet Mass-Spectrometry. Biochemical Journal, 225(2): 441-448.

Jones, C. et al., 2011. Biogeochemistry of manganese in ferruginous Lake Matano, Indonesia. Biogeosciences, 8(10): 2977-2991.

Jørgensen, B.B., Kuenen, J.G., Cohen, Y., 1979. Microbial Transformations Of Sulfur-Compounds In A Stratified Lake (Solar Lake, Sinai). Limnology and Oceanography, 24(5): 799-822.

Joye, S.B., Connell, T.L., Miller, L.G., Oremland, R.S., Jellison, R.S., 1999. Oxidation of ammonia and methane in an alkaline, saline lake. Limnology and Oceanography, 44(1): 178-188.

Katsev, S. et al., 2010. Mixing and its effects on biogeochemistry in the persistently stratified, deep, tropical Lake Matano, Indonesia. Limnology and Oceanography, 55(2): 763-776.

Kroeger, K.F., di Primio, R., Horsfield, B., 2011. Atmospheric methane from organic carbon mobilization in sedimentary basins - The sleeping giant? Earth-Science Reviews, 107(3-4): 423-442.

Lidstrom, M.E., Somers, L., 1984. Seasonal Study of Methane Oxidation in Lake Washington. Applied and Environmental Microbiology, 47(6): 1255-1260.

Luther, G.W., 2005. Manganese(II) oxidation and Mn(IV) reduction in the environment - Two one-electron transfer steps versus a single two-electron step. Geomicrobiology Journal, 22(3-4): 195-203.

Martens, C.S., Berner, R.A., 1974. Methane Production In Interstitial Waters Of Sulfate-Depleted Marine Sediments. Science, 185(4157): 1167-1169.

Morgan, J.J., 2005. Kinetics of reaction between O-2 and Mn(II) species in aqueous solutions. Geochimica Et Cosmochimica Acta, 69(1): 35-48.

Reeburgh, W.S., 1980. Anaerobic Methane Oxidation - Rate Depth Distributions In Skan Bay Sediments. Earth and Planetary Science Letters, 47(3): 345-352.

Reeburgh, W.S., 2007. Oceanic methane biogeochemistry. Chemical Reviews, 107(2): 486-513.

Reid, R.C., Sherwood, T.K., Prausnitz, J.M., 1977. The Properties of Gases and Liquids. McGraw-Hill, New York.

Remsen, C.C., Minnich, E.C., Stephens, R.S., Buchholz, L., Lidstrom, M.E., 1989. Methane Oxidation in Lake-Superior Sediments. Journal of Great Lakes Research, 15(1): 141-146.

Rose, S., Long, A., 1988. Dissolved-Oxygen Systematics In The Tucson Basin Aquifer. Water Resources Research, 24(1): 127-136.

Rudd, J.W.M., 1980. Methane Oxidation In Lake Tanganyika (East-Africa). Limnology and Oceanography, 25(5): 958-963.

Rudd, J.W.M., Hamilton, R.D., Campbell, N.E., 1974. Measurement Of Microbial Oxidation Of Methane In Lake Water. Limnology and Oceanography, 19(3): 519-524.

Schmidt, U., Conrad, R., 1993. Hydrogen, Carbon-Monoxide, and Methane Dynamics in Lake Constance. Limnology and Oceanography, 38(6): 1214-1226.

Sloan, L.C., Walker, J.C.G., Moore, T.C., Rea, D.K., Zachos, J.C., 1992. Possible Methane-Induced Polar Warming in the Early Eocene. Nature, 357(6376): 320-322.

Stookey, L.L., 1970. Ferrozine - a New Spectrophotometric Reagent for Iron. Analytical Chemistry, 42(7): 779-781.

Trefry, M.G., Patterson, B.M., 2001. An experimental determination of the effective oxygen diffusion coefficient for a high density polypropylene geomembrane, PO Wembly WA 6913, Australia.

Valentine, D.L., Reeburgh, W.S., 2000. New perspectives on anaerobic methane oxidation. Environmental Microbiology, 2(5): 477-484.

Vary, P.S., Johnson, M.J., 1967. Cell Yields Of Bacteria Grown On Methane. Applied Microbiology, 15(6): 1473-1478.

Viollier, E., Inglett, P.W., Hunter, K., Roychoudhury, A.N., Van Cappellen, P., 2000. The ferrozine method revisited: Fe(II)/Fe(III) determination in natural waters. Applied Geochemistry, 15(6): 785-790.

Wankel, S.D. et al., 2010. New constraints on methane fluxes and rates of anaerobic methane oxidation in a Gulf of Mexico brine pool via in situ mass spectrometry. Deep-Sea Research Part Ii-Topical Studies in Oceanography, 57(21-23): 2022-2029.

Ward, B.B., Kilpatrick, K.A., Novelli, P.C., Scranton, M.I., 1987. Methane Oxidation and Methane Fluxes in the Ocean Surface-Layer and Deep Anoxic Waters. Nature, 327(6119): 226-229.

Whalen, S.C., Reeburgh, W.S., Sandbeck, K.A., 1990. Rapid Methane Oxidation in a Landfill Cover Soil. Applied and Environmental Microbiology, 56(11): 3405-3411.

Wilke, C.R., Chang, P., 1955. Correlation of diffusion coefficients in dilute solutions. AIChE Journal, 1(2): 264-270.

Zeebe, R.E., Zachos, J.C., Dickens, G.R., 2009. Carbon dioxide forcing alone insufficient to explain Palaeocene-Eocene Thermal Maximum warming. Nature Geoscience, 2(8): 576-580.

Zegeye, A. et al., 2012. Green rust formation controls nutrient availability in a ferruginous water column. Geology.

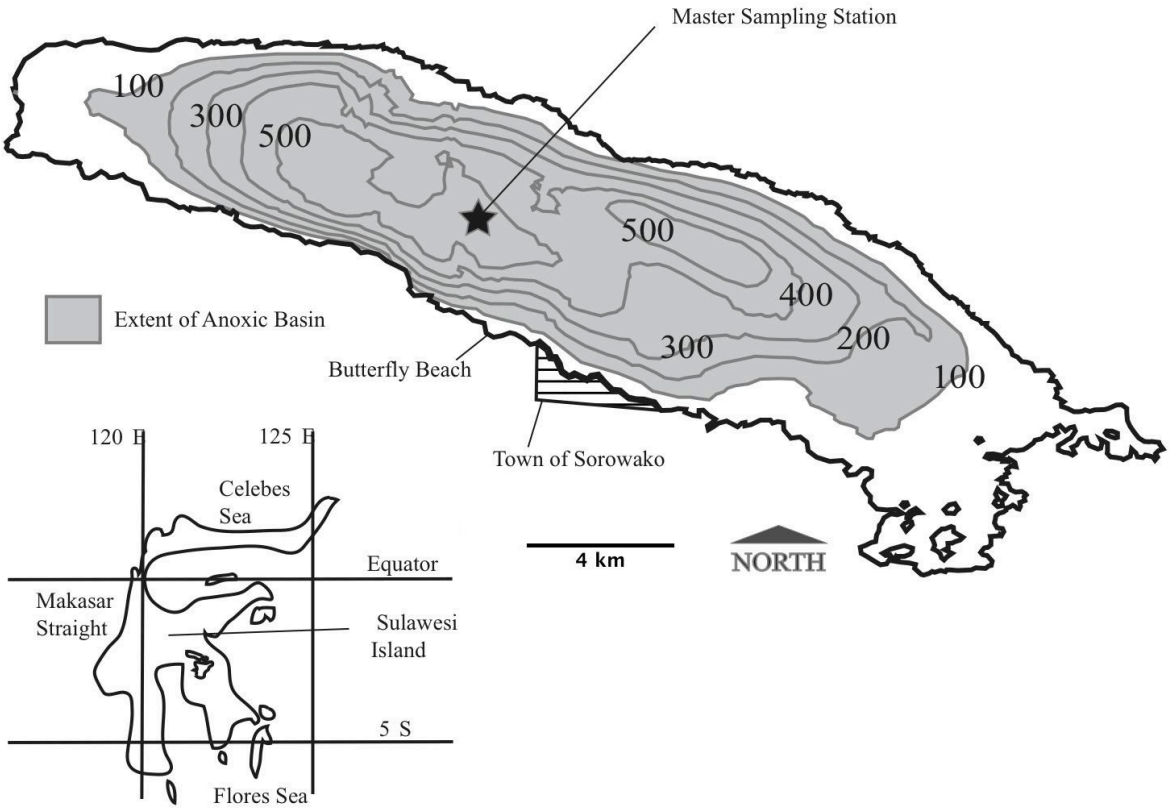

Figure 1 Map of Lake Matano bathymetry the extent of the anoxic basin is shaded and the location of the deep water master sampling station and the town of Sorowako are indicated (modified after Crowe et al.,2008).

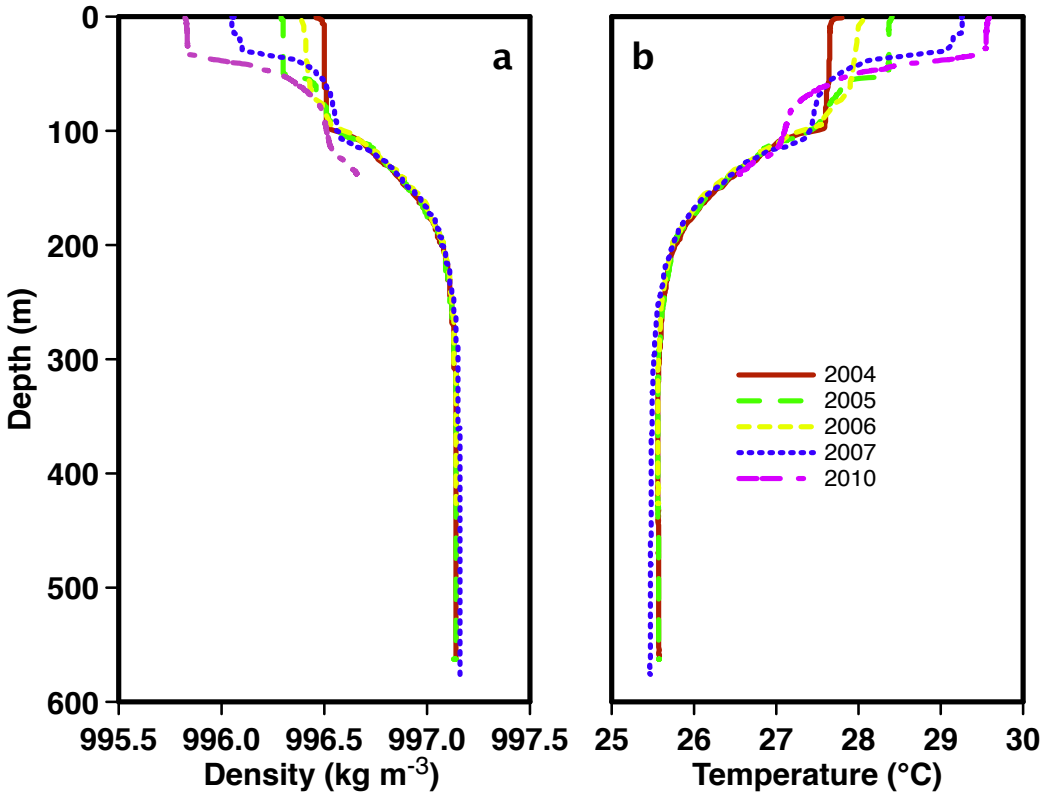

Figure 2 Multi-year density (a) and temperature (b) profiles for Lake Matano.

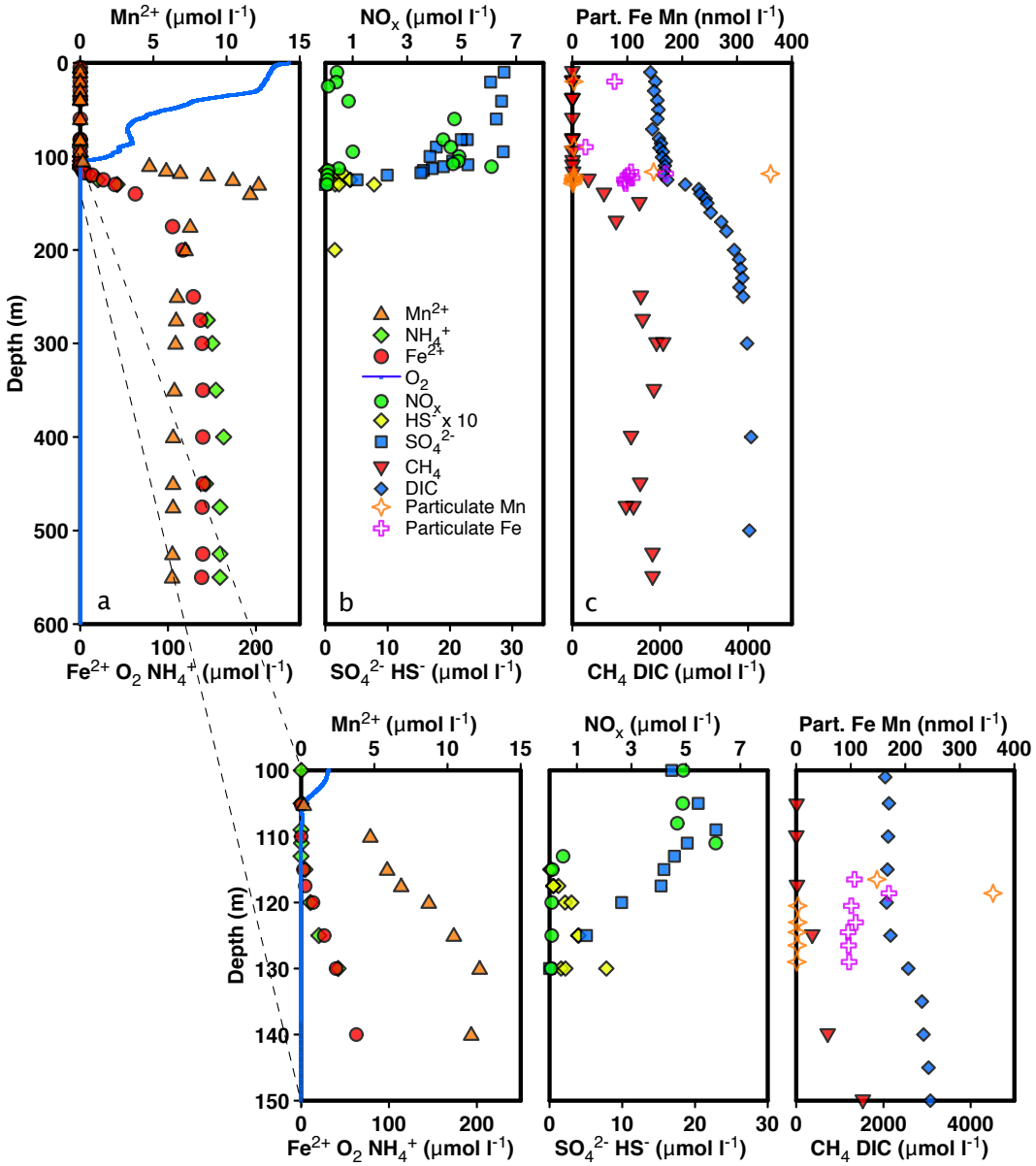

Figure 3 Lake Matano profiles for a: O_2, (CTD), aqueous Fe(II), Mn(II) and NH_4^+ b: aqueous NO_x, HS^- and SO_4^{2-}, and c: dissolved gases CH_4, DIC, particulate Fe and Mn (Jones et al. 2011).

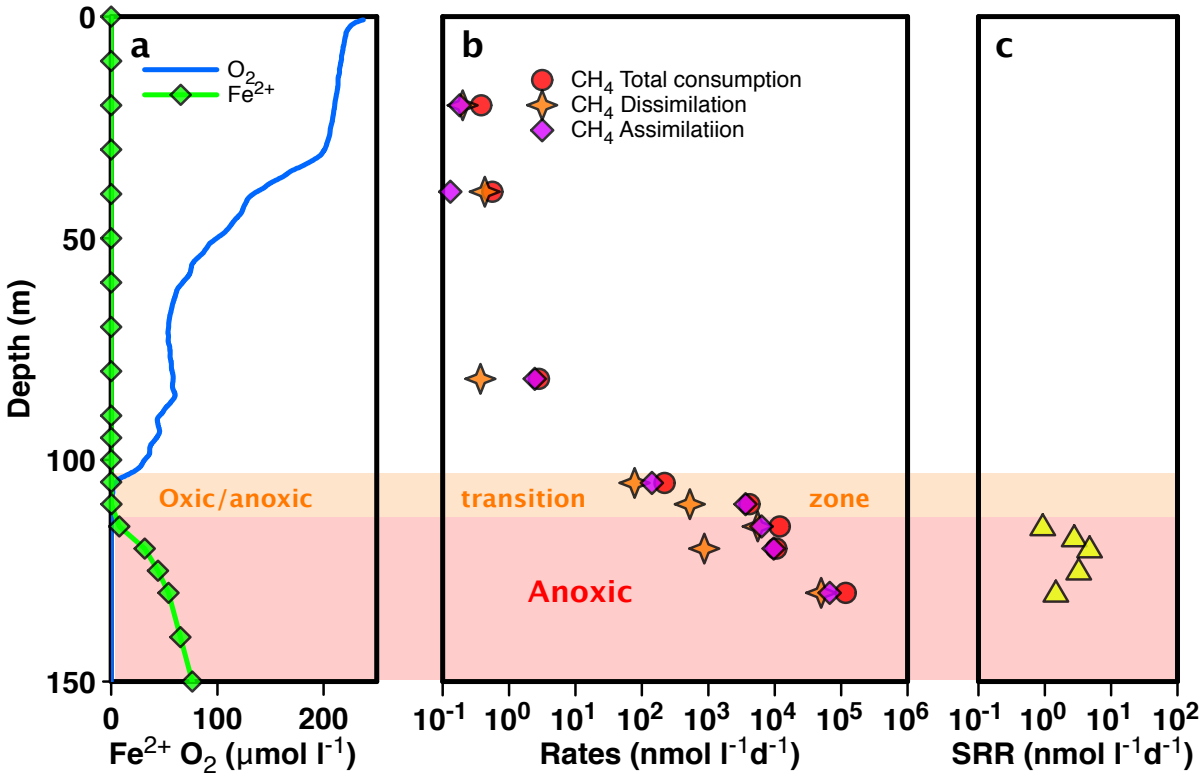

Figure 4 Dissolved biogeochemically active elements and process measurements as a function of depth a: dissolved Fe^{2+} and O_2; b: Rates of production of CO_2 (dissimilatory CH_4 oxidation), CH_4 assimilation and total methane consumption during the experiment; c: sulfate reduction rates.

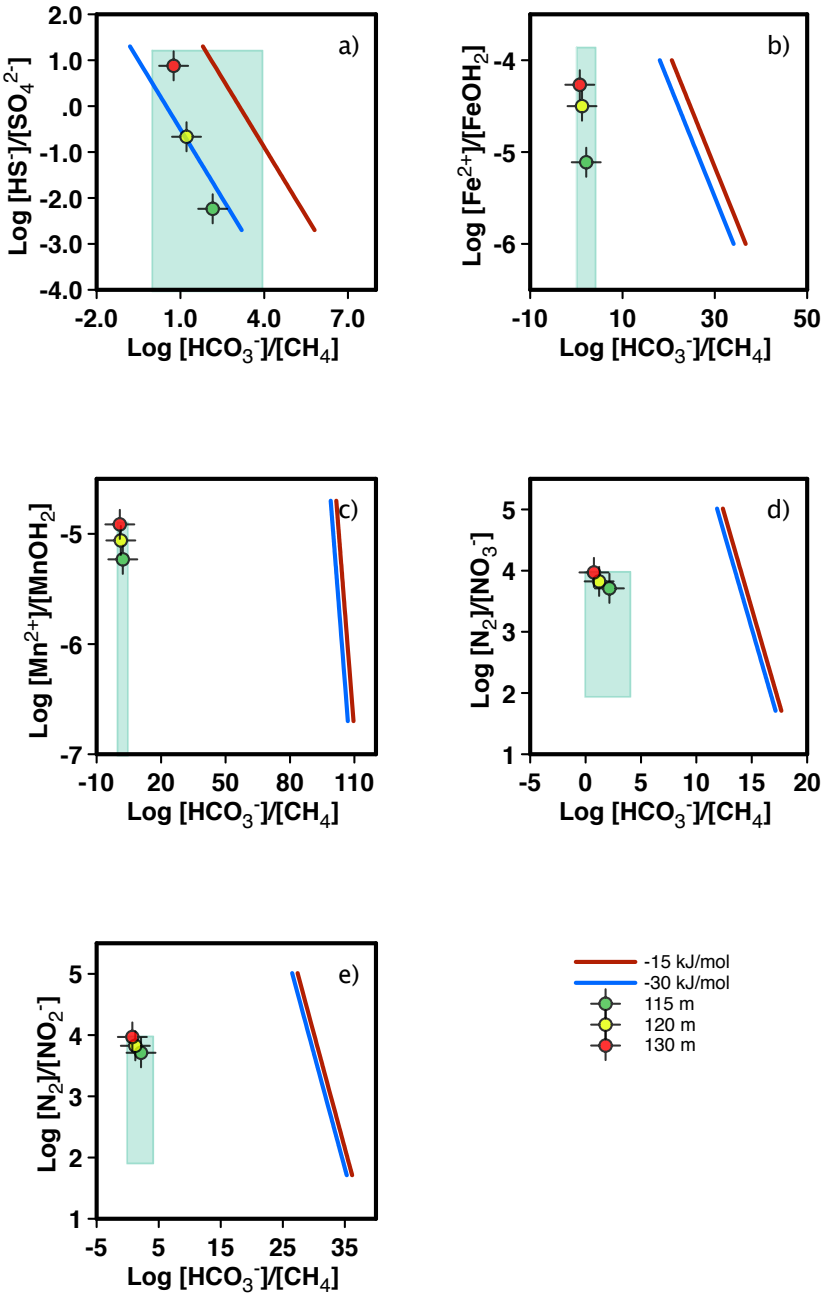

Figure 5 The plots show the energy availability at different concentrations of substrates and products for each reaction. The green areas show the range of substrate and product concentrations of Lake Matano, added are the specific anaerobic depth (115, 120, 130m) at which our experiments were conducted. The "Iso-energy" lines show that all proposed pathways of methane oxidation are favorable except for a) (SO_4^{2-}), where the Δ_rG values are very close to the previously proposed minimum values of -15 kJ mol^{-1} for cell survival.

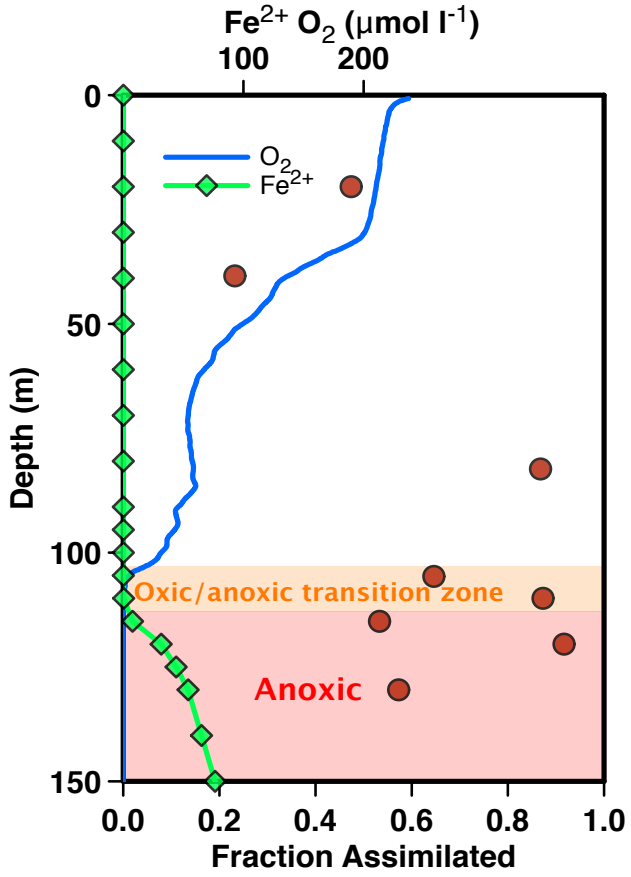

Figure 6 Fraction of CH_4 consumed through assimilation during the incubations (based on first order rate kinetics).

Lake / Reservoir	Oxidation rate μmol $l^{-1}d^{-1}$ Oxic / Oxic-Anaerobic transition / Anaerobic	Source
Lake Mendota (Madison, Wisconsin)	28.8 / 4.8 / 5.8	Harrits and Hanson, 1980
Lake Kivu, (Africa)	0.48 / 0.43 / 0.89	Jannasch, 1975
ELA, (Nothern Ontario)	72 / 890	Rudd and Hamilton, 1975
Lake Pavin, (France)	0.006-0.046 / - / 0.4	Lopes et al., 2011
Lake Kasumigaura, (Japan)	- / 0.12 / -	Utsumi et al., 1998a
Lake Nojiri, (Japan)	- / 17 / -	Utsumi et al., 1998b
Lake Erie, (USA, Canada)	- / 3.84 / -	Howard et al., 1971
Big Soda Lake (Nevada)	0.0013 / 0.01 / 0.064	Iversen et al., 1987
Mono Lake, (California)	0.04-3.8 / 0.5-37 /48-85 nM d-1	Joye et al., 1999
ELARP pond, FLUDEX reservoirs (ELA)	(360-1200)	Venkiteswaran and Schiff, 2005
Petit-Saut Reservoir, (Brazil)	1600 / - / -	Guerin and Abril, 2007
Lake 120 and 227 (ELA, Nothern Ontario)	1.3 / - / 0.49	Rudd et al., 1974
Lake Tanganyika, (Arfrica)	0.1-0.96 / 0.17-1.8 / 0.24-1.8	Rudd, 1980
Lillsjoen lake, (Sweden)	0.33 / 0.01 / -	Bastviken et al., 2002
Marn lake, (Sweden)	0.81 / 2.17 / 2.2	Bastviken et al., 2002
Illersjoen lake, (Sweden)	- / - / 1.3-3	Bastviken et al., 2002
Lake Kevätön, (Finland)	27 / - / -	Liikanen et al., 2002
Lake Matano (Sulawesi, Indonesia)	$3x10^{-4}$-$3.8x10^{-2}$ / 2.1 / 4.7-181	This Study
Brine pool (Gulf of Mexico)	- / - / 3.5	Wankel et al., 2010
Cariaco Basin, (Pacific)	$1x10^{-7}$ / $1x10^{-6}$ / $4x10^{-4}$	Ward et al., 1987
Black Sea	- / $1x10^{-6}$ / $1.64x10^{-3}$	Kessler et al., 2006
Lake Spirit, (Oregon)	0.144 / 0.065 / -	Lilley et al., 1988
Hudson River, (New York)	$4x10^{-6}$ – $6x10^{-4}$ / - / -	Deangelis and Scranton, 1993

Table 1 Methane oxidation rates complied from a variety of global aquatic settings. Values in brackets have uncertainties with respect to oxygen concentrations during measurements.

Incubation Depth (m)	Conc. in µmol l^{-1} (%) contribution to CH_4 oxidation					Max O_2 diffusion into Syringes in µmol l^{-1}, O_2 increase wrt background conc. [%] and its CH_4 oxidation Potential (%)	CH_4 converted to CO_2/CH_4 total nmol l^{-1} (%)
	Fe_{part}	Mn_{part}	SO_4^{-2}	NO_3^- & NO_2^-	O_2		
20	0.077 (452)	0.003 (35.2)	26.52 (1.25E6)	0.4 (9.4E3)	210.5 (4.94E6)	45 [22] (1.06E6)	2.13/3.84; (0.30/0.53)
39.5	no Data	0.003 (15.8)	28.28 (5.95E5)	0.85 (9.0E3)	137.2 (1.44E6)	129 [94] (1.35E6)	4.59/5.98; (0.50/0.65)
81.7	no Data	0.003 (197.4)	24.75 (6.5E6)	4.32 (5.7E5)	58.4 (7.68E6)	13 [23] (1.79E6)	0.38/2.56; (0.02/0.13)
105	no Data	no Data	20.44 (8.7E4)	4.88 (1.0E4)	4.4 (9.4E3)	5 [114] (1.07E4)	23.5/66.2; (0.36/1.01)
110	no Data	No Data	18.93 (3.3E4)	5.39 (4.8E3)	0.25 (2.2E2)	0.022 [2.2] (19.4)	56.7/448; (2.1/16.6)
115	0.107 (2.03)	0.148 (5.62)	31.55 (4.8E3)	0.1 (7.6)	0 (0.00)	0.024 [-] (1.86)	648/1408; (7.1/15.2)
120	0.101 (20.9)	0.003 (1.24)	9.91 (1.6E04)	0.077 (64)	0 (0.00)	0.014 [-] (11.8)	60.5/732; (0.05/0.61)
130	0.097 (0.36)	0.001 (0.008)	0.25 (7.5)	0.055 (0.83)	0 (0.00)	0.014 [-] (0.216)	3330/7092; (0.63/1.47)

Table 2 Availability of redox species in the incubation syringe in µmol l^{-1}, "oxidation potential (%)" is the potential contribution of each redox species towards oxidizing CH_4 to CO_2. Maximum O_2 introduction into syringes by diffusion and its possible increase of O_2 content compared to background in [%] and how much this amount of O_2 could have been part in the observed methane oxidation (%). Methane oxidation to CO_2 during the incubation is displayed in nmol l^{-1} and as % of total Methane available, along with total methane consumed.

Reaction	$\Delta G^{0'}$ in kJ mol^{-1} CH_4	Reference
$5CH_4 + 8NO_3^- + 8H^+ \rightarrow 5CO_2 + 4N_2 + 14H_2O$	-765	Raghoebarsing et al., 2006
$3CH_4 + 8NO_2^- + 8H^+ \rightarrow 3CO_2 + 4N_2 + 10H_2O$	-928	Raghoebarsing et al., 2006
$CH_4 + 8Fe(OH)_3 + 15H^+ \rightarrow HCO_3^- + 8Fe^{2+} + 21H_2O$	-572.2	Crowe et al., 2011
$CH_4 + 4MnO_2 + 7H^+ \rightarrow HCO_3^- + 4Mn^{2+} + 5H_2O$	-789.9	Crowe et al., 2011
$CH_4 + SO_4^- \rightarrow HCO_3^- + HS^- + H_2O$	-20 to -30	Boetius et al., 2000; Valentine et al., 2000

Table 3 Mass action equations and their corresponding Gibbs Free energy (ΔG°) of reaction at 298.15 K for demonstrated and theoretical AOM pathways.

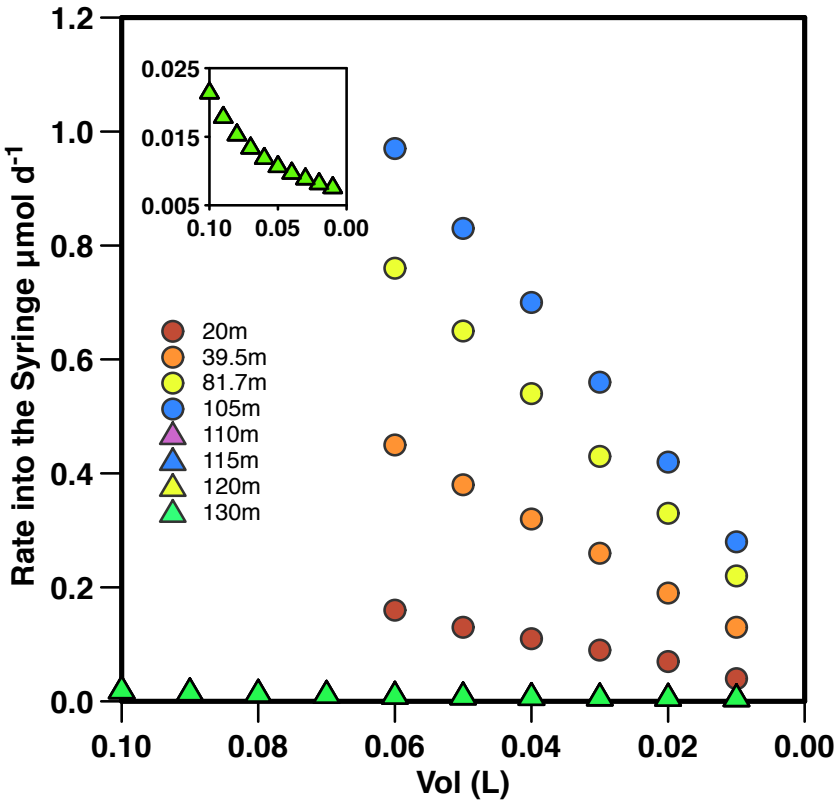

Figure S1 Rate at which O_2 leaks into the syringes vs. syringe volume, plastic syringes in (circles) and glass syringes in (triangles). Glass syringes have all identical rates since they all have the same initial concentration.

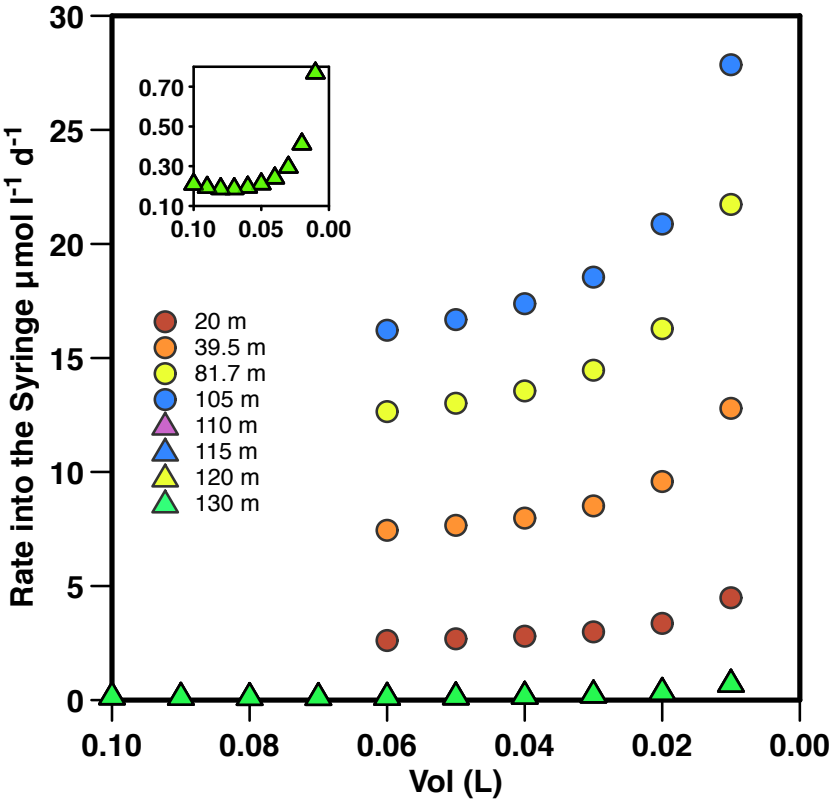

Figure S2 Rate of concentration change in the syringes due to diffusion into them vs. syringe volume, plastic syringes in (circles) and glass syringes in (triangles). Glass syringes have all identical rates concentration change since they all have the same initial concentration.

Sampling interval Depth 20m for Plastic Glass =all	Syringe type	Surface Area (cm^2)	Diffusion Path length dx (mm)	Diffusion rate into syringe ($\mu mol\ s^{-1}$)	Diffusive flux ($\mu mol\ cm^{-2}\ s^{-1}$)
T1	plastic	99.7	1.0	1.82E-6	1.82E-8
T2	plastic	85.4	1.0	1.56E-6	1.82E-8
T3	plastic	71.2	1.0	1.30E-6	1.82E-8
T4	plastic	57.0	1.0	1.04E-6	1.82E-8
T1	glass	0.215	55.0	2.49E-7	1.16E-6
T2	glass	0.215	65.9	2.08E-7	9.69E-7
T3	glass	0.215	76.8	1.78E-7	8.32E-7
T4	glass	0.215	87.6	1.57E-7	7.28E-7

Table S1 Variables related to O2 diffusion calculation into the Syringes are listed. Many of the variables are changing with sampling interval (Time), when assessing the diffusive fluxes into the glass and plastic syringes during incubations.

Depth (m)	Syringe type	Ambient O_2 concentration ($\mu mol\ l^{-1}$)	O_2 concentration differential $d_o = (O_{2\ sat}-O_{2\ syr})/1000$ ($\mu mol\ cm^{-3}$)	Diffusive O_2 Flux at T_0 ($\mu mol\ cm^{-2}\ s^{-1}$)	Average Diffusion Rate into Syringe ($\mu mol\ l^{-1}\ d^{-1}$)	Maximum reachable O_2 concentration ($\mu mol\ l^{-1}$)
20	plastic	210.5	0.0396	1.82E-8	2.7	250
39.5	plastic	137.8	0.1128	5.19E-8	7.8	250
81.7	plastic	58.4	0.1916	8.81E-8	13.4	72
105	plastic	4.9	0.2456	1.13E-7	16.7	9.4
110	glass	<2.5	0.250	1.1E-4	0.2	2.2E-2
115	glass	anoxic	0.250	1.1E-4	0.2	2.4E-2
120	glass	anoxic	0.250	1.1E-4	0.2	1.4E-2
130	glass	anoxic	0.250	1.1E-4	0.2	1.4E-2

Table S2 Values for diffusion coefficient and average values for the diffusive flux, average diffusion rate into the syringes and final accumulated concentration due to diffusion are given for the glass and plastic syringes used in the incubations.

Depth	Incubation Time (days)	$[CH_4]$ µmol l^{-1}	Initial DPM CH_4	Assimilation DPM	CO^2 DPM	Carbon Assimilated (nmol l^{-1})	CO_2 Produced (nmol l^{-1})	Total Methane consumed (nmol l^{-1})
20m	0	-	4523	0	0	0.00	0.00	0.00
	2.96	0.22	4523	-3.56	-2.03	-0.17	-0.10	-0.27
	10.65	0.43	4523	18.42	18.34	1.74	1.73	3.47
39m	0	-	4339	0	0	0.00	0.00	0.00
	2.98	0.16	4339	38.37	53.28	1.38	0.00	1.38
	10.68	0.22	4339	32.50	94.66	1.63	4.75	6.38
81.7m	0	-	10189	0	0	0.00	0.00	0.00
	0.01	0.16	10189	38.65	-3.19	0.62	-0.05	0.57
	0.30	0.22	10189	42.96	0.07	0.94	0.00	0.94
	1.02	0.21	10189	44.22	17.11	0.90	0.35	1.25
105m	0	4.61	12680	0	0	0.00	0.00	0.00
	0.01	4.23	12680	67.80	6.62	22.63	2.21	24.83
	0.30	4.06	12680	165.05	75.49	52.85	24.17	77.03
110m	0	21.48	6090	0	0	0.00	0.00	0.00
	0.03	20.32	6090	45.53	5.95	151.93	19.87	171.80
	0.11	24.32	6090	99.77	14.34	398.36	57.25	455.61
115m	0	53.68	5310	0	0	0.00	0.00	0.00
	0.05	57.72	5310	32.20	7.08	350.01	76.93	426.94
	0.12	75.62	5310	52.80	45.12	751.88	642.44	1394.32
120m	0	125.27	5466	0	0	0.00	0.00	0.00
	0.02	144.16	5466	21.21	2.29	559.45	60.31	619.76
	0.07	134.73	5466	29.63	2.74	730.26	67.60	797.86
130m	0	432.36	5938	0	0	0.00	0.00	0.00
	0.02	369.35	5938	27.95	45.48	1738.48	2828.86	4567.34
	0.06	1405.75	5938	17.43	14.21	4125.75	3364.46	7490.20

Table S3 Data used with Eq. 2 and 3 to calculate metabolic activity and carbon assimilation during incubations, from which time series then the 1st order rates of Fig. 4 were determined.

Chapter 3: Constraining the Carbon and Hydrological Cycles of Lake Matano, Indonesia

Abstract:

Lake Matano, Indonesia, is one of the Earth's largest known ferruginous aquatic ecosystems, where more than 50% of the organic matter produced in this system is thought be respired through methanogenesis, despite high concentrations of Fe (hydr)oxides available for reduction in the lake. In order to elucidate quantitatively the extent the carbon cycle of the lake is dominated by the production and consumption of methane, I developed a holistic model for the hydrological cycling of the lake using oxygen isotopes and Barium, as a tracer for groundwater influx into the lake. The two different approaches in the model were found to be consistent with each other and with previous studies of portions of this hydrological cycle and lake dynamics. The permanently stratified nature of the lake simplifies mass balance calculations, and together with my modeling approach made it possible to successfully develop the first proper mass balance for carbon in this system. Providing a conceptual model through the use of stable carbon isotopes on the production and consumption of DIC, CH_4 and particulate organic matter (POM) throughout the lake. This work showed clearly that carbon flow in this system is acutely different from other aquatic settings with methanogenesis and methanotrophy playing a dominant role in carbon cycle, in contrast to the typical photosynthetic production and respiration of autochthonous and allochthonous carbon. Lake Matano has been identified as one

of the best analogs for ferruginous Precambrian oceans. As such the possible changes in isotope carbon signatures resulting from intense recycling of Methane in the closely coupled carbon cycle of Lake Matano have to be considered when interpreting the biogeochemistry and redox proxies of ferruginous environments and by extension ancient oceans.

1. Introduction

The unique physical and chemical characteristics of Lake Matano, Indonesia has made it one of the most intensely studied early ocean analogues (Crowe et al., 2008a; Crowe et al., 2011; Crowe et al., 2014; Crowe et al., 2008b; Crowe et al., 2007; Jones et al., 2011; Katsev et al., 2010; Kuntz et al., 2015; Wicaksono et al., 2015; Zegeye et al., 2012). Specifically its low sulfate concentrations, its high aqueous iron content, and its general oligotrophic nature, mimic Proterozoic and Archean ocean biogeochemistry (Crowe et al., 2008a).

Initial studies of the lake system were prompted by concerns of high methane and carbon dioxide concentrations in the bottom waters of the lake, which in turn would make it a possible environmental threat in the case of a turnover and degassing event, similar to Lake Monoun and Lake Nyos in the 1980's (Kling et al., 1989; Kusakabe et al., 1989; Sigurdsson et al., 1987). In the events that occurred at these lakes, dissolved gasses (mainly CO_2) in the water columns were high or over saturated. The gas release, killing people and livestock in the area around the lake, was likely triggered by some common event such as internal seiches or mixing. However, calculations for Lake Matano by (Crowe et al. 2011) have established that total partial pressures of CO_2 and methane do not exceed 6% of the hydrostatic pressure and therefore gas ebullition at depth is unlikely and the risk of a gas driven limnic eruption is low. The high methane

concentrations in lake Matano remain intriguing from the perspective of the potential energy they represent that could drive biomass production from the bottom up in the lake, a hypothesis that has been proposed for early oceanic carbon cycling (e.g. (Konhauser, 2007)) and from a climate forcing perspective.

Previous work on methane cycling in lake Matano has shown that methane oxidation drives significant carbon assimilation by methane oxidation (Chapter 2). This assimilated carbon maybe critical for other microbial metabolisms as a carbon source, and may also influence the distribution and recycling of terminal electron acceptors, and ultimately the fate of organic carbon. Other parts of the carbon cycle such as primary production (Crowe et al., 2008a; Crowe et al., 2014; Haffner et al., 2001; Sabo, 2006), (Crowe et al., 2008b; Jones et al., 2011) have also previously been investigated. A holistic model was never attempted, except the approach by Kuntz et al. 2014, which was not constrained very well, as it made many of unsubstantiated assumptions about the carbon sinks and sources in the lake. The understanding of the overall carbon cycle of this unique lake is crucial for understanding both the paleoenvironment of this region (Russell et al., 2014) and the interpretation of paleoproxies of redox, climate and bio signatures of oligotrophic ferruginous environments. Therefore in this study I seek to evaluate the sources, sinks and cycling of carbon in Lake Matano. To facilitate this study we first constrain the hydrologic cycle of the lake system through the use of oxygen isotopes and conservative ion distribution (e.g. Na, Ba). Carbon cycling was constrained and quantified through the use of stable carbon isotopes and bulk concentrations of dissolved inorganic carbon (DIC), methane, and particulate organic matter (POM).

2. Materials and Methods

2.1 Sampling

Sampling was conducted at the deep water master station (2°28’00’’S and 121°17’00’’E) in May 2010. Deep water samples were of more then 14m depth were sampled with 5 L Go-Flow (Niskin; General Oceanics, Miami, FL, USA) bottles using a manual winch setup and a echo location sonar device (Furuno FCV585) for depth placement of the bottles. Using this technique we achieved and accuracy and precision of ±1meter. At depth less than 140m a pumping method was used (Jones et al., 2011), retrieving water directly at depth through a double coned intake (Jørgensen et al., 1979) allowing us to sample from a discrete 2cm thick layer of water. The placement of this sample device was much more accurate, as a (CTD) probe (Sea and Sun Technology) was attached to the cone and provided us with depth readings of approximately 10 cm vertical accuracy for positioning during sampling. The pump system was flushed with a minimum of 3 volumes prior to sample collection. Temperature, conductivity and oxygen was determined using the CTD with the following sensors: Temperature (SST PT100, accuracy ± 0.005 °C, precision ± 0.001 °C), conductivity (SST 7-pole platinum cell, accuracy ± 0.005 mS cm^{-1}, precision ± 0.0001 mS cm^{-1}), O_2 (Oxyguard Ocean (2009), Oxyguard Profile (2010), detection limit ~1% saturation, precision ± 1% saturation), light (LICOR PAR Sensor 193 SA, Accuracy ± 5%, detection limit 0.01 µmol m^{-2} s^{-1}), and turbidity (Seapoint). Samples for Fe(II) measurements were taken directly from the pump stream or the Niskin bottle spout using a 200 or 1000 µl pipette tip and was immediately fixed with ferrozine reagent (Viollier et al., 2000). The Fe samples were then measured within 4 hours by spectroscopic method (Stookey, 1970; Viollier et al., 2000). Measurements of pH were also immediately performed, by flushing a polypropylene bottle (100ml) with no headspace while stirring with a magnetic stirrer. Standardization was carried out with pH standards (4.01, 7.00 10.01, Fisher Scientific) and the

pH 7.00 standard was frequently read to correct for electrode drift. Major elements and trace elements were collected in acid cleaned HDPP bottles and acidified to 1% with trace metal grade and Optima grade nitric acid, DIC samples were collected in glass bottles, then poisoned with $HgCl_2$ and closed without headspace (Crowe et al., 2011). DIC Samples were then analyzed for concentration and ^{13}C; the isotope values have errors of less then ± 0.2‰. Cations and Anions were analyzed by ICP-OES (Perkin Elmer Optima 5300DV) and SO_4^{-2} and Cl^- by Ion Chromatography (Dionex ICS 1500, with an IONpac AS22 anion column and suppressor). Samples for methane concentrations were filled into pre-evacuated serum bottles with thick butyl rubber stoppers. The samples were directly withdrawn from the pump tubing or Niskin bottle spout with a piece of tygon tubing attached to a syringe needle, and directly injected into the pre-evacuated bottles. Samples were immediately poisoned by injecting 100 µl of $HgCl_2$ (Crowe et al., 2011), to prevent methanogenesis or methanotrophy from occurring. Samples for O_2 and H_2 isotopes were collected directly from the Niskin bottle spout into 15 ml screw cap filled to overflow, with little or no headspace. Additional samples were collected from two main tributaries (La Wa, La Molengku), a groundwater pool (Spring Kampung Matano), and a single rain event. The H and O stable isotopic composition was determined at GEOTOP laboratories (Katsev et al., 2010). Values were normalized to two internal reference waters and are reported in standard delta notation (δ^2H and $\delta^{18}O$) relative to Vienna standard mean ocean water (V-SMOW) and Vienna standard light Antarctic precipitation (V-SLAP) with an accuracy of replicate samples better then 0.1‰.

2.2 Physical Limnology

With >590m depth, lake Matano is one of the deepest lakes on Earth and at a depth of 100 meters Iron rich waters are covering a surface area of 107 km^2 and have a 35km^3 Volume (Figure 1). It has the largest ferruginous basin known to date (Crowe et al., 2008a; Crowe et al., 2008b). The lake is stratified and has a permanent anoxic monimolimnion, which is separated from oxic mixolimnion by a pycnocline between 100 and 250m depth, these physical features are very much the same as in past years as can be seen in the density and temperature profiles (Figure 2). A decrease in water temperature with depth is the primary reason for the persistent stratification of this pycnocline; a slight increase in solute concentrations with greater depth also contributes to this stable stratification. A seasonal pycnocline at 30m depth forms in the mixolimnion and separates the epilimnion from the underlying hypolimnion. This pycnocline is primarily driven by the intense solar surface radiation of the lake (Crowe et al., 2011). Density based transport calculations, CFC Data (Katsev et al., 2010) and major element data (Figure 3c) strongly suggest that the exchange from depth with the surface waters across the ~100m pycnocline is very slow, on the order of centuries to millennia (Crowe et al., 2008b). Even though Lake Matano is situated within a highly-active volcanic region, and is hosted by a rapid and extensive fault system, evidence for hydrothermal heating in the bottom waters has not been documented, nor does the ^{14}C content of Methane in the lake suggest that there are hydrothermal carbon inputs in the deep water (Crowe et al., 2011).

2.3 Chemical Limnology

The catchment of Lake Matano is composed of mainly lateritic soils with up to 60 wt% Fe (hydr)oxides (Crowe et al., 2008b; Golightly, 1981), supplies a particulate load rich in Fe to the

lake. The bottom waters are not well ventilated and thus oxidation of organic matter exhaust O_2 quickly within the pycnocline (Figure 3a). The slow physical transport limits not just O_2 transport across the permanent pycnocline but also all other aqueous species. Most redox species (O_2, Fe^{2+}, Mn^{2+},NO_3^-, NO_2^-, SO_4^{2-}, HS^-) behave as described in the traditional redoxcline (Canfield and Thamdrup, 2009; Jones et al., 2011). Reduced Iron and dissolved gases including CO_2 and CH_4 also accumulate to high concentrations in the monimolimnion due to this slow exchange (Figure 3b). Profiles of CH_4, DIC and Fe^{2+} suggest that their origin is in the bottom waters and sediment, and indicate along with profiles of other redox species and major ions, which have been identical over many years, that the lake is at or near steady state. The local environmental and physical characteristics of the lake produce its rigorous physical and chemical stratification, its dearth of sulfate suggests more abundant terminal electron acceptors such as Fe and Mn oxides replace SO_4^{-2} as a terminal electron acceptors, providing the oxidizing agents for most organic and inorganic matter degradation.

3. Results and Discussion

3.1 Hydrological Budget of Lake Matano

The water budget of Lake Matano was evaluated using annual precipitation data, evaporation and transpiration estimates for the local environment and the distribution of barium (Ba) in the system. The deep waters of Lake Matano have disproportionately high Ba concentrations when compared to surface waters in the catchment. The low concentrations of Ba in river and rain inputs into the system indicate that the source of this Ba must therefore originate in the deep waters of the lake. A groundwater source in the lake catchment has Ba concentrations

that are nearly identical to those in the deep waters of the lake; we thus postulate that the lake receives significant groundwater input below the pycnocline to maintain the concentrations of Ba that we see in the bottom of the lake despite a diffusive flux through the pycnocline. Within the lake, we consider Ba a conservative element as it typically does not play a significant role in any micro- or macro-biological metabolism or enzymatic system, and is highly soluble in the absence of high concentrations (SO_4^{-2}), which easily forms Barium sulfate (Ba SO_4) as a precipitate. Maximum concentrations of Ba (0.74 μM) and SO_4^{-2} (29 μM) in the water column are low enough that no precipitation of $BaSO_4$ or any other Ba species is expected.

With the average precipitation of 2875 mm $year^{-1}$ in the catchment we calculate an average inflow of 11.90 m^3 s^{-1}, an outflow rate of 16.42 m^3 s^{-1}, a surface evaporative rate of 10.41 m^3 s^{-1}, and direct precipitation on the lake of 14.94 m^3 s^{-1} (Table 1). Barium concentrations were obtained for all the sources and sinks, and the inflow in the bottom of the lake was assumed to come from ground water as the lower portion of the deep water has the same concentration as the groundwater spring. Applying Fick's law (Eq 1) to the concentration gradient of Ba we calculated the eddy diffusivity coefficient (Kz) needed to sustain a Ba flux across the pycnocline (as define in Chapter 2 section 3.2 and area of lowest diffusion in the lake) that matched the Ba flux out of the Lake through the Petea river. This yielded a value of Kz = 0.205 m^2 d^{-1} when we considered the Ba concentration gradient over the 105 -95m depth interval. To test the sensitivity of Kz to uncertainties in the concentration gradients we tested other depth intervals, which yielded variability of at most 17% for different diffusion paths (120 - 95 m to 105 - 95 m) across the pycnocline and is much better as the range predicted by previous models (Katsev et al., 2010), which is 1-2 orders of magnitude. The value also seems to be reasonably robust with respect to changes in evaporation and rainfall, as they behave fairly linearly for the range of

values we used to perturb the system. To evaluate rates of evaporation we utilized a ± 20% change in annual irradiance, and a ± 3 sigma for rainfall amounts to the data. Adding the errors introduced by variances in the chemocline with the precipitation and irradiance errors, we get a value of 0.205 ± 0.1 m^2 d^{-1} for Kz in the pycnocline.

$$F = Kz\frac{dC}{dx} \quad (1)$$

This result agrees with values that were calculated by other methods in previous years (Table 2). Lake Matano has no other significant Ba sources besides the bottom waters, and therefore a simple mass balance between the bottom waters and the outflow of the lake can be utilized to provide an estimate of groundwater inflow into the bottom waters of 2.0 m^3 s^{-1}.

3.2 Oxygen Isotopes constraining groundwater inflow

Oxygen isotope profiles look much like other chemical water column profiles (Figure 4). In the surface waters $\delta^{18}O_{H_2O}$ = -4.4 ‰ and remains unchanged within error (± 0.1‰) down through 20m depth (Figure 4). Between 44 and 90 m $\delta^{18}O_{H_2O}$ is constant at approximately -4.6 ‰ and then decreases linearly to 140m. The 160m depths has the same value a 140m depths, producing a step in the profile. The isotopic signature decreases from 160 to 180m with a clear inflection point. Between 180 and 250m the profile has a sharp curvature and then remains near constant at $\delta^{18}O_{H_2O}$ = -7.1 with the exception of the deepest measurement at 550m where there is a slight increase. This is indicative of subsurface groundwater input, which is depleted in ^{18}O between 400 and 500m. If we presume the bottom waters have a source of isotopically light ^{18}O, we can estimate its magnitude, for which we obtained isotopic signature of the same

groundwater source we sampled for barium. These waters had a $\delta^{18}O_{H_2O}$ of -8.55. Using the oxygen isotopes for other sinks and source (Table 2) and the Kz value of 0.2 m^2 d^{-1} calculated from Ba concentration gradients we can calculate the groundwater inflow from O isotope values using equation (2).

$$Q_G(\delta^{18}O_G - \delta^{18}O_{mon}) = \frac{AK_z}{e}(\delta^{18}O_{mon} - \delta^{18}O_{mix}) \quad (2)$$

In this equation "A" is the area of the interface between monimolimnion and mixolimnion, Kz is the eddy (turbulent) diffusion coefficient for the chemocline and e is the length of the diffusion path (122 - 90 m), the subscripts used are defined as mon = monolimnion, mix = mixolimnion, G = groundwater. Solving this equation for Q_G and using the values in Table 3 enable us to determine the volume of groundwater flowing into the lake per unit time, which we calculated to be 1.4 ± 1 m^3 s^{-1}. This result is very similar to the value of 2.0 m^3 s^{-1} calculated by using Ba as a conservative tracer. This agreement gives confidence in both the Ba mass balance as well as the Kz value.

3.3 Oxygen isotopes constraining lake surface evaporation

Lake Matano experiences large amounts of surface evaporation because of the large input of solar radiation with its near equator location. Preferentially ^{16}O H_2O enters the vapor phase (Einstein, 1905) during evaporation and therefore the residual water in the epilimnion is continuously enriched in heavier ^{18}O H_2O. Although the transport between upper waters and lower water layers of the lake is very slow and on the order of hundreds of years (Crowe et al., 2008b; Katsev et al., 2010), the bottom of the lake will slowly become enriched in ^{18}O H_2O as it

defuses down from the surface waters. The groundwater source in Lake Matano that is supplying water below the pycnocline which is enriched in ^{16}O though, and is making the water in the bottom of the lake significantly lighter. Our knowledge of $\delta^{18}O_{H_2O}$ of the ground water influx, along with the fluxes of other sources and sinks and their oxygen isotope values enables us to calculate the amount of surface evaporation of the lake.

To be able to estimate the other inputs and sinks for the lake, we have evaluated Lake Matano's water budget by comparing it and its basin to similar tropical environments. The values in Table 1 enable us to estimate the approximate inflow and outflow of the lake. Calculations estimating that most of the solar radiative flux is absorbed by the lake and reveal that the surface of Lake Matano evaporates approximately 70% of water that it receives in rainfall. For the remaining basin that is covered with dense jungle growth we estimate 52% of the water is returned to the atmosphere by evapotranspiration as determined for jungle foliage in a study near Bogor (Calder et al., 1986). Therefore the rainfall and the evapotranspiration of the jungle and this basin provides a net influx of approximately 11.9 $m^3\ s^{-1}$ into the lake. Together with data for rainfall and river outflow (Table 1) we can determine the evaporative flux of the lake by using oxygen isotopes in Table 3 and by rearranging the formula below for Q_p (Eq. 3) using the same conventions for labeling as equation 2.

$$Q_{Pe}\delta^{18}O_{Pe} + Q_{ev}\,(\delta^{18}O_{mix} - \delta^{18}O_{ev}) = \frac{AK_z}{e}(\delta^{18}O_{mon} - \delta^{18}O_{mix}) +$$

$$Q_G\delta^{18}O_G + Q_{Lw}\delta^{18}O_{Lw} + Q_P\delta^{18}O_P \qquad (3)$$

The evaporation flux calculated this way was 15.8 $m^3\ s^{-1}$ and considering the uncertainty in the Kz value (~20%), the annual precipitation measurements (~5%) and irradiance estimates (~15%)

is in good agreement with the 16.8 m^3 s^{-1}, that was estimated using solar irradiance for its calculation. There is a lack of sensitivity with respect to the water sources in determining evaporation. Because the $\delta^{18}O_{H_2O}$ isotope values for most of the sources except precipitation are very close to each other, redistribution of water among the sources will not change the outcome, only changes in rainwater input would make a significant difference.

3.4 Carbon

Figure 3b displays concentration profiles of methane within lake Matano. At the surface of the lake concentrations of 0.5 μmol l^{-1} indicate it is supersaturated with respect to the atmosphere determined by gas equilibrium calculations using Henry's law with a constant of K_H = 1.3x10^{-3} M atm^{-1} (Canfield et al., 2005). Below the surface layer, methane concentrations remain relatively constant throughout the upper mixolimnion, increase in the lower mixolimnion and then sharply increase across the pycnocline and in the upper monimolimnion, reaching concentrations of 2 mmol l^{-1} in the deepest parts of the lake. DIC and Fe (Figure 3) follow similar trends with depth, the difference between the profiles being that DIC is also high in the mixolimnion and nearly constant at 2 mmol l^{-1} though slowly increasing with depth. Similar to CH_4 the DIC and Fe concentrations increase sharply across the pycnocline, and reach a near steady-state concentration of 4 mmol l^{-1} and 140 μmol $l^{-}1$ respectively between 250 m and the bottom of the lake.

3.4.1 Processes controlling sources and sinks of DIC, their concentration and $\delta^{13}C_{DIC}$ signature.

Concentrations of DIC and their $\delta^{13}C_{DIC}$ are used to provide insight into the predominant processes that affect DIC concentrations and isotope signatures in the different zones (mixiolimnion, pycnocline, and monimolimnion) of the lake. In Figure 6, we show how current DIC concentration and isotope signatures in the water are related to processes that may modify these concentrations and isotope signatures. Ranges of typical isotopic values are marked on the $\delta^{13}C_{DIC}$ axis with grey bars. As to our current state of knowledge ((Crowe et al., 2008a; Crowe et al., 2011; Crowe et al., 2008b; Jones et al., 2011; Chapter 2) the important metabolic processes in Lake Matano are phototropic primary production, anoxygenic phototrophy, heterotrophic carbon oxidation, methanogenesis, and methane oxidation. In most water layers only few of these metabolisms are active simultaneously and the remainder can likely be considered negligible, this in most cases reduces the number of variables and simplifies the isotope and mass balance.

$$1000ln\alpha = \frac{9.55\times10^3}{T} - 24.10 \qquad (4)$$

3.4.2 Characterization of the DIC in the mixolimnion and pycnocline

In the mixolimnion DIC concentrations and $\delta^{13}C_{CO_2}$ values are affected most likely by these processes: (1) atmospheric CO_2 exchange; (2) surface and river DIC inputs; (3) photosynthetic activity; (4) organic matter oxidation; (5) methanotrophy; and (6) methanogenesis.

(1) CO_2 exchange with the atmosphere.

The surface water of Lake Matano has a DIC concentration of 1.9 mmol l^{-1} and has 50% saturation with respect to the atmosphere, indication that there is a net DIC flux into the lake. DIC has a $\delta^{13}C_{DIC}$ of -7.5‰ near the surface, absorption of this DIC would decrease $\delta^{13}C_{DIC}$ in the surface waters. Fractionation calculated at ambient temperature (Equation 4 where α is the isotopic fractionation factor for a given temperature and T is the ambient temperature in K)(Gorka et al., 2011; Mook et al., 1974) between $CO_{2(g)}$ and $HCO_3^-{}_{(aq)}$ is 7.6‰ and the atmospheric $\delta^{13}C_{atmospherCO_2}$ is approximately -7.8‰, predicting a $\delta^{13}C_{DIC}$ of ≈ 0‰ in the waters near the surface. We do not know if we have this fractionation effect, as we have no DIC measurements right at the surface and the closest spatial value was obtained at 10m depths. It is also possible that the large amounts of isotopically light DIC that are provided from the chemocline and the river inputs result in a negligible isotope effect when CO_2 exchanges at the lakes surface. As for this process we may have a steady state scenario and may not be in equilibrium with atmospheric CO_2, for which we unfortunately have no data.

(2) Surface and river DIC inputs of lake Matano have low $\delta^{13}C_{DIC}$ values, Lawa river = -22.2 ± 0.2. These values are close to C isotope signatures of organic detrital matter and are likely the result of organic matter degradation, which usually has no fractionation effect itself. Extrapolating from the lakes phototrophic primary production record, contributing rivers will also not have strong photosynthetic primary production and thus will not increase the $C^{13}{}_{DIC}$ signature. Surface rainwater at equilibrium with the atmosphere is estimated for $\delta^{13}C_{DIC}$ between -1 and +3 ‰ according to similar environments (Amiotte-Suchet et al., 1999; Helie et al., 2002).

The DIC C isotopes at 10m depth may not be in equilibrium with the surface waters and therefore present a lower then usual value of -7.5‰ instead of the ~ 0‰ as would be expected from lake water in equilibrium with the atmosphere. The very low molar influx of DIC by rain water, about 100 times less compared to river or atmospheric influx, makes this effect nearly negligible. Additionally it is also possible that precipitation has isotopic values that are not in equilibrium with average atmospheric CO_2 and are more negative because of interaction with more negative sources of CO_2 prior to deposition (Gorka et al., 2011).

(3) Oxygenic photosynthesis in Lake Matano is relatively low with primary production rates of $3.8x10^{-3}$ mol C m^{-2} d^{-1} ,which are comparable to ultraoligotrophic high alpine lakes (Crowe et al., 2008a). DIC consumption by photosynthetic activity is not evident from DIC concentration profiles (Figure 6), likely because the comparably large DIC fluxes from other sources (river influx, upward transport and atmospheric diffusion) are masking the signal. Yet a small positive $\delta^{13}C_{DIC}$ excursion around 40m depths is showing some evidence for photosynthetic activity, which also was previously observed to be at a maximum around this depth (Crowe et al., 2008a).

(4) Organic Matter oxidation

Organic matter oxidation by itself hardly has any noticeable fractionation associated with it (Fritz et al 1978; Peterson and Fry 1989; Barker and Fritz 1981). In general it still decreases $\delta^{13}C_{DIC}$, as lighter carbon from POM ($\delta^{13}C_{POM}$ = -20 to -30) or dissolved organic matter is moved to the DIC pool and therefore will result in a more negative total signature. Organic matter oxidation occurs in Lake Matano throughout most of the water column, it could be responsible for part of the negative DIC excursion in the pycnocline, but most of it will likely happen in the

sediments, as a significant amount of detrital matter sediments (0.85 – 1.3 mmol C m^{-2} $d^{-}1$) at the bottom of the lake (Crowe et al., 2011).

(5) Methanotrophy will fractionate methane at $\delta^{13}C_{CH_4\text{-}DIC}$ of 5 to +31 ‰ (Barker and Fritz, 1981; Whiticar, 1999), though the observable DIC fractionation will depend much on the size of the DIC pool. Even though biogenic CH_4 has already a very light carbon isotope signature, it will get further fractionated and will obtain an even lighter isotope signature of $\delta^{13}C_{DIC}$ = -119 ‰, which was calculated for methane defusing across the pycnocline using concentration gradients and isotope measurements between 120 and 110m. This signature may not be very noticeable as the DIC pool is very large but in Lake Matano it is evident that methanotrophy is having an effect on DIC, and the production of a noticeable light DIC signature. As methanotrophic rates increase with depth (Chapter 2) we witness that $\delta^{13}C_{DIC}$ decreases in the mixolimnion. Methane oxidation rates are even higher in the pycnocline and even though we have higher DIC concentrations the $\delta^{13}C_{DIC}$ values are still decreasing to a low of -12 to -13‰. A sure indication for methane oxidation that accompanies these DIC isotope trends is the fractionation of $\delta^{13}C_{CH_4}$ during this process. Values of $\delta C^{13}_{CH_4}$ increase in the pycnocline (Figure 5) and CH_4 concentrations decrease rapidly where the highest methane oxidation rates were measured (Chapter 2).

(6) Methanogenesis produces a $\delta^{13}C_{DIC}$ between +7 and +18‰ and can produce C isotope values for methane of less then -100 ‰. Changes in C isotope values ($\delta^{13}C_{DIC\text{-}CH4}$) for CH_4 can reach between 24 to 77 ‰ depending on which microbial pathway generated the CH_4(Whiticar, 1999). Isotope separation factors can be used when two species are linked by an isotope fractionation process and can help determine what pathway of methanotrophy is predominantly used. The

separation factor is simply the difference in isotopic value, before and after the fractionation process. Isotope separation factors in the mid 50s in the upper pycnocline (120-140m) indicate that likely both, CO_2 reduction and some acetate fermentation methanogenesis is occurring. Isotope separation factors in the high 50s and low 60s (150-550m) are a good indication that CO_2 reduction is the main pathway for methanogens (Whiticar, 1999), as this pathway has a high $^{13}C_{CH_4\text{-}DIC}$ fractionation creating these larger (50-95 ‰) separation factors. 120m is the only depth that would suggest that some methanogenesis by acetate fermentation is occurring according to the separation factor of 37, but it could also be that the high CH_4 oxidation rate at this depth is the reason for less fractionation.

Even though a lot of methanogenesis is believed to be occurring in the sediments, it has been recently discussed (Bogard et al., 2014) that in deep lakes a significant amount also occurs in the water column. It has been proposed that for deep lakes a significant amount of methanogenesis has to occur in the water column in order to balance concentration gradients, rates of methanotrophy and outgassing. There are, in fact, many studies showing that this process is occurring not just in the anoxic, but also in in the oxic water column (Grossart et al., 2011; Tang et al., 2014), which is quite unusual, as for a long time the general censuses was that methanotrophy was a strictly anaerobic process because of its oxygen sensitive enzyme system (Jarrell, 1985; Mah et al., 1977). In the oxic waters the production of methane occurs in micro-anoxic environments such as metazoan guts and on particles (Deangelis and Lee, 1994; Karl et al., 2008; Tilbrook and Karl, 1995), but it has also been shown that methane is produced in particle free oxic waters (Damm et al., 2010; Grossart et al., 2011; Tang et al., 2014). I suggest, that to a large extent aerobic and anaerobic water column methanogenesis is also occurring in Lake Matano in order to balance the high methane oxidation Rates observed (Chapter 2).

3.4.3 Carbon distribution

Isotope values for DIC are in general lower than would be expected in similar aquatic ecosystems. Figure 6 depicts both DIC concentrations and $\delta^{13}C_{DIC}$ as a function of depth. Sampling for DIC isotopic signatures began at 10 m depth with a $\delta^{13}C_{DIC}$ = -7.5, which decreases to -9.0 and -8.0 at 40m and 41m respectively. The zone between 40-50 m has been previously characterized as a hotspot photosynthetic activity (Crowe et al., 2008a). Below this zone the carbon isotopic composition of $\delta^{13}C_{DIC}$ = -10.9 is constant (within the error) down to 95m, during this depth interval [DIC] also stays constant at 2 mmol l^{-1}. The isotope values decrease quickly between 95 and 100m but then remain almost constant at about $\delta^{13}C_{DIC}$ = -11.6 between 100 and 118m, and again [DIC] is constant as well in this interval. A decrease in $\delta^{13}C_{DIC}$ at 120m with -12.9 ‰ at [DIC] = 2.3 mmol l^{-1} after which $\delta^{13}C$ is increases ($\delta^{13}C_{DIC}$ = -7.9) at 170m depth and then decreases again at 200m. We also observe a sharp increase of [DIC] to 3.2mmol l^{-1} over this depth interval.

Concentrations of particulate organic matter (POM) at the surface of the lake are 7.8 uM with a $\delta^{13}C_{POM}$ of -31.2 ‰ and increase to 16.6 uM at 10m depth with a concomitant increase in $\delta^{13}C$ to -27.9 ‰ (Figure 7). POM concentration and carbon isotopic composition decrease steeply until 39m depth (5.8uM) and then progress to lower values at between 39 and 95m (3.3uM). Through the chemocline (95 to 200m) POM increases up to 14.1 uM with a small recess at 130 m. Carbon isotope values drop to -43.1 ‰ at 110m and then quickly increase again through the chemocline, with a small inversion at 120m to -28.3 ‰ at 200m depth.

If organic matter oxidation is the predominant DIC generating process in the mixolimnion and pycnocline the expected trend would be that $\delta^{13}C_{DIC}$ becomes more negative with increasing oxidation of organic material. Therefore organic matter oxidation should correlate between the surface water [DIC] and its $\delta^{13}C_{DIC}$ = -7.5 value and the initial organic matter, which is the end member, in this case with $\delta^{13}C_{DIC} \approx$ -31.2. Figure 9 depicts this relationship as the group of round markers that show DIC concentrations and their isotope values for the oxic part of the mixolimnion extending into the pycnocline. It is notable that data are in good agreement with the predicted trend for organic mater oxidation line $y = 43.8x - 31.2$, which was determined by the end points previously described. POM concentrations have dropped from 15 uM in the surface to less then 5 µM (Figure 7) in this zone, supporting the hypothesis that organic matter oxidation is controlling DIC and isotopic composition in the upper waters of the lake. DIC concentrations and isotopic composition increase and respectively become enriched with heavier carbon at the bottom of the pycnocline (Figure 6). I propose that this isotopic signal is related to more positive DIC diffusing upwards from the deep waters of the lake. Similar features have been described in other lakes (Myrbo and Shapley, 2006; Oana and Deevey, 1960). These studies broadly summarized that the high DIC isotope signature could not be sourced simply by POM oxidation. Instead it was proposed that the isotope signature could be imparted from fermentation products and from the deep sediments or carbonate rock dissolution. Though Lake Matano's DIC isotope values in the bottom waters do not quite approach the values in these studies, both of these hypotheses are worth considering, as we have a relatively high particulate load of detrital matter to the sediment which could lead to fermentation and a karst carbonate formation which clearly has groundwater connectivity to the lake as outlined in the water budget. However we offer another alternative hypothesis that the high methane production

in the lake may account for a significant proportion of the observed DIC signature, as methanogenesis can lead to fractionations of $\delta^{13}C_{DIC}$ between +7 and +18 (Camus et al., 1993; Herczeg, 1988).

In the oxic zone is a small group of outliers at lower (-10.5 to -11) $\delta^{13}C_{DIC}$ values, which have to originate from other sources than organic mater oxidation to obtain these values. This excursion could be caused by transport of light DIC from below (110m) or other metabolisms emerging around 80-90 m depth. We suggest that it is mainly caused by an emerging metabolism, as the large decrease of $\delta^{13}C_{POM}$ would not be expected during typical organic mater oxidation, in fact the opposite would be expected for the POM. Increasing methane oxidation instead could facilitate the features we are seeing. In this process isotopically light methane, most likely produced by CO_2 reduction ($\delta^{13}C_{CH_4} \approx$ -50 to -70 ‰), is oxidized and generates isotopically light DIC and biomass. This process explains the lower $\delta^{13}C$ signature we are seeing in POM along with the decreasing $\delta^{13}C$ signature of DIC. These observations are supported by observations made in Chapter 2, reporting that 50 to 90% of the CH_4 consumed during methane oxidation was assimilated by the organisms.

At the top of the anaerobic zone an even more pronounced decrease in $\delta^{13}C_{DIC}$ is observed (Figure 6), the simultaneous increase of $\delta^{13}C_{CH_4}$ (Figure 5) and the decrease of $\delta^{13}C_{POM}$ to -45‰ (Figure 7) endorse the idea of a very active methane oxidation zone. Other lines of evidence also support this magnitude of methane oxidation, such as an inversion in the methane profile at the same depth of 110m, which is right in the oxic anoxic transition zone. The limited transport (low Kz) of the pycnocline and the high transport of the mixolimnion, create a steep concentration gradient of CH_4 and DIC lowering the concentrations in the upper pycnocline

substantially. This decrease in the CH_4 and DIC pool also makes the isotope effects that the metabolisms cause much more noticeable, as the dilution effect is much lower in this zone compared to the monimolimnion. The high rates of methane oxidation in this zone also contribute to the depletion of CH_4 as can be seen from the concentration profiles (Figure 3) and isotope profiles (Figure 5).

A third trend is emerging on the Kelling plot (Figure 9) to higher $\delta^{13}C_{DIC}$ values with increasing [DIC] for depth below 120m. This trend is in parallel with the modeled line for methanotrophy, it may be caused by enriched ^{13}C DIC diffusing upward from the bottom waters where the isotope signature suggests methanogenesis and carbonate dissolution as a sources, or it may be caused by water column methane production. This pathway can also play a role creating high $\delta^{13}C_{DIC}$ and certainly should be considered a source. Plotting the conservative ion Ba versus DIC (Figure 10) shows us the variation of DIC from the regular diffusion line. The plot reveals that there is an actual sink for DIC right in the pycnocline, which fits well with the DIC conversion to methane and with the heavier $\delta^{13}C_{DIC}$ signal involved in methanogenesis. As many types of metabolisms that have different substrates and isotope fractionations are occurring at the same time, the cumulative DIC isotope signature and [DIC] are not easy to interpret. In the pycnocline we most likely have the isotopically heavy DIC flux from below, and fractionation by methanotrophic activity in the water column. This is possibly shifting the points on the Keeling plot (Figure 9) upwards, which may cause samples that have ample evidence for CH_4 oxidation, appear to lie on the organic matter oxidation line or even above it. For this reason the 100 and 120 m samples look like they are sitting on the organic matter oxidation line, even though large amounts of methane oxidation are occurring at these depths. Deeper samples seem even more

influenced by this trend and we can see that methane oxidation, as well as methanogenesis are probably at work here simultaneously, shifting the trend down so it runs parallel to mixing line for pure methanogenesis. Unfortunately we do not have DIC carbon isotopic composition below 200m for the year 2010 so we are only able to see the onset. Though data from 2009 shows a good correlation with the same trends and even a more detailed transition from lower depth. Here it can be seen from concentration and isotope profiles for methane, that methane oxidation and methanotrophy are primarily occurring. The trends shown in Figure 9 are also confirmed by the C^{13} enriched CH_4 in the upper pycnocline, resulting from increasing CH_4 oxidation and the decrease in C^{13} CH_4 in the deep water, as a result of increasing methanogenesis. POM from the pycnocline is also becoming more enriched in ^{13}C with depth again, likely due to organic matter degradation or biomass accumulation by methanogenesis.

The increase in methane production in the bottom waters and the sediments is a common occurrence, as in most aquatic environments a fair quantity of the methane actually gets produced in sediments and diffuses into the water above. Water column profiles confirm rapid increase of CH_4 in the bottom waters, $\delta^{14}C_{CH_4}$ values also confirm that the CH_4 in the lake is relatively "young" This means that the carbon of the CH_4 was produced in the atmosphere by nitrogen decaying to C^{14} by cosmic radiation bombardment (Ralph and Michael, 1974). It is then oxidized with atmospheric O_2 to CO_2, following incorporation into organic matter via photosynthesis. This organic carbon has a high C^{14} signature indication to us that it was recently produced by atmospheric CO_2 fixation. Carbon from hydrothermal sources would contain only methane with very low C^{14} signal, as the carbon in this methane usually comes from the subsurface being a remnant of long buried carbon. Our C^{14} measurements for methane indicated

that bottom water methane is not older then 2300 years and therefore did originate by methanogenesis of organic matter rather then coming from the subsurface.

Near the sediment interface in the deep waters a small decrease in DIC and a small increase in $\delta^{13}C_{DIC}$ confirms an increase in methanogenic activity. Additionally increases seen in $\delta^{13}C_{CH4}$ may be caused by the heavier source DIC pool, or a less pronounced isotope effect due to increased methanotrophic rates (Templeton et al., 2006). Higher rates of methanogenesis near the sediment water interface would be reasonable, as we likely have higher microbial density as well as increased nickel concentrations here, resulting from reductive dissolution of Ni bearing Fe oxides. Nickel is an important cofactor in the methyl-coenzyme M reductase (MCR) which is critical to methanogenesis and can thus control methanogenesis rates. (Konhauser et al., 2009) suggested that a Ni famine was likely responsible for a reduction in methanogenesis in Archean times, and may have even brought on the oxygenation of the atmosphere. Considering this, the large quantities of methane in lake Matano are not entirely surprising due to the relatively high Ni availability from the Ni bearing laterites, compared to the availability of Cu.

Alternatively there may be a shift in substrate use for methanogenesis, moving from mainly methanol based metabolisms ($\delta^{13}C_{CH_4}$ = -68 to -77‰) to CO_2 reduction ($\delta^{13}C_{CH_4}$ = -55 to -58‰) or acetate fermentation ($\delta^{13}C_{CH_4}$ = -24 to -27‰) pathways (Whiticar, 1999). $\delta^{13}C_{DIC}$ vs. $\delta^{13}C_{CH_4}$ (Figure 11) does shows us similar results in this regard, and indicates that we have more acetoclastic methanogenesis occurring in the shallower waters, and more methanogenesis by CO_2 reduction in the bottom waters or near the sediments.

To quantitatively evaluate the carbon fluxes in lake Matano I constructed two separate box models based on mass balances of DIC fluxes and their isotopic compositions, one

for the mixolimnion and one for the monimolimnion.. To estimate how much authigenic carbon was exported from the mixolimnion to the monimolimnion, a box model for the mixolimnion was formulated according to equation 5 which was solved for the export flux particulate organic Matter (C_{POM}). Parameters in Table 4 were used in the calculation, where the major components are the Lawa (La) river inflow (a proxy for total inflow), direct precipitation on the lake (pre), atmospheric exchange (atm), Petea (Pe) river outflow, DIC (DIC_{mon}) diffusing up from the monimolimnion and DIC (DIC_{CH4}) produced from the oxidation of upward diffusing methane.

$$Q_{La}(\delta^{13}C_{La}) + Q_{pre}(\delta^{13}C_{pre} - \delta^{13}C_{mix}) +$$
$$[DIC]_{mon}\frac{AK_z}{dx}\left(\delta^{13}C_{mon} - \delta^{13}C_{pyc}\right) + Q_{atm}\,(\delta^{13}C_{atm} - \delta^{13}C_{mix}) +$$
$$[DIC]_{CH4}\frac{AK_z}{dx}(\delta^{13}C_{CH4\,mix} + \delta^{13}C_{CH4\,DIC}) = Q_{POM}\;\delta^{13}C_{POM} + Q_{Pe}\,\delta^{13}C_{mix} \qquad (5)$$

The box model for the monimolimnion (equation 6) was set up to determine the amount of particulate organic carbon that is oxidized to DIC (i.e. respired) in the bottom waters and underlying sediments of the lake. Upward diffusion of DIC and CH_4, methanogenesis, ground water influx, and respiration of POM to DIC were included in the model. Equation 6 was rearranged and solved for POM respiration, and values in Table 4 were used for the calculations. Carbon transport across the pycnocline was calculated using the Kz values that were derived from water budgets constrained through the distributions and fluxes of O isotopes as well as barium. This water budget afforded a much more precise and accurate measure of Kz than was previously available allowing superior estimates for the fluxes for CH_4 (1.02 mmol $m^{-2}d^{-1}$) and DIC (9.00 mmol $m^{-2}d^{-1}$) diffusing across the pycnocline. These revised fluxes are an order of

magnitude higher then those estimated by Kuntz et al. 2015, and this is due exclusively to the revised Kz. Note that this revised Kz is in much better agreement with Kz previously derived through multiple independent measurements (Katsev et al. 2010, Crowe et al. 2015). Values for the DIC concentration and isotopic composition of the groundwater influx to the monimolimnion, were taken as similar to those of the monimolimnion, and the riverine input, respectively. The appropriateness of these estimates was evaluated through an analysis of the model output, POM respiration, and combinations of parameter values that yielded extraneous solutions were eliminated from the parameter space considered. This process gave a possible range for DIC concentrations (2070-4970 μmol l^{-1}) and groundwater inflow rates (1 - 2.4 $m^3 s^{-1}$) that yielded valid solutions for POM degradation rates. The final values used in the calculations were [DIC] = 4000 μmol l^{-1} and a flow rate of 1.2 m^3 s^{-1}.

$$Q_{gr}\delta^{13}C_{gr} + Q_{POMmon}\,\delta^{13}C_{POMmon} + d[DIC]_{CH4}\frac{AK_z}{dx}\delta^{13}C_{DIC\,CH4} =$$

$$d[DIC]_{CH4}\frac{AK_z}{dx}\delta^{13}C_{CH4\,exp} + d[DIC]_{mon}\frac{AK_z}{dx}\left(\delta^{13}C_{mon} - \delta^{13}C_{pyc}\right) \quad (6)$$

The box model for the mixolimnion yielded organic matter export rates to the deep water from the mixiolimnion of 4.58 mols s^{-1}, which, converted to an area flux of 3.95 mmol m^{-2} d^{-1}, is in exceptional agreement with the organic matter (primary) production rates measured previously (3.8 mmol m^{-2} d^{-1}) (Crowe et al., 2008a). The agreement between these values give us confidence that they are reasonable and robust and that the mixolimnion box model is well constrained. Notably, the box model also predicts that Lake Matano is a strong sink for atmospheric CO_2, capturing 7.8 x10^8 mols of C annually.

Previous models for C degradation in Lake Matano's monimolimnion and underlying sediments suggest very inefficient rates of respiration and methanogenesis, which translate to exceptional sedimentary organic C burial and preservation (Kuntz et al. 2015). As mentioned, however, this model was based on an underestimate of water column transport, and this on underestimates of CH_4 fluxes and production rates. With the revised Kz and CH_4 production rates, the rate of POM degradation to DIC in the monimolimnion is 0.13 mols s^{-1} or an area specific respiration rate of 0.11 mmol m^{-2} d^{-1}. Given that ferric Fe represents the only possible electron acceptor, this respiration rate can be reconciled with electron acceptor availability by considering Fe deposition rates (0.81 - 1.86 mmol m^{-2} d^{-1}) (Kuntz et al., 2015), of which approximately 27 % is reactive Fe (Raiswell and Canfield, 1998). Based on a ratio of 1:4 for full oxidation, the respiration rate calculated can be supported with a reactive Fe flux of 0.44 mmol m^{-2} d^{-1}, which is in the range observed.

The total flux of carbon to the monimolimnion can be considered as the sum of total degradation (Fe respiration and methanogenesis) in addition to burial. Considering calculated C burial rates (Kuntz et al.) and the range of values the box modeling yields for respiration and methanogenesis gives a total C flux of between 3.23 mmol m^{-2} d^{-1} and 5.04 mmol m^{-2} d^{-1}. Comparing this value with the export of authigenic organic matter from the mixolimnion suggests that primary production within the lake supplies between 78 -100% of the total organic carbon, of which 56 to 75% is degraded and the remainder is preserved in the sediments. Notably, only a small fraction (10-40%) of the total C degradation proceeds through Fe reduction, despite the ferruginous nature of Lake Matano's sediments. We also show that the burial efficiency in lake Matano is relatively high (between 25-44%) though not a high as previously proposed (Kuntz et al., 2015).

Conclusions:

The development of hydrological budget and box models for Lake Matano enabled a more quantitative analysis of carbon cycling in this system and further constrained the magnitude of its influence on the lakes biogeochemical cycles. Carbon stable isotopes of all major carbon species in the lake facilitated the forensic investigation of the evolution and sources of DIC throughout the lake. Particulate organic matter (POM) carbon isotopic signatures provided verification in situ for high assimilation rates of methane C into microbial biomass. This in turn, when considered with the consumption and then production of POM in the chemocline, suggests a significant deposition of isotopically light organic matter through autochthonous assimilation, and biomass production into the iron-rich sediments of the lake. Methanogenesis was found to be proceeding in the lake through carbon dioxide reduction and acetoclastic methanogenesis with a larger proportion of CO_2 reduction pathways at the greatest depths. These findings have significant divergence from the perceived cycling of carbon in both Lake Matano and marine settings of Precambrian eons and thus must integrated into future models of these systems.

References:

Amiotte-Suchet, P. et al., 1999. δ13C pattern of dissolved inorganic carbon in a small granitic catchment: the Strengbach case study (Vosges mountains, France). Chemical Geology, 159(1–4): 129-145.

Barker, J.F., Fritz, P., 1981. Carbon isotope fractionation during microbial methane oxidation. Nature, 293(5830): 289-291.

Bogard, M.J. et al., 2014. Oxic water column methanogenesis as a major component of aquatic CH4 fluxes. Nature Communications, 5.

Calder, I.R., Wright, I.R., Murdiyarso, D., 1986. A study of evaporation from tropical rain-forest - west java. Journal of Hydrology, 89(1-2): 13-31.

Camus, G. et al., 1993. Risques d'eruption gazeuse carbonique en Auvergne. Bulletin de la Societe Geologique de France, 164(6): 767-781.

Canfield, D.E., Thamdrup, B., 2009. Towards a consistent classification scheme for geochemical environments, or, why we wish the term 'suboxic' would go away. Geobiology, 7(4): 385-392.

Canfield, D.E., Thamdrup, B., Kristensen, E., 2005. Aquatic Geomicrobiology. Advances in Marine Biology, 48. Elsevier Academic Press, 640 pp.

Crowe, S.A. et al., 2008a. Photoferrotrophs thrive in an Archean Ocean analogue. Proceedings of the National Academy of Sciences of the United States of America, 105(41): 15938-15943.

Crowe, S.A. et al., 2011. The methane cycle in ferruginous Lake Matano. Geobiology, 9(1): 61-78.

Crowe, S.A. et al., 2014. Deep-water anoxygenic photosythesis in a ferruginous chemocline. Geobiology, 12(4): 322-339.

Crowe, S.A. et al., 2008b. The biogeochemistry of tropical lakes: A case study from Lake Matano, Indonesia. Limnology and Oceanography, 53(1): 319-331.

Crowe, S.A. et al., 2007. Reductive dissolution of trace metals from sediments. Geomicrobiology Journal, 24(3-4): 157-165.

Damm, E. et al., 2010. Methane production in aerobic oligotrophic surface water in the central Arctic Ocean. Biogeosciences, 7(3): 1099-1108.

Deangelis, M.A., Lee, C., 1994. Methane production during zooplankton grazing on marine-phytoplankton. Limnology and Oceanography, 39(6): 1298-1308.

Einstein, A., 1905. On the movement of small particles suspended in a stationary liquid demanded by the molecular-kinetic theory of heat. Annalen der Physik, 17: 549-560.

Golightly, J.P., 1981. Nickeliferous Laterite Deposits. Economic Geology, 75th Aniversary Volume: 710-735.

Gorka, M., Sauer, P.E., Lewicka-Szczebak, D., Jedrysek, M.-O., 2011. Carbon isotope signature of dissolved inorganic carbon (DIC) in precipitation and atmospheric CO2. Environmental Pollution, 159(1): 294-301.

Grossart, H.-P., Frindte, K., Dziallas, C., Eckert, W., Tang, K.W., 2011. Microbial methane production in oxygenated water column of an oligotrophic lake. Proceedings of the National Academy of Sciences.

Haffner, G.D., Hehanussa, P.E., Hartoto, D., 2001. The biology and physical processes of large lakes of Indonesia: Lakes Matano and Towuti. The great lakes of the world, 183-192 pp.

Helie, J.F., Hillaire-Marcel, C., Rondeau, B., 2002. Seasonal changes in the sources and fluxes of dissolved inorganic carbon through the St. Lawrence River - isotopic and chemical constraint. Chemical Geology, 186(1-2): 117-138.

Herczeg, A.L., 1988. Early diagenesis of organic-matter in lake-sediments - a stable carbon isotope study of pore waters. Chemical Geology, 72(3): 199-209.

Jarrell, K.F., 1985. EXTREME OXYGEN SENSITIVITY IN METHANOGENIC ARCHAEBACTERIA. Bioscience, 35(5): 298-302.

Jones, C. et al., 2011. Biogeochemistry of manganese in ferruginous Lake Matano, Indonesia. Biogeosciences, 8(10): 2977-2991.

Jørgensen, B.B., Kuenen, J.G., Cohen, Y., 1979. Microbial Transformations Of Sulfur-Compounds In A Stratified Lake (Solar Lake, Sinai). Limnology and Oceanography, 24(5): 799-822.

Karl, D.M. et al., 2008. Aerobic production of methane in the sea. Nature Geoscience, 1(7): 473-478.

Katsev, S. et al., 2010. Mixing and its effects on biogeochemistry in the persistently stratified, deep, tropical Lake Matano, Indonesia. Limnology and Oceanography, 55(2): 763-776.

Kling, G.W., Tuttle, M.L., Evans, W.C., 1989. The evolution of thermal structure and water chemistry in lake nyos. Journal of Volcanology and Geothermal Research, 39(2-3): 151-165.

Konhauser, K.O., 2007. Introduction to Geomicrobiology. Blackwell Publishing, 440 pp.

Konhauser, K.O. et al., 2009. Oceanic nickel depletion and a methanogen famine before the Great Oxidation Event. Nature, 458(7239): 750-U85.

Kuntz, L.B., Laakso, T.A., Schrag, D.P., Crowe, S.A., 2015. Modeling the carbon cycle in Lake Matano. Geobiology, 13(5): 454-461.

Kusakabe, M., Ohsumi, T., Aramaki, S., 1989. The lake nyos gas disaster - chemical and isotopic evidence in waters and dissolved-gases from 3 cameroonian crater lakes, nyos, monoun and wum. Journal of Volcanology and Geothermal Research, 39(2-3): 167-185.

Mah, R.A., Ward, D.M., Baresi, L., Glass, T.L., 1977. BIOGENESIS OF METHANE. Annual Review of Microbiology, 31: 309-341.

Mook, W.G., Bommerso.Jc, Staverma.Wh, 1974. Carbon isotope fractionation between dissolved bicarbonate and gaseous carbon-dioxide. Earth and Planetary Science Letters, 22(2): 169-176.

Myrbo, A., Shapley, M.D., 2006. Seasonal water-column dynamics of dissolved inorganic carbon stable isotopic compositions (delta C-13(DIC)) in small hardwater lakes in Minnesota and Montana. Geochimica Et Cosmochimica Acta, 70(11): 2699-2714.

Oana, S., Deevey, E.S., 1960. Carbon-13 in lake waters, and its possible bearing on paleolimnology. American Journal of Science, 258: 253-272.

Raiswell, R., Canfield, D.E., 1998. Sources of iron for pyrite formation in marine sediments. American Journal of Science, 298(3): 219-245.

Ralph, E.K., Michael, H.N., 1974. Twenty-five Years of Radiocarbon Dating: The long-lived bristlecone pines are being used to correct radiocarbon dates. American Scientist, 62(5): 553-560.

Russell, J.M. et al., 2014. Glacial forcing of central Indonesian hydroclimate since 60,000 y BP. Proceedings of the National Academy of Sciences of the United States of America, 111(14): 5100-5105.

Sabo, E., 2006. Characterization of the pelagic plankton assemblage of Lake Matano and determination of factors regulating primary and secondary production dynamics., University of Windsor.

Sigurdsson, H. et al., 1987. Origin of the lethal gas burst from lake monoun, cameroun. Journal of Volcanology and Geothermal Research, 31(1-2): 1-16.

Stookey, L.L., 1970. Ferrozine - a New Spectrophotometric Reagent for Iron. Analytical Chemistry, 42(7): 779-781.

Tang, K.W., McGinnis, D.F., Frindte, K., Bruchert, V., Grossart, H.-P., 2014. Paradox reconsidered: Methane oversaturation in well-oxygenated lake waters. Limnology and Oceanography, 59(1): 275-284.

Templeton, A.S., Chu, K.H., Alvarez-Cohen, L., Conrad, M.E., 2006. Variable carbon isotope fractionation expressed by aerobic CH4-oxidizing bacteria. Geochimica Et Cosmochimica Acta, 70(7): 1739-1752.

Tilbrook, B.D., Karl, D.M., 1995. Methane sources, distributions and sinks from California coastal waters to the oligotrophic North Pacific gyre. Marine Chemistry, 49(1): 51-64.

Viollier, E., Inglett, P.W., Hunter, K., Roychoudhury, A.N., Van Cappellen, P., 2000. The ferrozine method revisited: Fe(II)/Fe(III) determination in natural waters. Applied Geochemistry, 15(6): 785-790.

Whiticar, M.J., 1999. Carbon and hydrogen isotope systematics of bacterial formation and oxidation of methane. Chemical Geology, 161(1-3): 291-314.

Wicaksono, S.A., Russell, J.M., Bijaksana, S., 2015. Compound-specific carbon isotope records of vegetation and hydrologic change in central Sulawesi, Indonesia, since 53,000 yr BP. Palaeogeography Palaeoclimatology Palaeoecology, 430: 47-56.

Zegeye, A. et al., 2012. Green rust formation controls nutrient availability in a ferruginous water column. Geology.

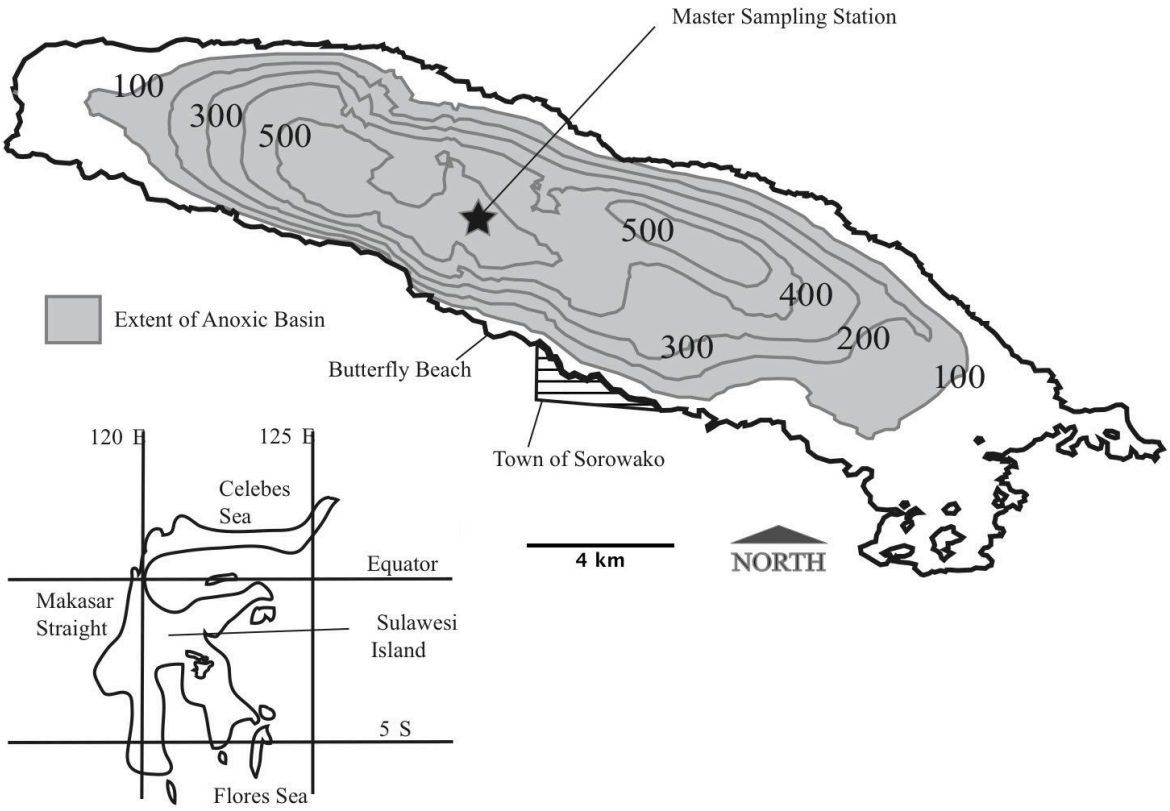

Figure 1 Map of Bathymetry showing the extent of the anoxic basin, location of the deep water master sampling station and the town of Sorowako (modified after Crowe et al.,2008 Biogeosciences)

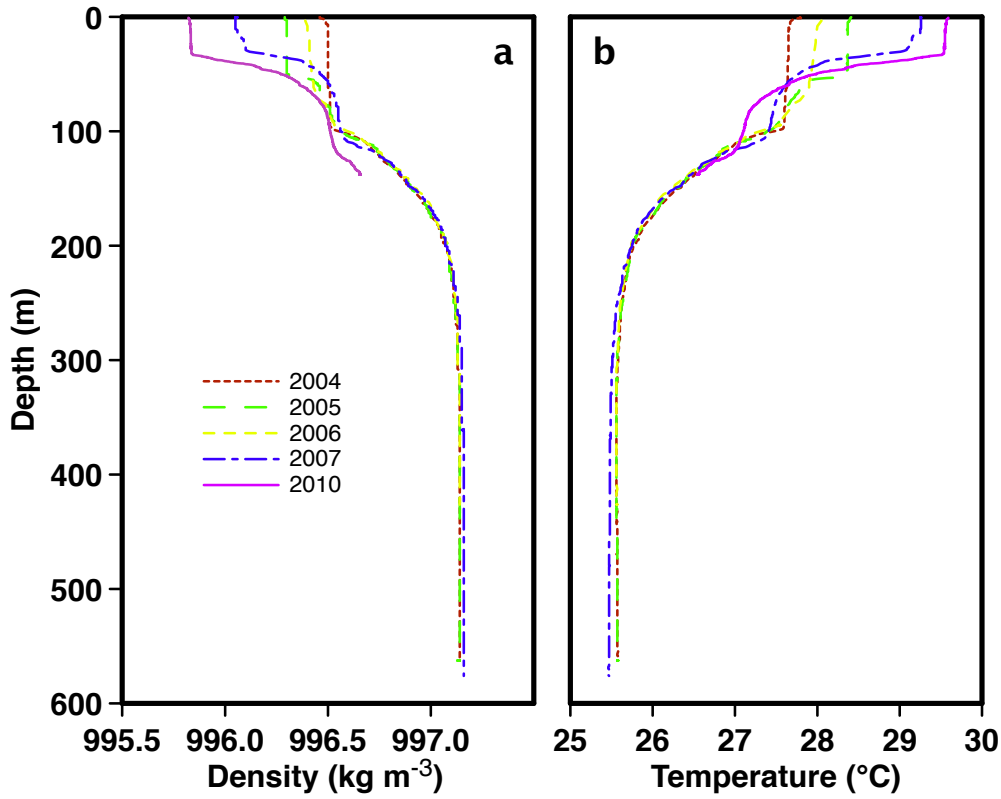

Figure 2. Density and Temperature over several years of Lake Matanos water column, emphasizing the lakes physical Stability

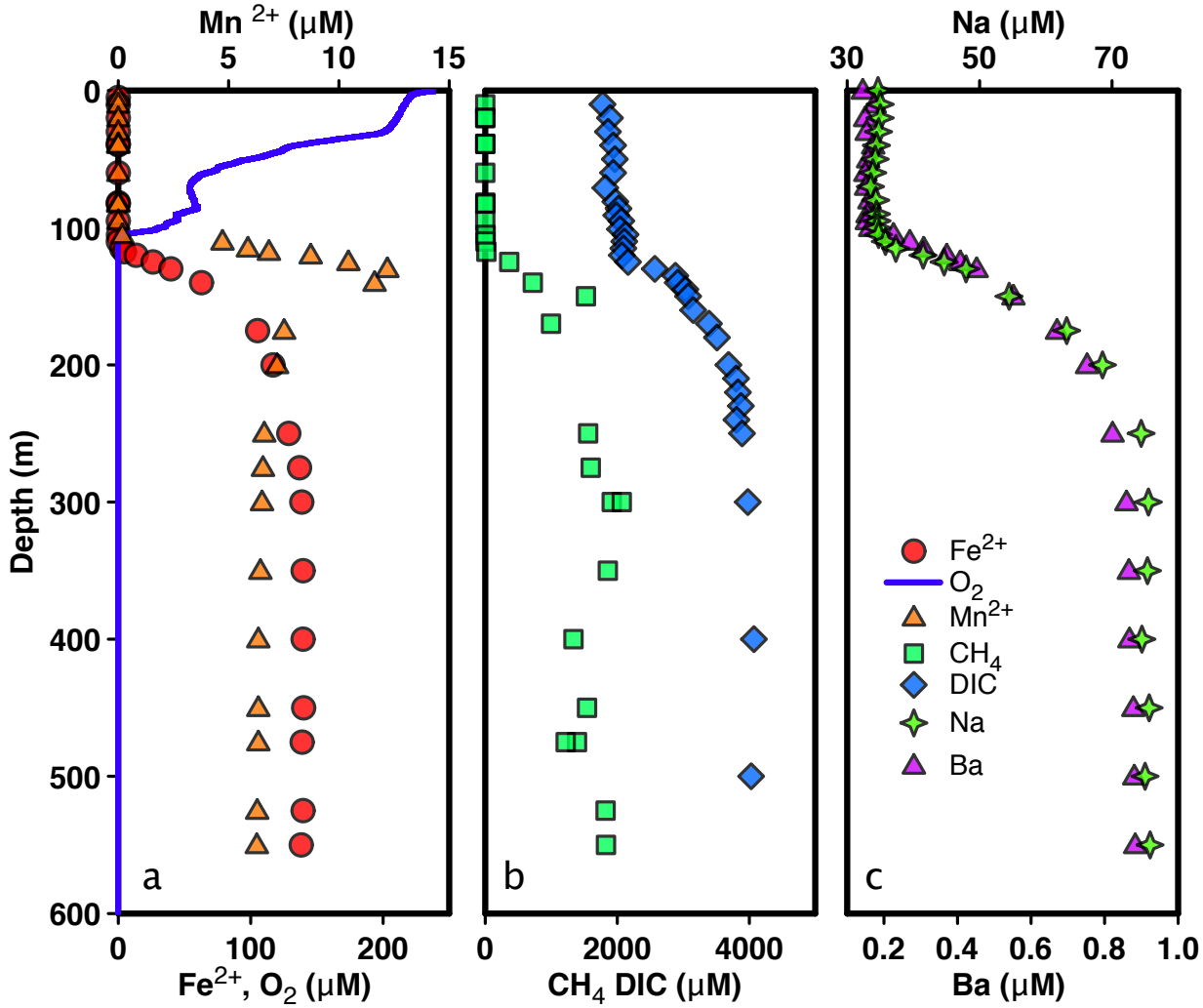

Figure 3 Water column profiles for a) redox elements, b) dissolved gases and c) conservative major elements.

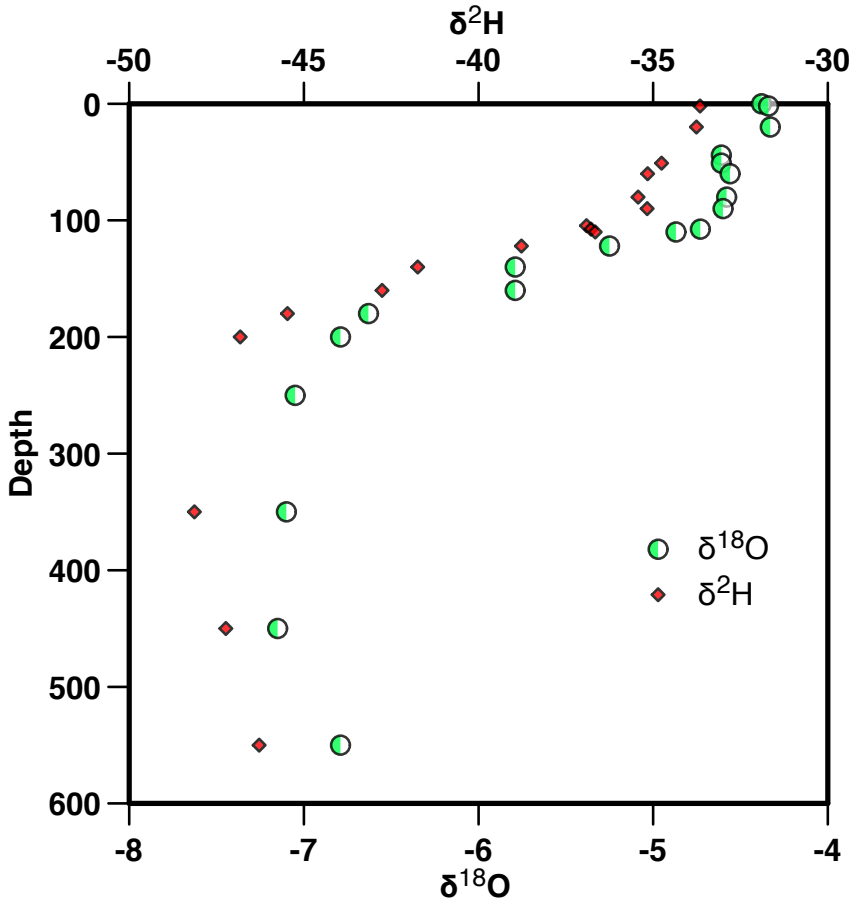

Figure 4 Oxygen and Hydrogen Isotopes in Lake Matanos water column. Heavy Isotope signatures in the surface waters (evaporation) and light isotope values in the bottom waters resulting from groundwater input. The slow diffusion across the pycnocline clearly separates the sources of light and heavy isotope signatures.

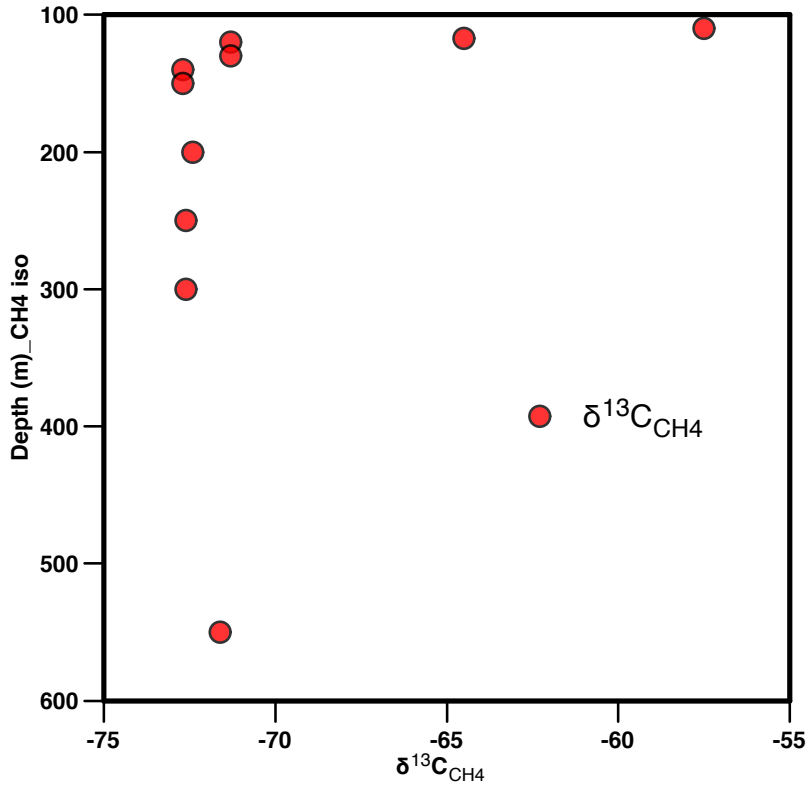

Figure 5 Methane ^{13}C isotope profile of Lake Matano water column 2010.

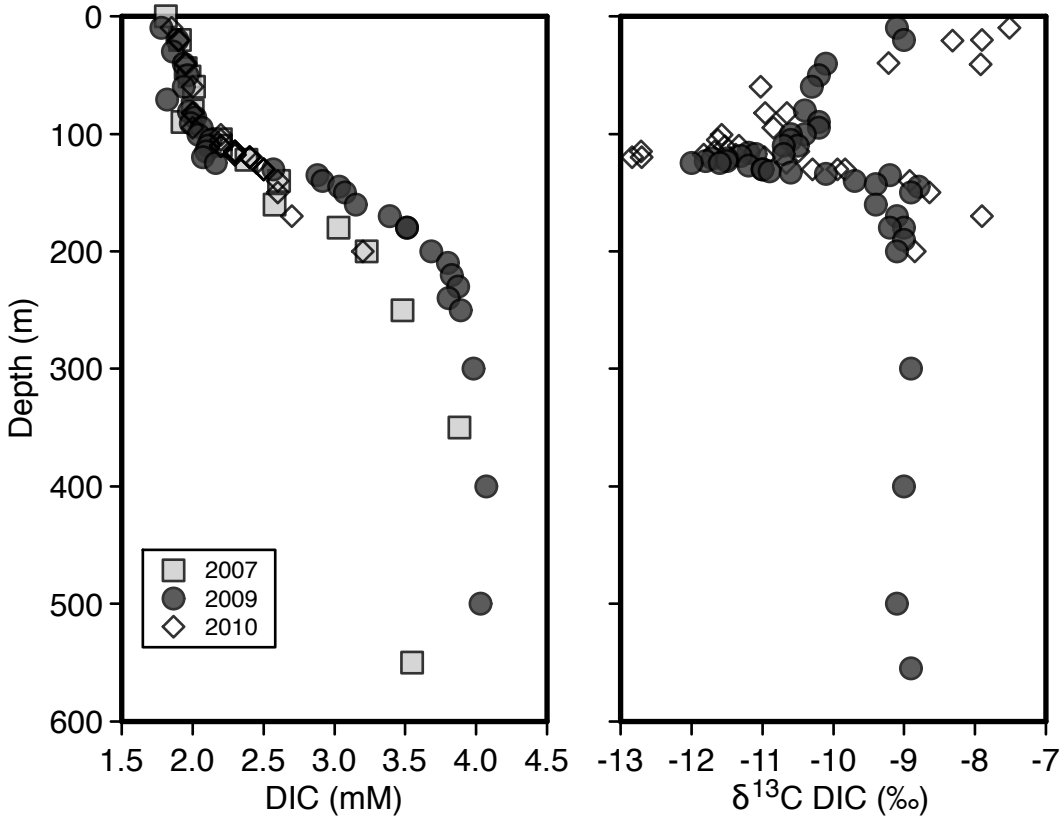

Figure 6 DIC concentrations (2007, 2009, 2010) and Isotope values (2009 and 2010).

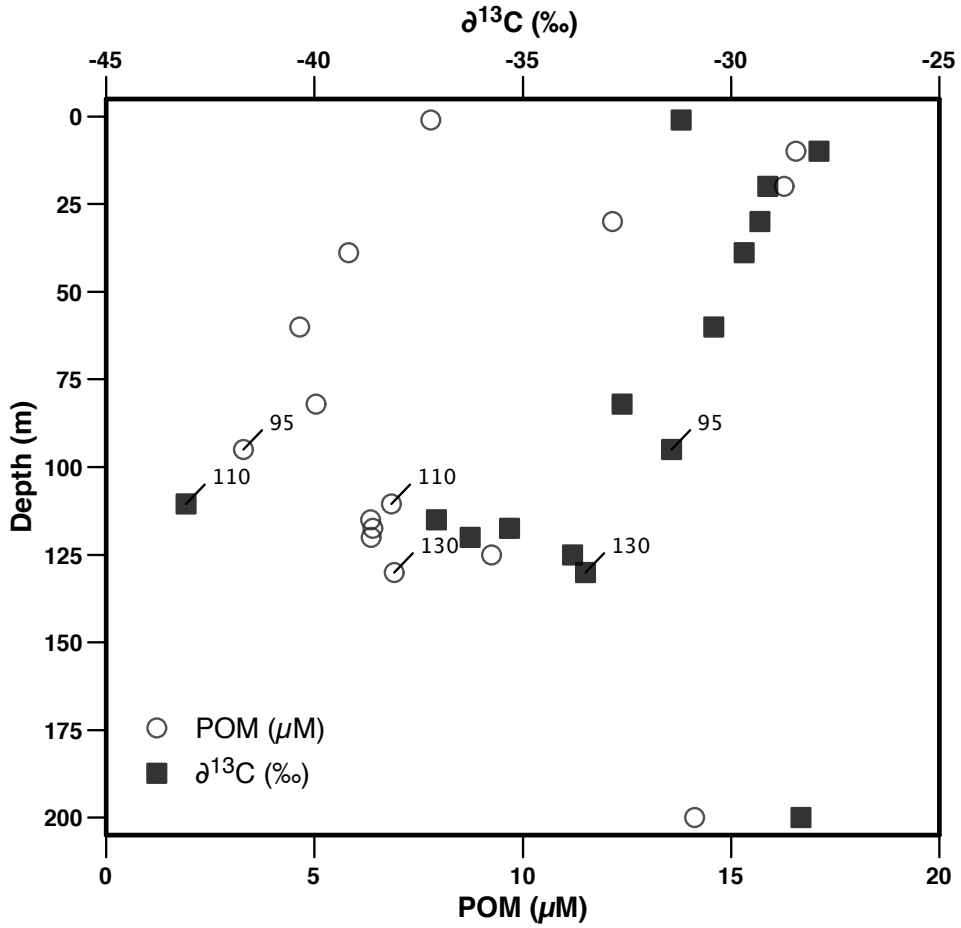

Figure 7 POM concentrations and Isotope values through the mixolimnion and pycnocline.

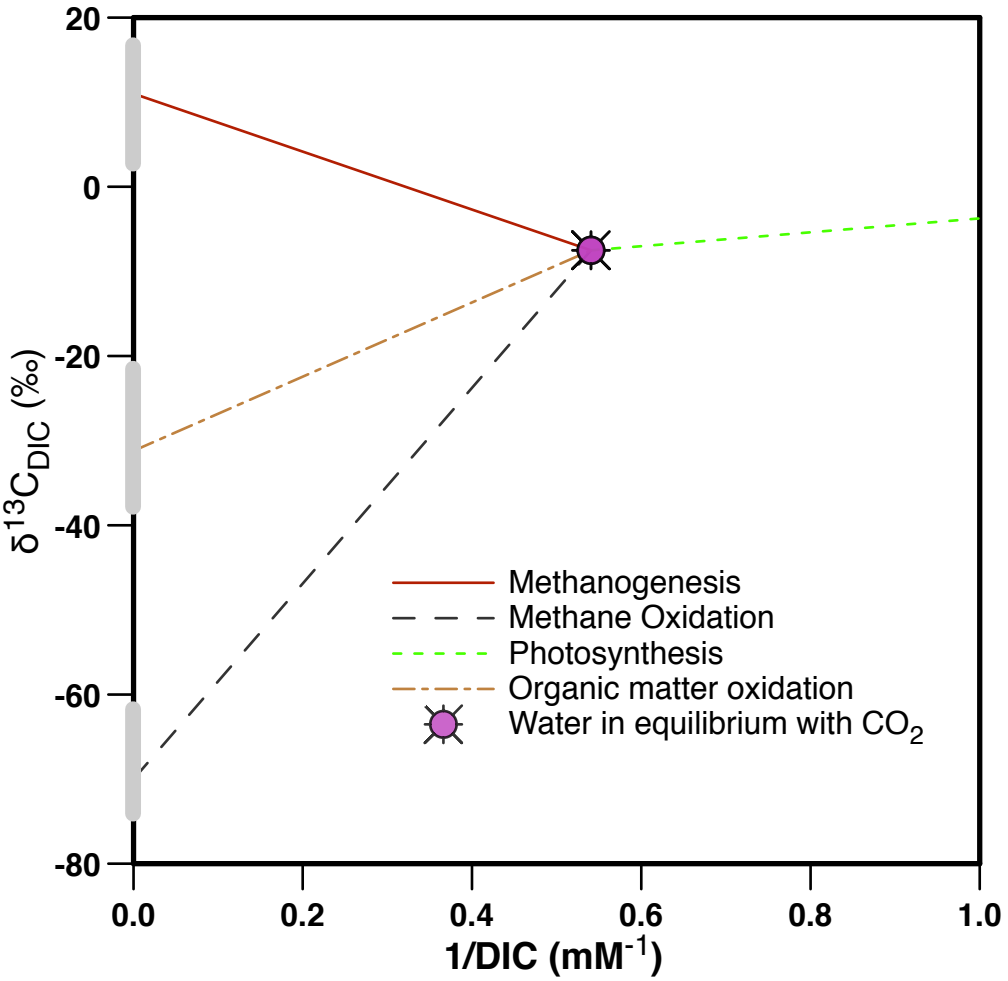

Figure 8 Kelling Plot showing end members and path specific lines for each main processes in Lake Matano

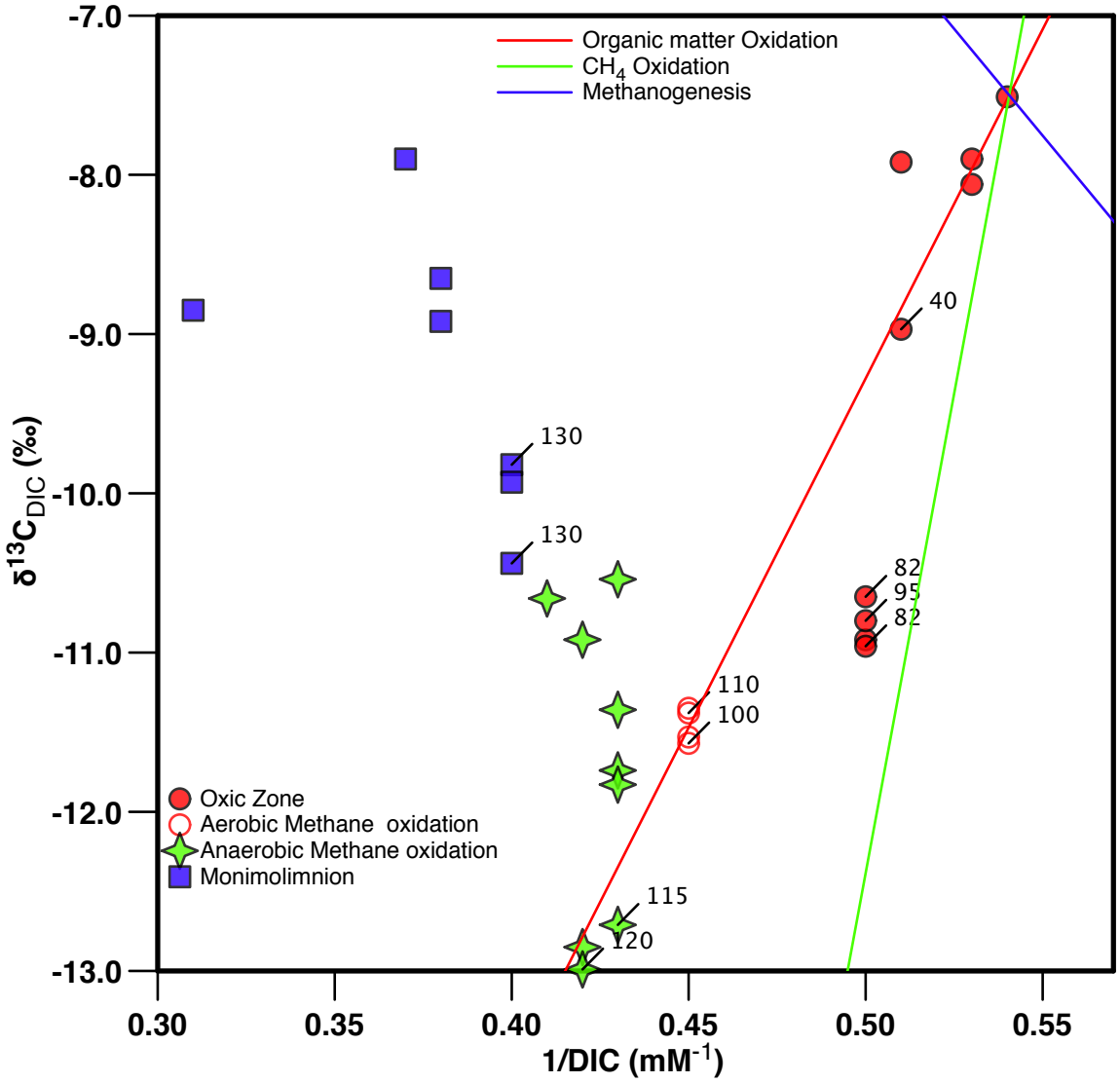

Figure 9 Kelling Plot showing data of the oxic zone (Solid circle), the oxic/anoxic boundary (open circles), zone of of anaerobic methane oxidation (Stars) and Deep water samples (squares). The lines are mixing lines between the surface waters at equilibrium with the atmosphere and the end members of organic matter oxidation, methane oxidation and methanogenesis .

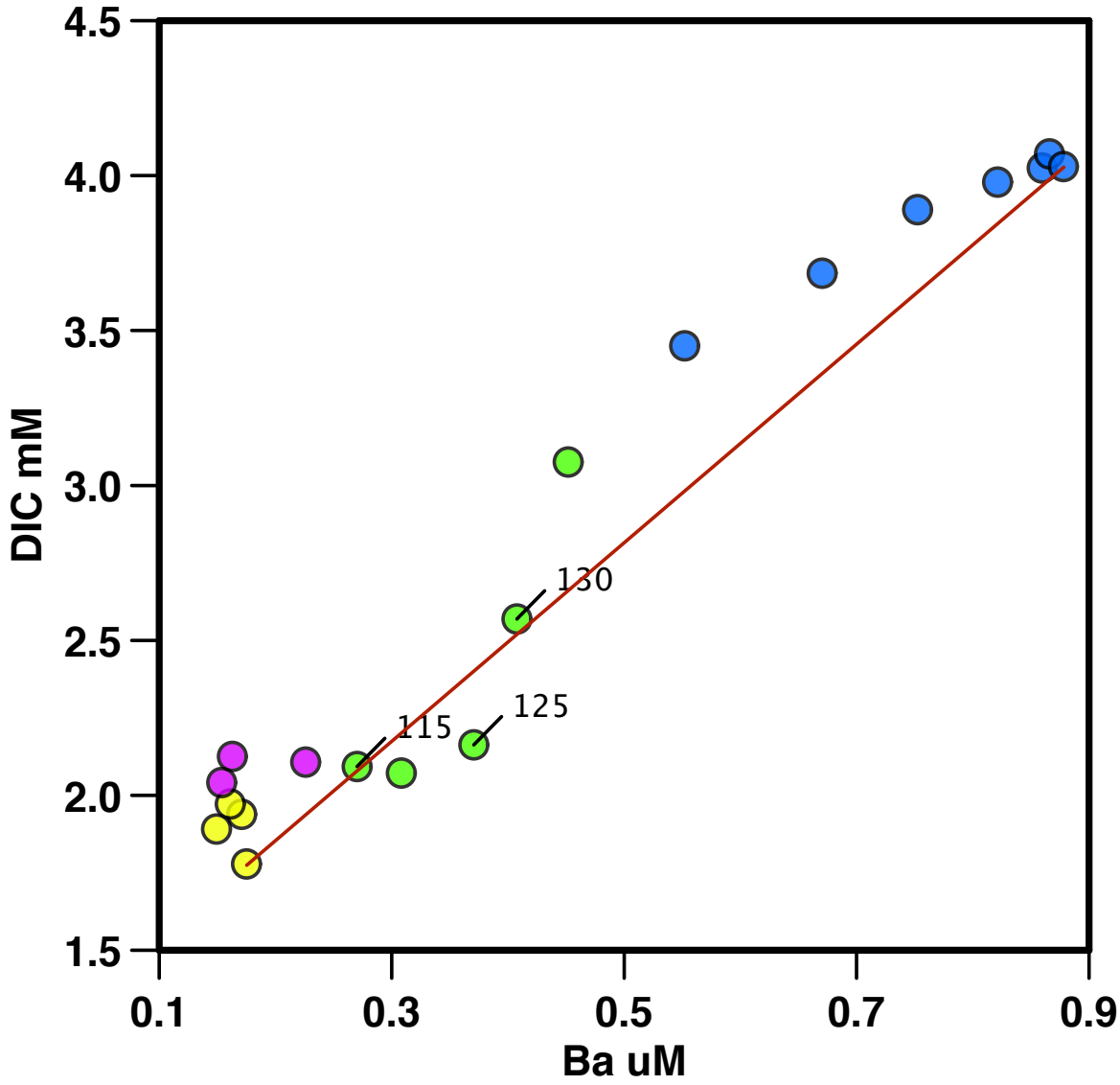

Figure 10 DIC concentration versus Barium. Bottom waters (blue), Pycnocline (green), oxic anoxic Transition zone (purple) and surface waters (yellow).

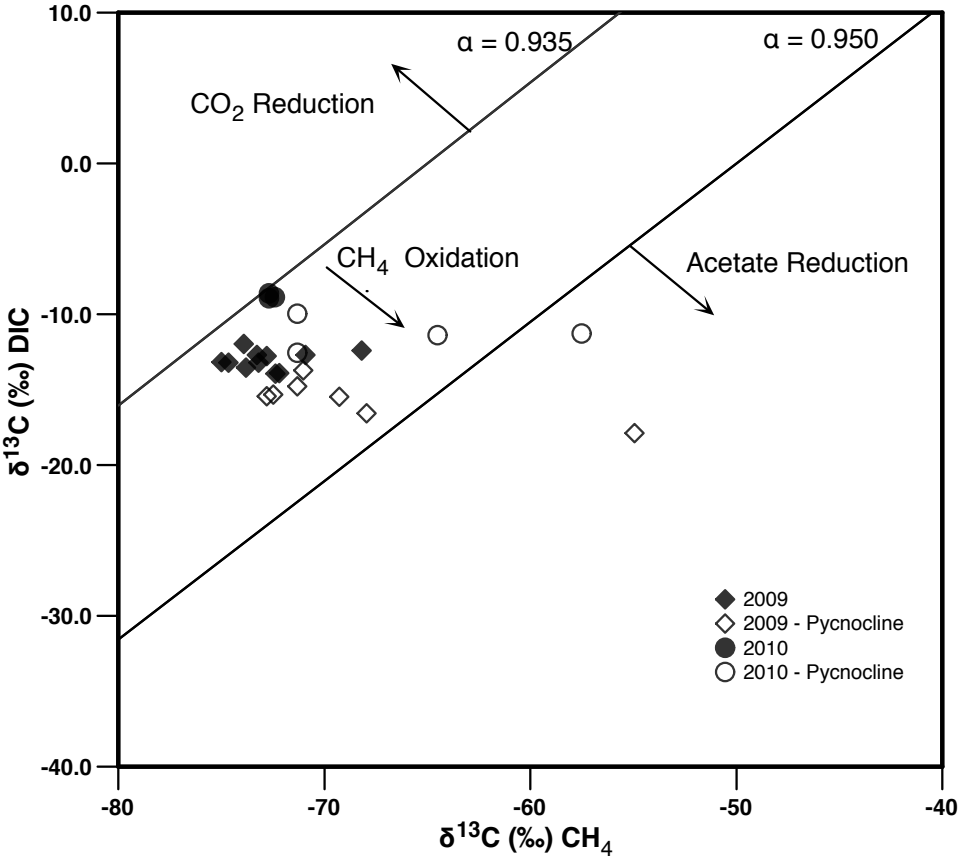

Figure 11 Combination Plot of $\delta^{13}C_{DIC}$ and $\delta^{13}C_{CH4}$ with isotope fractionation lines drawn from isotope separation factors.

Physical Properties of Lake Matano

Catchment Area (km^2)	436
Lake Surface Area (km^2)	164
Anoxic Basin Surface Area (km^2)	100
Elevation lake surface (m)	380
Temp change from surface to bottom (°C)	3.5
Volume (km^3)	38
Oxic basin Volume (km^3)	11.4
Anoxic basin Volume (km^3)	26.6
Radiation Average input (Wm^{-2})	173
Hydrological Budget Data	
Annual Precipitation (mm $year^{-1}$)	2875
Evaporation from Rainforest (%)	52
Combined inflow from Catchment (m^3 s^{-1})	11.9
Surface Evaporation Average (m^3 s^{-1})	10.4
Precipitation Average on lake surface (m^3 s^{-1})	14.9
Outflow Petea River (m^3 s^{-1})	16.4

Table 1 Physical Data for Lake Matano

Kz in m^2 d^{-1}	2007	2009	2010
Kz from SRR	0.09 – 0.2 (Crowe et al 2011)	0.31	0.10
Kz from Thorpe	0.432	0.65±0.02	0.27±0.02
Kz from Modeling	0.86 3D Model		
Katsev et al. 2010	0.48 1D Model		
	0.5 Thorpe displacement		
	0.086 – 0.86 Brunt–Väisälä correlation		
Crowe et al. 2008	0.39 Brunt–Väisälä correlation		

Table 2 Summary of previously determined Kz values for Lake Matano.

Parameters and results for calculations of groundwater inflow and Evaporation			
A (m^2)	10E+8	$\delta^{18}O_P$(‰) (Katsev et al. 2010)	-10.6
Kz(m^2 d^{-1})	0.2	$\delta^{18}O_{Pe}$ (‰)	-4.4
e (m)	32	$\delta^{18}O_{Lw}$ (‰)	-8.7
$\delta^{18}O_{mix}$ (‰)	-4.6	Q_{Lw} (m^3 s^{-1})	9.51
$\delta^{18}O_{mon}$ (‰)	-5.2	Q_{Pe} (m^3 s^{-1})	16.42
$\delta^{18}O_G$ (‰)	-8.6	Q_P (m^3 s^{-1})	14.94
$\delta^{18}O_{ev}$ (‰) (Majoube, 1971)	+9.1	Q_G (m^3 s^{-1})	2.0

Table 3 Aqueous oxygen isotope data and physical system parameters water budget modeling.

Parameters and results for carbon model calculations			
A (m^2)	10E+8	$\delta^{13}C_{CH4\ mix}$ (‰)	-57. 5
Kz ($m^2\ s^{-1}$)	$2.315x10^{-6}$	$\delta^{13}C_{CH4\ DIC}$ (‰)	-61.5
dx (m)	10	$\delta^{13}C_{La}$(‰)	-22.23
$\delta^{13}C_{mix}$ (‰)	-7.51	Q_{La} (mol s^{-1})	19.02
$\delta^{13}C_{pyc}$ (‰)	-10.5	Q_{Pe} (mol s^{-1})	27.01
$\delta^{13}C_{mon}$ (‰)	-11.6	Q_{pre} (mol s^{-1})	0.198
$\delta^{13}C_{atm}$ (‰)	0	$d[DIC]_{CH4}$ (mol m^{-3})	0.051
$\delta^{13}C_{POM}$(‰)	-30	$d[DIC]_{mon}$ (mol m^{-3})	0.45
Q_{atm} (mol s^{-1})	24.71	Q_{POM} (mol s^{-1})	4.58
Q_{gr} (mol s^{-1})	4.8	$\delta^{13}C_{pre}$ (‰)	0
$\delta^{13}C_{gr}$(‰)	-22.05	$\delta^{13}C_{POMmon}$(‰)	-30
Q_{POMmon} (mol s^{-1})	0.11	$\delta^{13}C_{DIC\ CH4}$(‰)	12.5
$\delta^{13}C_{CH4\ exp}$ (‰)	-71		

Table 4 Parameters for Modeling Calculations for Carbon budget in lake Matano

Chapter 4: Biogeochemical controls on Copper Cycling in a Ferruginous Ancient Lake

Abstract:

We have analyzed the distribution of Copper (Cu) in ferruginous, permanently stratified Lake Matano—A modern analogue for iron dominated oceans of Precambrian Eons. There is a dearth of Cu in Lake Matano with measured concentrations that are much lower than typical freshwaters (110 nmol l^{-1}) as well as most oceanic environments (1-5 nmol l^{-1}). Using a combination of selective chemical extractions, geochemical modeling, and X-ray spectroscopy, we find that the distribution of Cu is strongly controlled by particulate organic matter throughout the lake. Within the Lake's chemocline we find evidence for the redistribution of Cu, possibly related to respiration of particulate organic matter, and redox reactions of Fe, Mn, and S. Indeed, evidence points to an important role for Cu-sulfide species despite the very low overall sulfide concentrations that characterize this ferruginous environment. Overall, we find that a variety of particulate phases control Cu speciation and distribution in Lake Matano, and we suggest that, by extension, organic particles and sulfides need to be considered in models of Precambrian marine Cu biogeochemistry, even under ferruginous conditions.

1. Introduction

Copper (Cu) is a critical micronutrient used by microorganisms as a co-factor in several enzymes and as such is essential to life. Some copper based enzymes are needed for

denitrification (Zumft, 1997), ammonia oxidation (Zahn et al., 1996), iron oxidation (Ilbert and Bonnefoy, 2013), photosynthesis (Katoh, 2003) and methanotrophy (Hakemian and Rosenzweig, 2007), for example. These microbially catalyzed reactions play key roles in global biogeochemical cycles, today, and in the past. Through their control on concentrations and distributions of principal chemical species (e.g. O_2, Fe, HS^-), redox conditions exert an important control on the cycling and availability of Cu. Under the modern, well oxygenated atmosphere, oxic conditions prevail in near surface environments(Canfield and Thamdrup, 2009). Physical stratification and other barriers to O_2 transport, like low porosity in soils or sediments, together with O_2 demand can lead to the consumption of O_2 and the development of anoxia (Canfield and Thamdrup, 2009). In the distant geologic past, however, atmospheric O_2 concentrations were low, and anoxia generally prevailed (Canfield, 1998).

Under anoxic conditions the availability of alternative electron acceptors like sulfate or ferric Fe plays an overwhelming role in regulating the principle dissolved chemical species. Anoxia can be broadly classified as euxinic when sufficient availability of sulfate favors anaerobic respiration through microbial sulfate reduction leading ultimately to the accumulation of hydrogen sulfide (H_2S) (Canfield and Thamdrup, 2009). When sulfate availability is low, but ferric Fe is in abundant supply, respiration proceeds through dissimilatory Fe reduction, and ferrous iron accumulates leading to ferruginous conditions. The overwhelming abundance of sulfate in modern seawater leads to a prevalence of euxinic conditions in anoxic marine waters today. Indeed, the oxidative weathering of continental rocks also leads to appreciable sulfate in freshwaters, which tend also to develop euxinia when O_2 transport from the atmosphere is restricted. Throughout much of geologic history, however, sulfate abundances at Earth's surface were low and anoxic environments including the deep oceans were generally ferruginous

(Canfield et al., 2008; Poulton and Canfield, 2011). With some notable exceptions (Lake Kivu, Lake Malawi, Lake Pavin, Lake La Cruz, Lake Matano), ferruginous conditions are rare on Earth today.

The biogeochemical cycling of Cu, and its dissolved concentrations, speciation, and bioavailability differ dramatically under oxic, ferruginous, and euxinic conditions (Saito et al., 2003). Under aerobic conditions, Cu partitions between sorption to relatively low abundance Fe and Mn oxyhydroxides, association to organic matter, and stabilization as dissolved chelated organic complexes or sulfide colloids (Masson et al., 2011; Pokrovsky et al., 2012; Weber et al., 2009). As a chalcophyllic element, Cu speciation under euxinic conditions is overwhelmingly dominated by reactions with HS^- and the generally very low solubility ($\log K = -36.2$), of Cu sulfides tends to limit dissolved Cu concentrations to pmol l^{-1} (Anbar and Knoll, 2002; Dupont et al., 2010; Saito et al., 2003). Under ferruginous conditions, sulfide concentrations are very low, but Cu sorption to high abundance, strong affinity, high surface area Fe oxyhydroxides is expected to maintain very low dissolved Cu concentrations. While modern euxinic basins have provided real world tests for the behavior of Cu under euxinia, biogeochemical cycling of Cu under ferruginous conditions remains largely untested. Lake Matano is a large modern ferruginous basin with biogeochemistry similar to the ferruginous environments and oceans of the Precambrian Eons(Crowe et al., 2008a). We have examined the biogeochemical behavior of Cu in Lake Matano, and as predicted for ferruginous environments in general, we find very low dissolved Cu concentrations. We also, however, find that Cu is strongly associated with organic matter and microbial biomass, and that within the chemocline, Cu sulfide species can form and may play an important role in dictating dissolved Cu concentrations, even under ferruginous conditions.

2. Methods

2.1 Sampling for general limnology and geochemistry

Samples were collected in May 2009 at a deep water master station (2°28'00''S and 121°17'00''E) (Crowe et al., 2008b). Niskin bottles (5LGo-Flow, General Oceanics, Miami, FL.USA) were used with a manual winch setup in conjunction with a Furuno FCV585 fish finder to sample at depths < 100m and >140m. Bottles were placed at depth by echolocation , achieving an accuracy and precision of ± 1m, for the intermediate depths >100m and <140m a pump profiling method was used (Jones et al. 2011), where water was pumped up from sampling depth using a double-conical pump intake (Joergensen et al 1979) capable of sampling a horizontal layer <2cm thick. A conductivity, temperature, depth (CTD probe (Sea and Sun Technologies) was fastened to the intake allowing very accurate (~10cm) vertical intake placement during pumping. Three or more tubing volumes were flushed through the pump system and tubing before samples were collected. Conductivity, Oxygen concentrations and Temperature were determined using the CTD, which was equipped with the following array of sensors: oxygen, Oxyguard Ocean (2009), Oxyguard Profile (2010) (detection limit ~1% saturation, precision ± 1% saturation), Temperature (SST PT100, accuracy ± 0.005 °C, precision ± 0.001 °C), conductivity (SST 7-pole platinum cell, accuracy ± 0.005 mS cm^{-1}, precision ± 0.0001 mS cm^{-1}), light (LICOR PAR Sensor 193 SA, Accuracy ± 5%, detection limit 0.01 μmol m^{-2} s^{-1}), and turbidity (Seapoint). Oxygen concentrations were also determined by classical Winkler titrations (detection limit 6μmol l^{-1}, (APHA, 1985; Rose and Long, 1988)) and the location of the oxycline was verified at the surface independently in pumped water with a potentiometric Clark-style microelectrode (Unisense, detection limit 0.2μmol l^{-1}) and voltametry

using Au/Hg amalgam microelectrodes (detection limit 1μmol l^{-1}(Brendel and Luther, 1995)). Iron(II) samples were withdrawn directly from the spout of the Niskin bottle or the pump stream and fixed immediately in ferrozine reagent. Samples for major elements were taken from Niskin bottles with acid washed plastic syringes and filtered through 0.2 μm syringe filters (polycarbonate, nucleopore), or were pumped from depth through 0.2 μm syringe filters (polycarbonate, nucleopore) directly into acid clean 60 ml HDPP bottles. Samples were then acidified to 2% with trace metal grade nitric acid.

2.2 Sampling for Cu

To minimize the chance of metal contamination we conducted our sampling for Cu analyses from a small rubber dinghy, which was wiped down with acetic acid and rinsed with lake surface water prior to use. The dinghy was towed to our central master sampling station using local fishing boats. The dinghy was paddled using plastic oars several hundred meters from the fishing boat. Samples were taken with a single 5 L Go-Flow bottle (Niskin; General Oceanics, Miami, FL, USA), lowered on a braided nylon cord and triggered with a painted brass messenger wrapped in several layers of Teflon tape. Niskin bottles were cleaned with Acetic acid, de-ionized water, and filtered lake surface water prior to sampling, and between samples. Samples were filtered through 0.2 μm Teflon syringe filters, were stored at 4°C in HDPP Bottles and acidified to 2% with optima grade HNO_3. Prior to sampling the HDPP bottles were acid washed overnight consecutively in 13% HCl and 13% HNO_3, after which they were rinsed 5 times with 18 MΩ cm^{-1} Milli-Q water (HMD Millipore) and dried in a HEPA filtered laminar airflow cabinet.

2.3 Solid Phase Samples

Particles from the water column were recovered by filtration, pumping water from depth through an in-line filtration device at the surface onto 0.2 μm Nucleopore polycarbonate filters. Our filtration device was situated in an N_2 filled glove bag to avoid oxidation during filtration. Air tight vials were used to store the filters under and N_2 atmosphere at 4°C in the dark until they were analyzed. For determining particulate Mn and associated elements (Cu), two assays were used, an acidified peroxide extraction (0.5N HNO_3 and 30 % peroxide applied for 0.5 hours), from here on referred to as (Org-PO) and a 0.1M hydroxylamine-HCl assay applied for 2 hours, referred to as (Mn-HA). The Org-PO digestion targets reactive Mn phases but also liberates appreciable metals from organic matter(Neaman et al., 2004). The Mn-HA extraction is able to dissolve pure Mn-minerals, pyrolusite, birnesirte, δMnO_2 and lithiophorite, as well as small amounts of Fe minerals (<20%) (Jones et al., 2011; Neaman et al., 2004). Cases where Org-PO exceeds Mn-HA imply Cu association to particulate organic carbon. For biologically reactive Fe phases, a one hour 0.5M HCl extraction (Fe-HCl) was used (Cooper et al., 2000; Lovley and Phillips, 1986) and a 6M HCl sub boiling (100 °C, 24hr) extraction was used to retrieve totals (Lovley and Phillips, 1986; Poulton and Canfield, 2005). The Mn specific extractions were performed in parallel and the Fe targeting and total extractions were performed sequentially, the extracts were analyzed on an ICP-OES (Perkin Elmer Optima 5300 DV).

2.4 General Analysis

Samples for Fe(II) were stored refrigerated and analyzed by standard spectrophotometric methods (Stookey, 1970; Viollier et al., 2000) with in 8 hours of sampling. Sulfate was measured by ion chromatography (Dionex ICS 1500, with an IONpac AS22 anion column and suppressor),

nitrite and nitrate were combined (NO_x) and determined by chemiluminescence (Braman and Hendrix 1989). Major element samples were run on an Inductively Coupled Plasma-Optical Emissions Spectrometer (ICP-OES; Perkin Elmer Optima 5300 DV).

2.5 ICP-MS measurements

Analyses for elemental Cu concentrations were made on a Perkin-Elmer NexION 300 quadrapole Inductively Coupled Plasma-Mass Spectrometer (qICP-MS). Before analysis the instrument was allowed to warm up and tuning was preformed using SmartTune (Perkin-Elemer) solution. Multi-element standard Stock-4 was used for calibration at 5ppb Cu. Milli-Q (18 $M\Omega cm^{-1}$) acidified to 2% HNO_3 was used for dilutions and as a blank, while SLRS-5 (NRC) river water standard was used as a certified reference material (CRM). The average measured Cu concentration of the CRM was 18.6±0.5ppb, within error of the certified value of 17.4±1.3ppb. Acidified samples, standards, CRM, and blanks were spiked with 100ppb Sc as an internal standard. The blank and CRM were analyzed every 5-6 samples to account for any instrumental drift throughout the analyses. A sample rinse of 1% HNO_3 was run for 2 minutes between samples to prevent any carry over between sample runs.

2.6 Synchrotron based speciation

Particulate matter samples were collected and then preserved on polycarbonate filters (142 mm). Maps for Micro X-ray Fluorescence (μXRF) and (micro) X-ray absorption near edge structure (XANES and μXANES) spectra were collected at the Advanced Photon Source (APS) on beamline 20-BM-B (PNC-CAT) at Argonne National Laboratory, Illinois. Samples were

mounted in a plastic holder oriented 45° to the beam in the horizontal plane. A pair of Kirkpatrick –Beaz mirrors and a Si(111) double monochromator were used to focus a monochromatic X-Ray beam onto the sample. Filters were subsampled and pieces of the filter paper were sealed in kapton film under N_2 atmosphere. Elemental maps using μXRF were collected using monochromatic X-rays focused to a spot size of 5 by 5 μm and tuned to 14000 eV (λ = 5.508 nm). The sample was mapped in step sizes of 5μm with an exposure time of 1 second per step. X-ray fluorescence emission spectra were collected simultaneously for 9 elements (Ti *Kα*, V *Kα*, Cr *Kα*, Mn *Kα*, Fe *Kα*, Co *Kα*, Ni *Kα*, Cu *Kα*, and Zn *Kα*). Integrated counts of the raw intensity data for Fe, Mn and Cu were calibrated to mols using the concentration values determined from total extractions of the filter membranes. More details on the beam line setup and calibrations can be found in Jones et al 2011.

2.7 Modeling

Saturation indices and speciation calculations were performed using the geochemical modeling software Geochemist's Workbench Version 10 (Aqueous Solutions LLC, Champaign, IL, USA) specifically using the geochemist spreadsheet and React. Data used for the calculations included all major cations and anions, pH and the relevant redox pairs for each depth. Calculations indicated the system was charge balanced within 2%.

3. Results and Discussion

3.1 General Limnology

Lake Matano is a persistently stratified tropical lake on Sulawesi Island, Indonesia, it has a depth of about 600 meters and has an extensive ferruginous basin below about 110m depth

(Figure 1). At the time of sampling (Jan-Mar 2009) the lake was similar in both physical structure (Figure 2) and chemical composition to previous studies of the lake (Crowe et al., 2011; Crowe et al., 2014; Crowe et al., 2008b), where a permanent pycnocline was present around 110m (Figure 3) separating the oxygenated mixolimnion from the poorly ventilated bottom waters (monimolimnion). Here we define the waters to be anoxic at the depth where no O_2 was undetectable (>0.2 μmol l^{-1}) and Fe(II) was detectable (>0.5 μmol l^{-1}) . The zone where O_2 was below the detection limit but no Fe(II) or sulfide was detected we define as the oxic-anoxic transition zone, as we cannot rule out the presence of trace O_2 at these depths. The mixolimnion also exhibited a seasonal pycnocline, which was present at 30m at the time of sampling. Redox active species (e.g. H_2S^-, Fe^{2+}, Mn^{2+}) displayed (Figure 3) the expected redox cascade (Canfield and Thamdrup, 2009) in the water column with Mn and O_2 profiles overlapping within a narrow depth interval near the permanent pycnocline (as defined in section 3.1 of chapter 2) (Jones et al., 2011). This is prototypical and a result of the generally slow reaction kinetics of Mn-oxidation at low O_2 concentrations (Luther, 2005; Morgan, 2005). Ammonium (NH_4^+) and Fe^{2+} were both below detection in the mixolimnion, but concentrations sharply increase below the permanent pycnocline and are nearly constant at depths greater then 250m. In the lower mixolimnion, Nitrite (NO_2^-) and Nitrate (NO_3^-) accumulated, and combined (NO_x) reached 8 μmol l^{-1} in the vicinity of the permanent pycnocline at 120 meters. Notably, Mn and Fe particulates also showed concentration increases near the pycnocline, indicative of oxidation of upward diffusing Fe(II) and Mn(II) upon O_2 (Jones et al., 2011).

3.2 Aqueous Cu concentrations

As predicted, copper concentrations ranging from 0.44 to 0.13 nmol l^{-1} (Figure 4) in the surface waters of lake Matano are orders of magnitude lower than typical freshwaters and seawater which are generally in the single to hundreds of nmol l^{-1} range (e.g. average stream water (110 nmol l^{-1}), average seawater (4.72 nmol l^{-1})) and other lakes and rivers (1.63 to 680 nmol l^{-1}) (e.g. Table 1). At <0.44 nmol l^{-1} concentrations in the lake are comparable to the North Pacific (0.5 nmol l^{-1}) (Bruland, 1980) and lower than in the North Atlantic surface waters (1 nmol l^{-1}) (Bruland and Franks, 1983), which are some of the lowest aqueous concentrations measured in aquatic ecosystems.

Within the vicinity of the permanent pycnocline, Cu concentrations are somewhat variable, suggesting some dynamics with respect to the redistribution of Cu between various particulate phases and the dissolved phase, which we address in more detail in section 3.3 below. Within this depth interval, however, dissolved Cu concentrations (Figure 4) reach some of their highest values of up to 0.35 nmol l^{-1}, which, though still low, may signify the release of Cu from sinking particulates in response to the redox reactions that characterize this depth interval (see section 3.1). In the deep monimolimnion, Cu concentrations reach 0.13 nmol l^{-1}, higher than the mixolimnion, suggesting that different, yet currently unresolved controls on concentration operate in these two water masses. Overall, our data from Lake Matano illustrate that ferruginous conditions can be associated with low overall dissolved Cu concentrations. To gain more detailed insight into the role of particulate matter in controlling Cu speciation, we have conducted a suite chemical and X-ray spectroscopic analyses to test Cu associations to different phases.

3.3 Particulate Cu Concentrations and speciation

Particulate Cu concentrations (Figure 4) in Lake Matano range from 0.87 - 0.09 nmol l^{-1}, illustrating that particulate Cu is generally, though not dramatically, more abundant than dissolved Cu. This implies that particles play a key role in Cu speciation within the Lake. A prediction about ferruginous environments in general is that particulate Cu speciation is dominated by sorption to or co-precipitation with Fe (oxy)hydroxides (Coughlin and Stone, 1995; Tessier et al., 1996), and that these Fe (oxy)hydroxides therefore limit dissolved Cu concentrations. To test this prediction we conducted a suite of sequential extractions to target Cu associated with reactive particulate Fe, Mn, and organic particles. These extractions reveal (Figure 5) that Cu is distributed through a variety of different phases depending on the depths considered.

The Org -PO extraction is designed to liberate Cu associated with either Mn oxyhydroxides, or organic matter (Neaman et al., 2004), while the 0.1 M Mn-HA extraction liberates Cu exclusively associated with Mn oxyhydroxides. The Fe-HCl extraction liberates Cu associated with reactive Fe oxyhydroxides (generally ferrihydrite). While definitive assignment of Cu to specific phases based on sequential extractions is not strictly possible, some general observations can be made. Strikingly, the Org-PO extraction liberated more Cu than the Mn-HA or Fe-HCl extractions from particles in the mixolimnion (Figure 5). This indicates that an important component of the particulate Cu in the mixolimnion is associated with organic particles. Since the Mn-HA liberates Cu exclusively from Mn oxides, while the Fe-HCl extraction should dissolve Fe and Mn oxyhydroxides, we can estimate that 2-10% of the Cu in mixolimnion particles is associated with organic materials and 2-10% is associated with reactive Mn and Fe oxyhydroxides (Figure 5). The remaining 85-90 % of the Cu in mixolimnion particles

is associated with poorly reactive phases, which could be soil particulate from the surrounding laterites.

Abundant reactive authigenic Mn and Fe oxyhydroxides are generated within the vicinity of the permanent pycnocline (Crowe et al., 2008b; Jones et al., 2011). The near equivalence of Cu liberated by the 3 extractions between 116.8 and 118.6m depth indicates association principally to Mn and Fe oxyhydroxides, and this is consistent with the accumulation of these phases within this depth interval (Jones et al., 2011; Zegeye et al., 2012). Strikingly, Cu liberated by the Org-PO extraction is a substantial component of the particulate Cu between 120.5 and 122.5m, and is therefore likely associated with organic particles or biomass. Organic associated Cu may, indeed, represent more than about 20% of the total reactive particulate Cu in this depth interval. This implies redistribution of Cu from aqueous and particulate Fe and Mn oxyhydroxides into particulate organics or biomass, and is suggestive of uptake by methanotrophic and nitrogen metabolizing organisms for their enzymatic requirements. Notably, particulate Cu concentrations are highest within this depth interval, which also implies not only that organic particles or biomass exert a key control on Cu speciation here, but likely also throughout the Lake as a whole. Cu speciation in deeper depths is harder to interpret, yet the generally appreciable fraction of Cu extracted with Org-PO and the correspondingly smaller fraction of Cu liberated with Mn-HA and Fe-HCl implies some association with organic matter, except at 124.5m. Fe-HCl liberates marginally more Cu at 124.5 and 129m, which can be attributed to Cu associated with Fe oxyhydroxides and/or acid volatile sulfides. General support for Cu association with organic particles also comes from strong linear correlations between particulate Cu concentrations and POM concentrations (Figure 6). A role for acid volatile sulfide species comes from thermodynamic considerations of the solubility of Cu containing sulfide

minerals. These calculations reveal supersaturation in Chalcopyrite and Covellite mineral phases (Table 2).

Overall, our chemical data imply that particulate Cu in Lake Matano is distributed between a diversity of different reactive and non-reactive phases. Organic particles or biomass appears to be an important component of the reactive particulate Cu fraction, and may ultimately play an important role in maintaining low dissolved Cu concentrations. Sulfides may also play a key role within narrow intervals in proximity to the permanent chemocline in which HS- accumulates to low but detectable concentrations. The very low solubility of Cu HS- species may restrict dissolved Cu concentrations to very low levels within this depth interval. Further support for these observations comes from synchrotron based μXRF analyses, as described below.

Spatially resolved μXRF concentration maps illustrate the distribution of Mn, Fe and Cu on the filter membranes and these maps let us visually correlate the distributions of different elements. Map data along with scatter plots (Figure 7) for concentrations of Cu, Fe and Mn let us evaluate semi quantitatively show how much Cu is associated with the Mn or Fe phases and how much may be bound to some other phase like POM (including microbial biomass) , or sulfides.

At 20 m depth the μXRF maps show no strong, direct correlation between Cu and Mn. There is, however, a correlation at two hotspots between Cu and Fe, which is also supported by the extraction data. The scatter plot reveals that Fe is much stronger represented then Mn, but neither Fe or Mn are particularly well associated with Cu, and there is a significant amount of copper that has no apparent association to Fe and Mn. This Cu is likely bound to POM as we determined from the Org-PO extraction.

A better association of Cu with Fe and Mn can be observed at 118.6m. As the extractions revealed, the amount of particulate Mn is considerably higher than Fe and this is also apparent in

μXRF maps and the scatter plots. Correlation on the scatter plot between Cu and Mn and Fe is quite strong, confirming the associations between these metals apparent from the extraction data. The Cu distribution on the μXRF is very homogeneous at 123m, demonstrating the amorphous and uniform distribution of Cu. Fe and Mn are also quite amorphous compared to the 118.6m depth. With the exception of a small distribution of hotspots on the μXRF map, there is no significant association noticeable between Cu and Mn or Cu and Fe. The scatter plots show some correlation between Cu, Fe and Mn phases, but again compared to the particle max sample (118.6m) there is more Cu that is not associated. This unassociated Cu may have been bound by microbes, POM or precipitated as sulfide minerals. The amorphous nature of Fe, Mn leads to the conclusion that this is freshly precipitated or formed mineral (Jones et al., 2011), which may also be the reason for the higher extraction yields compared to samples from the oxic pycnocline.

The dissolution of Mn phases at the 129m depth and redistribution of Cu is supported by μXRF maps, where Cu and Mn are very homogeneously distributed and Fe, which did not as readily dissolve during the extractions shows more structure and clusters of material. On the scatter plot a reasonable association of Cu with Fe and Mn can be observed, though Mn concentrations are fairly low. A significant amount of Cu is still not associated with Fe, and may be in cooperated into biomass, complexed by POM.

As the analysis of the surface waters indicates, a significant amount of Cu comes into the lake in a very refractory mineral form, unfortunately the extractions could not shed much light on the structure of these refractory phases. The other particles were split quite evenly between organic matter and Fe and Mn oxyhydroxides, a significant fraction of the Cu is bound to organic matter, which is most likely transported into the lake as detrital material. The complexation to

POM is supported by the surface structure of organic matter which has a large negative surface charge, and has been known to bind to trace metals (Fontes and Gomes, 2003; Mbila et al., 2001; Sodre et al., 2001; Soumare et al., 2003) in tropical soils. Cu has been demonstrated to binds preferentially to organic matter (Mbila et al., 2001; Soumare et al., 2003), even when Fe and Mn (oxy)hydroxides are present (de Matos et al., 2001). Having a significant amount of trace metals (Cu) associated to POM is very different from the common consensus, where Fe or Mn oxides are expected to be the main bearer of trace metals.

As Cu is very scarce, the scavanging of it by microbes during the re-distribution is very likely, as it is the only time when Cu is made available for microbial uptake. In lake Matano the process for the release of Cu is not only reductive dissolution, as it is suggested for many other environments that have large Iron or Mn particulate content. In this case Cu will also be release released when the POM that it is associated with is consumed by microbes through regular carbon respiration pathways. This means that the release of Cu is not purely associated with and bound to a particular redox environment. This might make it more available, easier for microbes to cycle and retain and thus increase Cu acquisition efficiency and decrease the apparent demand for Cu.

4. Conclusions

This study has presented an intriguing window into the distribution of Copper (Cu) in ferruginous modern analogue to iron dominated oceans of Precambrian Eons. When compared to Cu concentrations in other aquatic environments the biological communities of Lake Matano face a copper famine of sorts, the same conditions often imposed in conceptual models of Earth's

early oceans. We demonstrate that the particulate organic matter found within the lake is the major control on the distribution of Cu in this system by using a combination of selective chemical extractions, geochemical modeling, and X-ray spectroscopy. In the lakes biogeochemically active zone we find evidence for the mobilization of Cu into different solid phase reservoirs, seemingly tied to respiration of particulate organic matter, and redox reactions of Fe, Mn, and S. This role for sulfur could be considered particularly unexpected with the minimal aqueous sulfide available. Yet a preponderance of evidence seems to align with a critical role for Cu-sulfide species in this iron dominated environment. Thus even under ferruginous conditions particulate organic matter and sulfur geochemistry must be incorporated in biogeochemical models of Precambrian marine Cu biogeochemistry.

References:

Anbar, A.D., Knoll, A.H., 2002. Proterozoic ocean chemistry and evolution: A bioinorganic bridge? Science, 297(5584): 1137-1142.

APHA, 1985. Standard Methods for the Examination of Water and Waste Water, Washington, DC, pp. 413-426.

Brendel, P.J., Luther, G.W., 1995. Development of a Gold Amalgam Voltammetric Microelectrode for the Determination of Dissolved Fe, Mn, O-2, and S(-Ii) in Porewaters of Marine and Fresh-Water Sediments. Environmental Science & Technology, 29(3): 751-761.

Bruland, K.W., 1980. Oceanographic distributions of cadmium, zinc, nickel, and copper in the north pacific. Earth and Planetary Science Letters, 47(2): 176-198.

Bruland, K.W., Franks, R.P., 1983. Mn, Ni, Cu, Zn and Cd in the Western North Atlantic. In: Wong, C.S., Boyle, E., Bruland, K.W., Burton, J.D., Goldberg, E.D. (Eds.), Trace Metals in Sea Water. Springer US, Boston, MA, pp. 395-414.

Canfield, D.E., 1998. A new model for Proterozoic ocean chemistry. Nature, 396(6710): 450-453.

Canfield, D.E. et al., 2008. Ferruginous conditions dominated later neoproterozoic deep-water chemistry. Science, 321(5891): 949-952.

Canfield, D.E., Thamdrup, B., 2009. Towards a consistent classification scheme for geochemical environments, or, why we wish the term 'suboxic' would go away. Geobiology, 7(4): 385-392.

Cooper, D.C., Picardal, F., Rivera, J., Talbot, C., 2000. Zinc immobilization and magnetite formation via ferric oxide reduction by Shewanella putrefaciens 200. Environmental Science & Technology, 34(1): 100-106.

Coughlin, B.R., Stone, A.T., 1995. Nonreversible Adsorption Of Divalent Metal-Ions (Mn-Ii, Co-Ii Ni-Ii Cu-Ii And Pb-Ii) Onto Goethite - Effects Of Acidification, Fe-Ii Addition, And Picolinic-Acid Addition. Environmental Science & Technology, 29(9): 2445-2455.

Crowe, S.A. et al., 2008a. Photoferrotrophs thrive in an Archean Ocean analogue. Proceedings of the National Academy of Sciences of the United States of America, 105(41): 15938-15943.

Crowe, S.A. et al., 2011. The methane cycle in ferruginous Lake Matano. Geobiology, 9(1): 61-78.

Crowe, S.A. et al., 2014. Deep-water anoxygenic photosythesis in a ferruginous chemocline. Geobiology, 12(4): 322-339.

Crowe, S.A. et al., 2008b. The biogeochemistry of tropical lakes: A case study from Lake Matano, Indonesia. Limnology and Oceanography, 53(1): 319-331.

de Matos, A.T., Fontes, M.P.F., da Costa, L.M., Martinez, M.A., 2001. Mobility of heavy metals as related to soil chemical and mineralogical characteristics of Brazilian soils. Environmental Pollution, 111(3): 429-435.

Dupont, C.L., Butcher, A., Valas, R.E., Bourne, P.E., Caetano-Anolles, G., 2010. History of biological metal utilization inferred through phylogenomic analysis of protein structures. Proceedings of the National Academy of Sciences of the United States of America, 107(23): 10567-10572. Falkner, K.K. et al., 1997. Minor and trace element chemistry of Lake Baikal, its tributaries, and surrounding hot springs. Limnology and Oceanography, 42(2): 329-345.

Falkner, K.K. et al., 1997. Minor and trace element chemistry of Lake Baikal, its tributaries, and surrounding hot springs. Limnology and Oceanography, 42(2): 329-345.

Faure, G., 1998. Principles and Applications of Geochemistry. Prentice-Hall, Upper Saddle River, 600 pp.

Fontes, M.P.F., Gomes, P.C., 2003. Simultaneous competitive adsorption of heavy metals by the mineral matrix of tropical soils. Applied Geochemistry, 18(6): 795-804.

Hakemian, A.S., Rosenzweig, A.C., 2007. The biochemistry of methane oxidation, Annual Review of Biochemistry. Annual Review of Biochemistry, pp. 223-241.

Ilbert, M., Bonnefoy, V., 2013. Insight into the evolution of the iron oxidation pathways. Biochimica et Biophysica Acta (BBA) - Bioenergetics, 1827(2): 161-175.

Jones, C. et al., 2011. Biogeochemistry of manganese in ferruginous Lake Matano, Indonesia. Biogeosciences, 8(10): 2977-2991.

Knauer, K., Ahner, B., Xue, H.B., Sigg, L., 1998. Metal and phytochelatin content in phytoplankton from freshwater lakes with different metal concentrations. Environmental Toxicology and Chemistry, 17(12): 2444-2452.

Katoh, S., 2003. Early research on the role of plastocyanin in photosynthesis. Photosynthesis Research, 76(1-3): 255-261.

Lovley, D.R., Phillips, E.J.P., 1986. Organic-Matter Mineralization with Reduction of Ferric Iron in Anaerobic Sediments. Applied and Environmental Microbiology, 51(4): 683-689.

Luther, G.W., 2005. Manganese(II) oxidation and Mn(IV) reduction in the environment - Two one-electron transfer steps versus a single two-electron step. Geomicrobiology Journal, 22(3-4): 195-203.

Masson, M., Blanc, G., Schafer, J., Parlanti, E., Le Coustumer, P., 2011. Copper addition by organic matter degradation in the freshwater reaches of a turbid estuary. Science of the Total Environment, 409(8): 1539-1549.

Mbila, M.O., Thompson, M.L., Mbagwu, J.S.C., Laird, D.A., 2001. Distribution and movement of sludge-derived trace metals in selected Nigerian soils. Journal of Environmental Quality, 30(5): 1667-1674.

Morgan, J.J., 2005. Kinetics of reaction between O-2 and Mn(II) species in aqueous solutions. Geochimica Et Cosmochimica Acta, 69(1): 35-48.

Neaman, A., Waller, B., Mouele, F., Trolard, F., Bourrie, G., 2004. Improved methods for selective dissolution of manganese oxides from soils and rocks. European Journal of Soil Science, 55(1): 47-54.

Ochieng, E.Z., Lalah, J.O., Wandiga, S.O., 2008. Water quality and trace metal distribution in a Pristine Lake in the lake Basin in Kenya. Bulletin of Environmental Contamination and Toxicology, 80(4): 362-368.

Pokrovsky, O.S. et al., 2012. Chemical and structural status of copper associated with oxygenic and anoxygenic phototrophs and heterotrophs: possible evolutionary consequences. Geobiology, 10(2): 130-149.

Poulton, S.W., Canfield, D.E., 2005. Development of a sequential extraction procedure for iron: implications for iron partitioning in continentally derived particulates. Chemical Geology, 214(3-4): 209-221.

Poulton, S.W., Canfield, D.E., 2011. Ferruginous Conditions: A Dominant Feature of the Ocean through Earth's History. Elements, 7(2): 107-112.

Rose, S., Long, A., 1988. Dissolved-Oxygen Systematics In The Tucson Basin Aquifer. Water Resources Research, 24(1): 127-136.

Saito, M.A., Sigman, D.M., Morel, F.M.M., 2003. The bioinorganic chemistry of the ancient ocean: the co-evolution of cyanobacterial metal requirements and biogeochemical cycles at the Archean-Proterozoic boundary? Inorganica Chimica Acta, 356: 308-318.

Sodre, F.F., Lenzi, E., da Costa, A.C.S., 2001. Applicability of adsorption models to the study of copper behaviour in clayey soils. Quimica Nova, 24(3): 324-330.

Soumare, M., Tack, F.M.G., Verloo, M.G., 2003. Distribution and availability of iron, manganese, zinc, and copper in four tropical agricultural soils. Communications in Soil Science and Plant Analysis, 34(7-8): 1023-1038.

Stookey, L.L., 1970. Ferrozine - a New Spectrophotometric Reagent for Iron. Analytical Chemistry, 42(7): 779-781.

Tessier, A., Fortin, D., Belzile, N., DeVitre, R.R., Leppard, G.G., 1996. Metal sorption to diagenetic iron and manganese oxyhydroxides and associated organic matter: Narrowing the gap between field and laboratory measurements. Geochimica Et Cosmochimica Acta, 60(3): 387-404.

Viollier, E., Inglett, P.W., Hunter, K., Roychoudhury, A.N., Van Cappellen, P., 2000. The ferrozine method revisited: Fe(II)/Fe(III) determination in natural waters. Applied Geochemistry, 15(6): 785-790.

Weber, F.-A., Voegelin, A., Kaegi, R., Kretzschmar, R., 2009. Contaminant mobilization by metallic copper and metal sulphide colloids in flooded soil. Nature Geosci, 2(4): 267-271.

Zahn, J.A., Arciero, D.M., Hooper, A.B., DiSpirito, A.A., 1996. Evidence for an iron center in the ammonia monooxygenase from Nitrosomonas europaea. Febs Letters, 397(1): 35-38.

Zegeye, A. et al., 2012. Green rust formation controls nutrient availability in a ferruginous water column. Geology.

Zumft, W.G., 1997. Cell biology and molecular basis of denitrification. Microbiology and Molecular Biology Reviews, 61(4): 533-616.

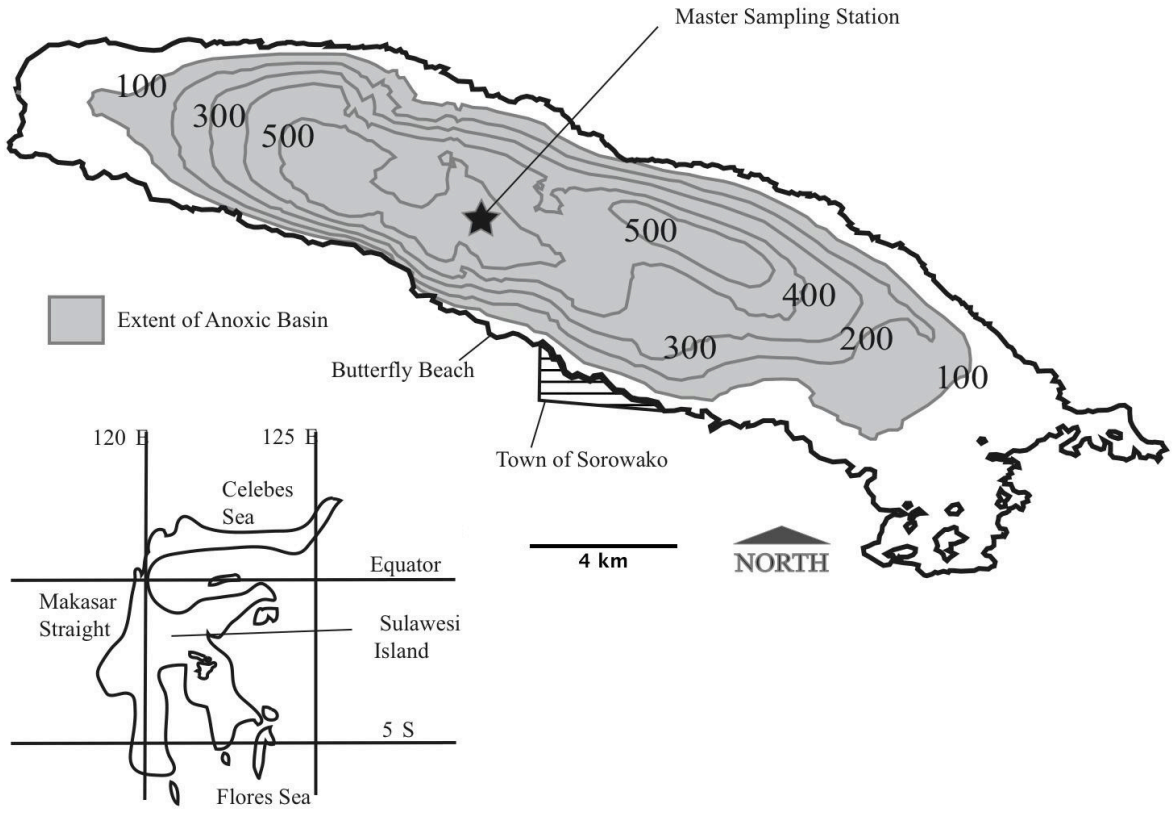

Figure 1 Map of Lake Matano bathymetry the extent of the anoxic basin is shaded and the location of the deep water master sampling station and the town of Sorowako are indicated (modified after Crowe et al., 2008).

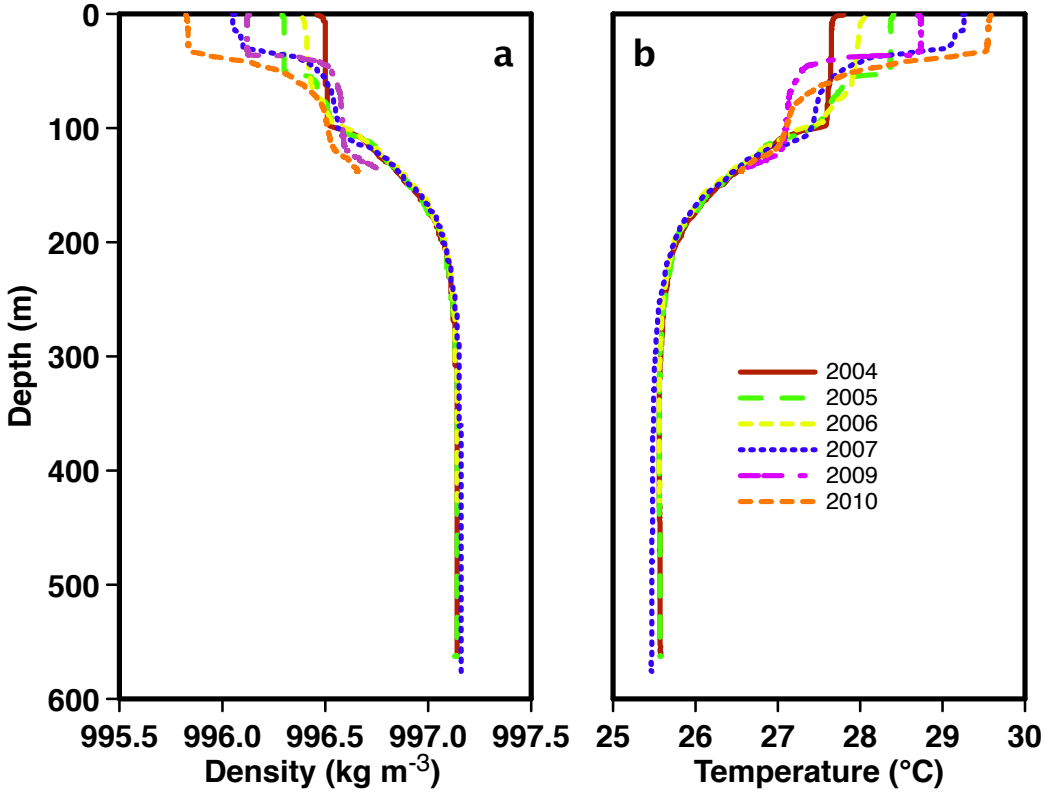

Figure 2 Density and Temperature profiles over several years.

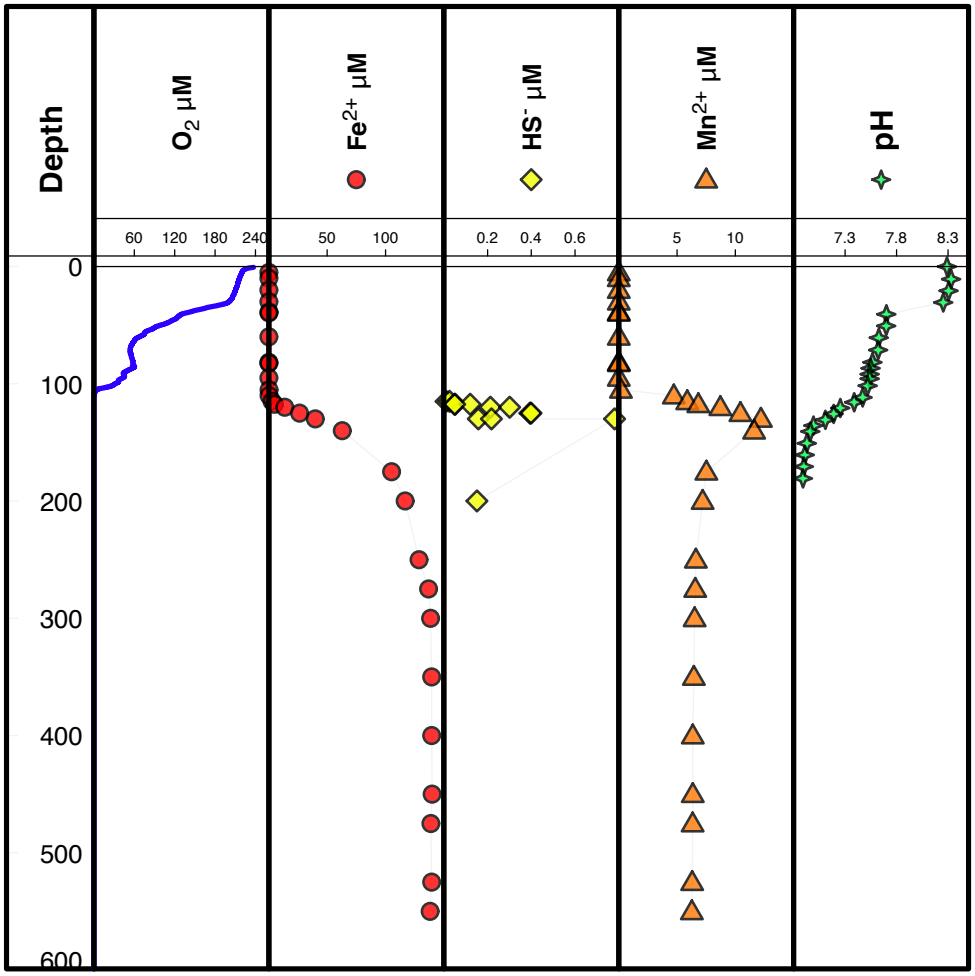

Figure 3 Profiles for the redox active elements in µmol l^{-1} and pH.

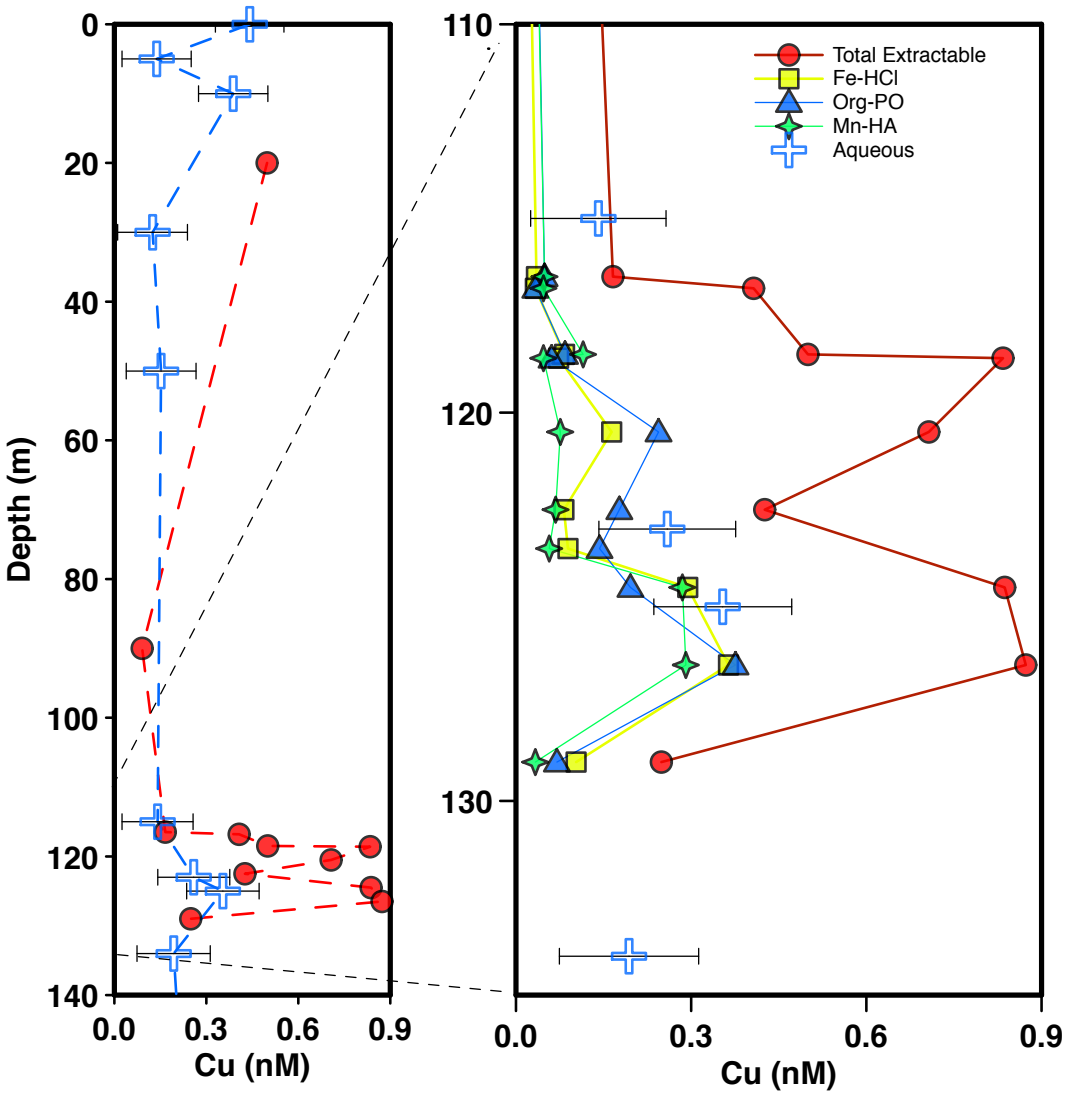

Figure 4 Aqueous and Extracted Copper.

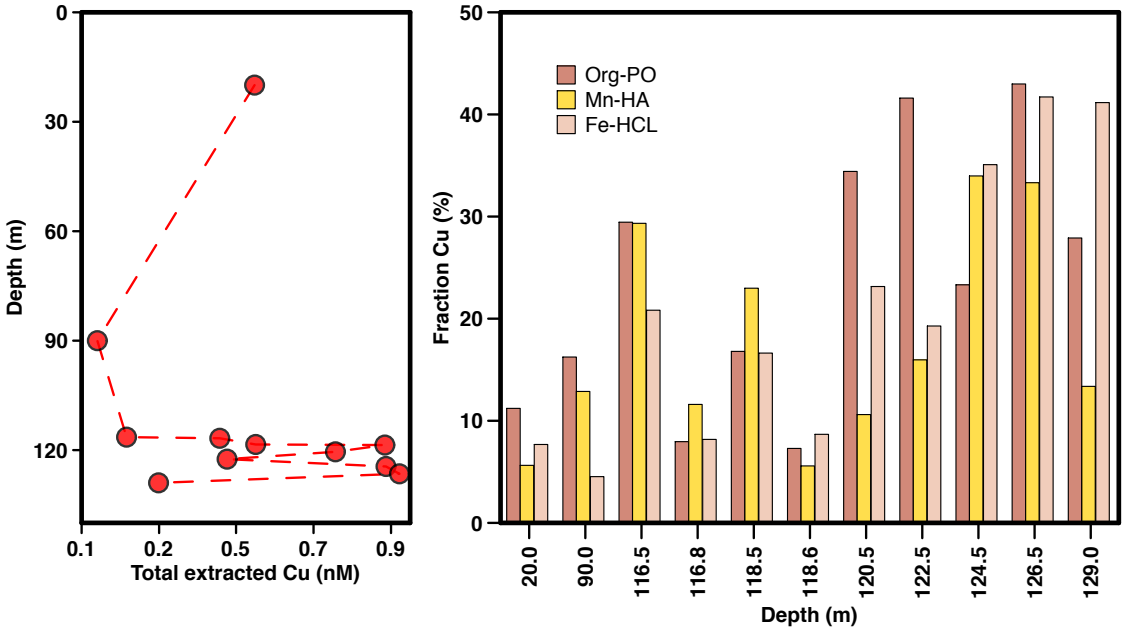

Figure 5 Fraction of Cu extracted from particulate using extraction targeting Fe, Mn and Organic phases.

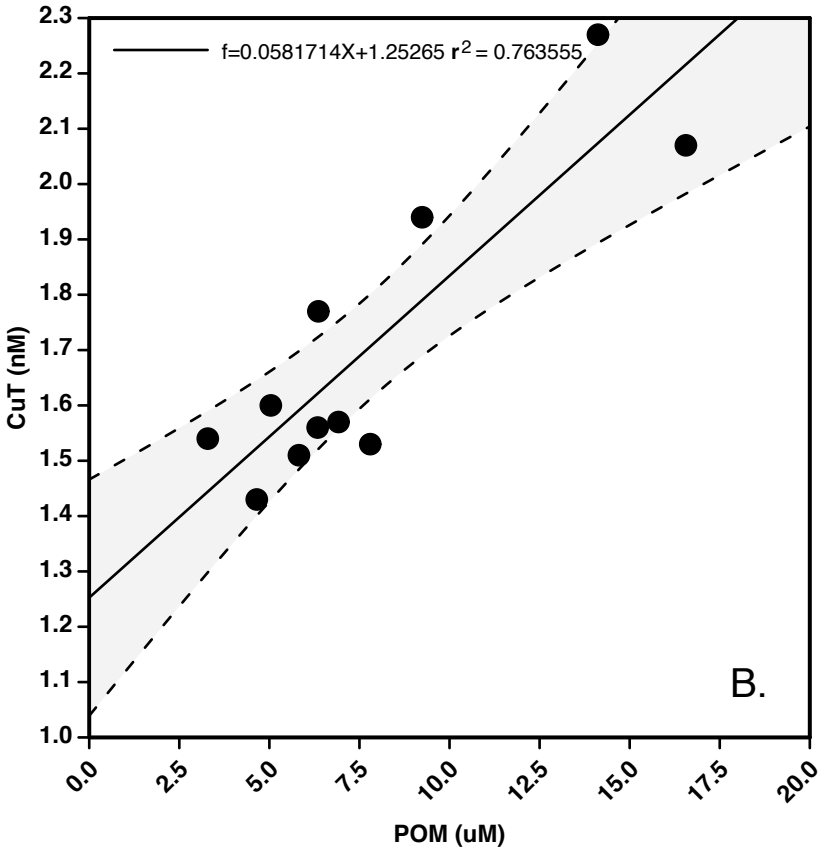

Figure 6 Particulate organic matter in relation to total extractable Cu.

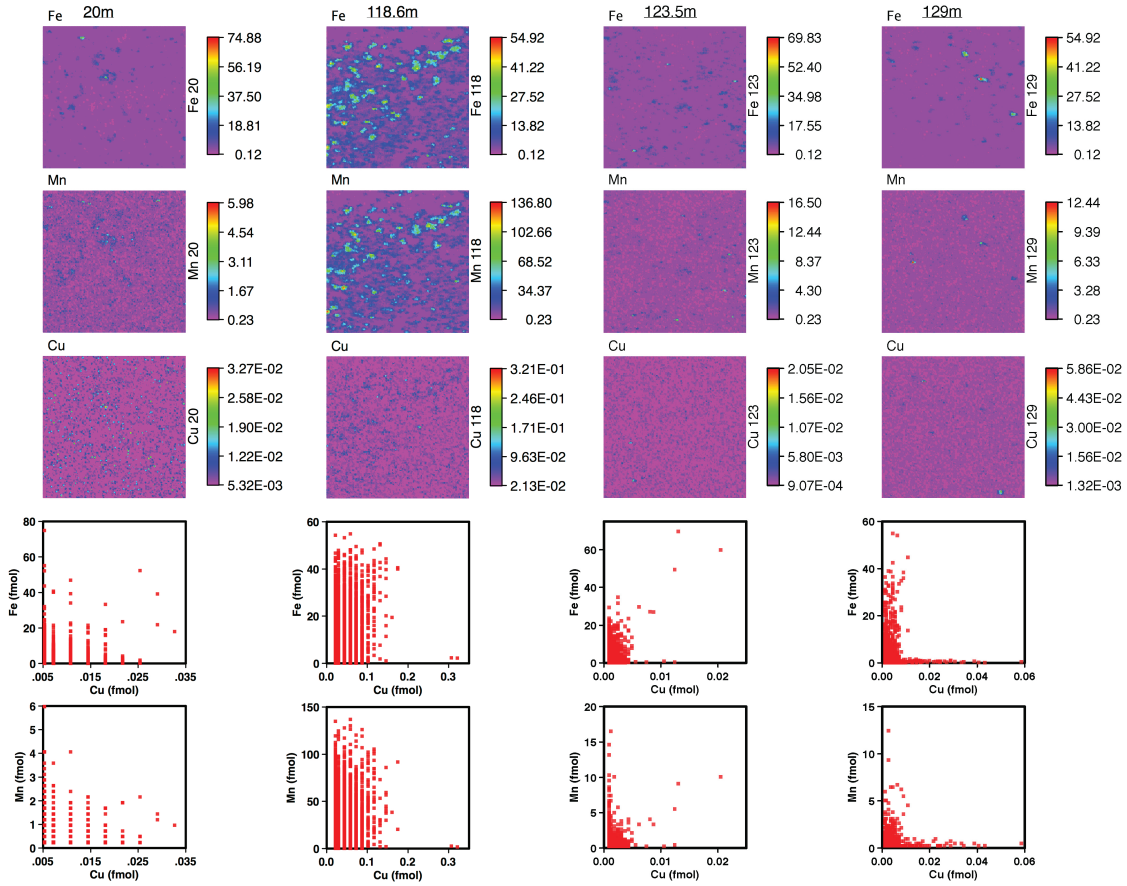

Figure 7 µXRF Maps and scatter plots for particulate matter.

Water body	Concentration nmol l^{-1}	Source
Lake Greifen, Switzerland	14.2 – 12.6 (Surface)	(Knauer et al., 1998)
Lake Senpach, Switzerland	7.78 – 6.30 (Surface)	(Knauer et al., 1998)
Lake Lucerne, Switzerland	4.72 - 9.05 (Surface)	(Knauer et al., 1998)
Lake Baikal, Russia	1.63 – 11.0	(Falkner et al., 1997)
Average Stream water	110.2	(Faure, 1998)
Average Seawater	4.72	(Faure, 1998)
Lake Kanyaboli, Kenya	173 -678 (Surface)	(Ochieng et al., 2008)
Selenga River, Russia	15.3	(Falkner et al., 1997)
Barguain River, Russia	13.6 – 14.7	(Falkner et al., 1997)
Turkar River, Russia	4.75	(Falkner et al., 1997)
Upper Angara River, Russia	11.4	(Falkner et al., 1997)

Table 1 Aqueous copper concentrations in a variety of aquatic ecosystems.

Depth	Chalcopyrite (SI)	Covellite (SI)	Pyrite (SI)	Tenorite (SI)	Calcite (SI)
10 m	-	-	-	-2.14	0.17
120.5 m	20.71	14.02	6.98	-3.51	-0.088
127 m	18.11	12.17	-	-5.17	-0.90

Table 2 Saturation indices of copper bearing minerals and other relevant phases in the surface and pycnocline waters of Lake Matano

Chapter 5: Conclusions

Our understanding of carbon and micronutrient cycling in ferruginous environments can be considered cursory at best owing to the lack of suitable modern environments to study (Konhauser et al., 2005; Poulton and Canfield, 2011). This is particularly problematic when there are attempts to interpret the biogeochemical processes that were ongoing in the Precambrian oceans as life and its underpinnings (such as micronutrient dependent enzymatic systems) were rapidly evolving. Unless we can find suitable large scale analogues to investigate these environments, we are left to develop box models with questionable boundary conditions and to overextend the interpretation of small scale laboratory studies to continue to develop our conceptual models of the biogeochemistry of our early oceans. With this dissertation I have significantly bolstered the use of Lake Matano in Sulawesi, Indonesia as such an analogue and in the process provided new insights into carbon and copper cycling in ferruginous systems.

Chapter 2

In Chapter 2 of this dissertation I investigated the mechanisms and rates of methane oxidation in Lake Matano. Although the lake has very high methane concentrations in its water column, nearly all of it is oxidized within the lake. Methane oxidation rates were high and represent to the best of my knowledge the fastest ever reported for anoxic water column rates. In this system using ^{14}C-based methane experiments I also discovered unusually high rates of carbon assimilation from methane. I propose that this is related to the highly oligotrophic nature

of the lake and redefines the role methane in carbon cycling as not simply the end product of organic carbon degradation but as both an energy and carbon source for biosynthesis within the lake.

Chapter 3

In Chapter 3 through the development of a holistic model for the hydrological system of the catchment I found confirmation and more insight into the significance of methane production and oxidation on the lakes carbon cycle. Using stable carbon isotopes I found evidence throughout the lake for the influence of methane, including signatures for high rate methane oxidation near the pycnocline and inflection points in the methane concentration gradient indicative of consumption are also noticeable (110m). Particulate organic matter (POM) carbon isotopic signatures provide further evidence of assimilation of methane into biomass, and ultimately deposition of isotopically light biomass in the sediments along with the potential for the recycling of this biomass again through fermentation and methanogenesis. Methanogenesis is occurring both through carbon dioxide reduction and Acetoclastic methanogenesis in the lake, however CO_2 reduction pathways appear to have prominence in the deeper (<140m) waters, thereby providing new and more quantitative evidence for mechanisms of methane production in this lake for models such as (Kuntz et al., 2015). Taken together this work will reset a number of ongoing academic discussions about interpreting the role of methane in early ferruginous oceanic environments.

Chapter 4

In Chapter 4 I investigated the bioavailability and cycling of Copper (Cu) in a Lake that is dominated by particulate Fe and Mn oxides. My original hypothesis which was formulated through both geochemical modeling and literature review was that Cu concentrations in the lake would be at nM levels and would be dominated in the solid phase by sorption to Fe and Mn oxides. However my results showed that instead a significant amount of the Cu is associated with POM and likely dissolved organic matter (DOM). Furthermore in a system where iron dominates the aqueous geochemistry and aqueous Sulfide is considered scarce, there is preliminary evidence supported by geochemical modeling that copper sulfides appear to be forming in the chemocline, where reductive dissolution is occurring. Perhaps the most intriguing find of this study is that several microbial metabolisms which at their heart are highly dependent on Cu for their enzymatic systems (e.g. Methanotrophic bacteria) providing strong evidence that these organisms are outcompeting abiotic reactions for this element as predicted in several laboratory studies e.g(Knapp et al., 2007; Kulczycki et al., 2011; Kulczycki et al., 2007).

Final Thoughts

This dissertation has provided a number of new key insights into carbon cycling and nutrient availability in a ferruginous aquatic environment including dispelling a number of assumptions that have provided the foundation for our interpretation of a variety of paleoenvironmental proxies. This certainly warrants further study of this lake system with a new focus on interpretation of how the cycling of these elements is reflected and preserved in the iron-rich sediments of this lake as they undergo diagenesis.

References:

Knapp, C.W., Fowle, D.A., Kulczycki, E., Roberts, J.A., Graham, D.W., 2007. Methane monooxygenase gene expression mediated by methanobactin in the presence of mineral copper sources. Proceedings of the National Academy of Sciences of the United States of America, 104(29): 12040-12045.

Konhauser, K.O., Newman, D.K., Kappler, A., 2005. The potential significance of microbial Fe(III) reduction during deposition of Precambrian banded iron formations. Geobiology, 3(3): 167-177.

Kulczycki, E. et al., 2011. Stimulation of Methanotroph Activity by Cu-Substituted Borosilicate Glass. Geomicrobiology Journal, 28(1): 1-10.

Kulczycki, E., Fowle, D.A., Knapp, C., Graham, D.W., Roberts, J.A., 2007. Methanobactin-promoted dissolution of Cu-substituted borosilicate glass. Geobiology, 5(3): 251-263.

Kuntz, L.B., Laakso, T.A., Schrag, D.P., Crowe, S.A., 2015. Modeling the carbon cycle in Lake Matano. Geobiology, 13(5): 454-461.

Poulton, S.W., Canfield, D.E., 2011. Ferruginous Conditions: A Dominant Feature of the Ocean through Earth's History. Elements, 7(2): 107-112.